Volume 88(91), Special Issue October 2017 ISSN 2248 – 2563

Romanian Journal of EARTH SCIENCES

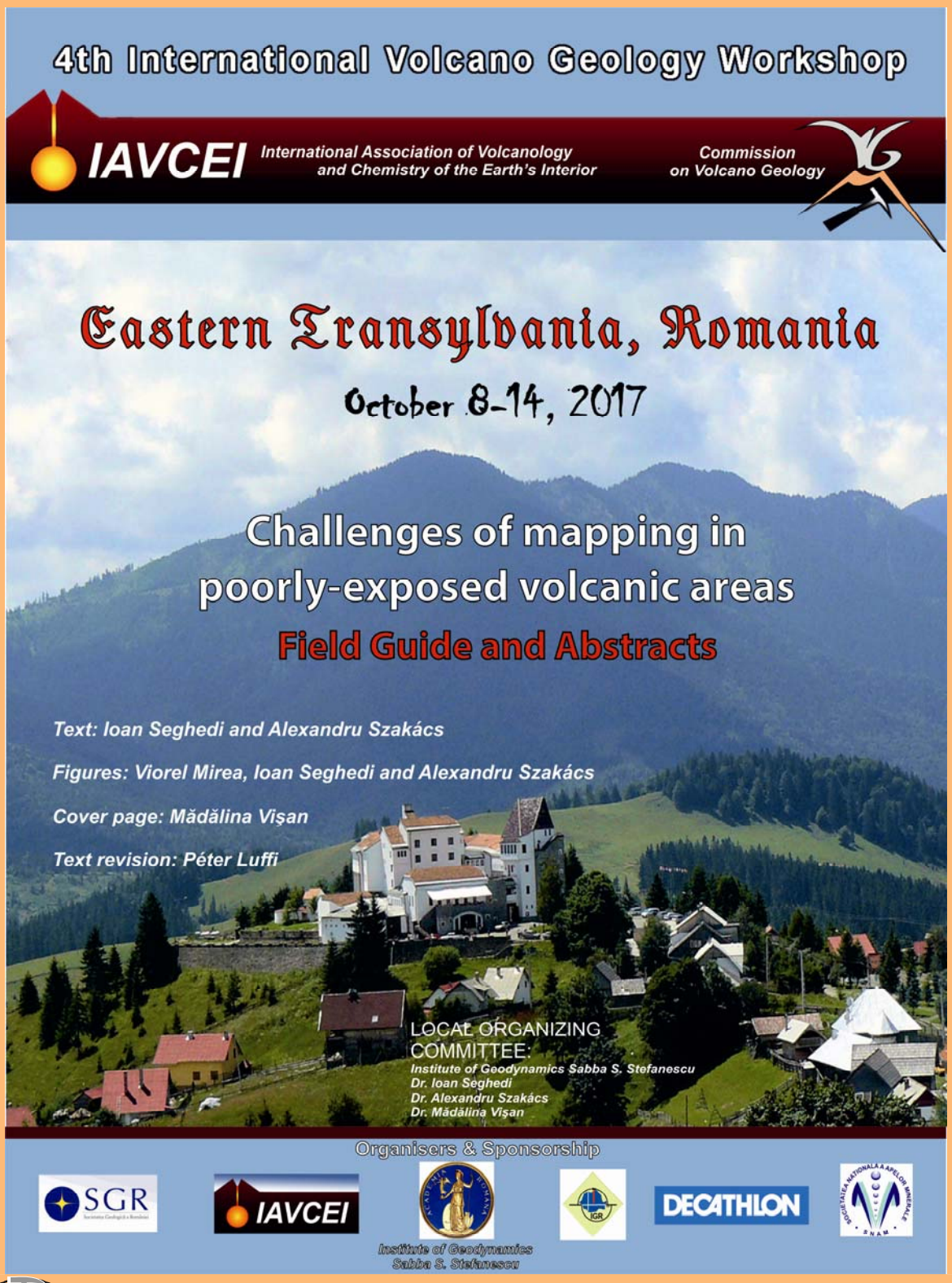

GEOLOGICAL INSTITUTE OF ROMANIA

4th International Volcano Geology Workshop Transylvania, Romania 8-14 October 2017

Challenges of mapping in poorly-exposed volcanic areas

Ioan SEGHEDI, Alexandru SZAKACS, Viorel MIREA, Mădălina VIŞAN, Péter LUFFI

1. Introduction

The 4th international Volcano Geology Workshop is organized in Eastern Transylvania, Romania 8-14 October 2017 under the auspices and with the sponsorship of the International Association of Volcanology and Chemistry of Earth Interior (IAVCEI). It is an action undertaken within the framework of activities run by the IAVCEI Commission on Volcano Geology (CVG). This Workshop follows previous actions initiated and run by the promoters of the CVG: Madeira (Portugal) in 2014, Prague (Czech Republic) in 2015, and Etna-Aeolian Islands (Italy) in 2016. It was proposed and largely agreed upon, including by an ad-hoc "plebiscite" by the participants of the 3rd Volcano Geology Workshop in Italy.

The idea laying at the very base of the initiative of the CVG and its activities is the recognition, by a group of volcanologists, of the fact that with the advent of the digital era and the opportunities offered by computerized techniques and software in the science of volcanology, enthusiastically embraced and effectively exploited mostly by the young generation of volcanologists, expertise in the "classical" fieldwork-based volcanological research started to diminish and in peril to be gradually lost. In particular, mapping skills are feared to be lost with the change of generations and gradual retirement of hard-rock geologists having those skills and expertise. Hence, there is an urgent need to pass the fieldwork-based experience to the next generation of volcanologists, which then may effectively combine those classical mapping techniques with the modern digital tools.

Field mapping is the first fundamental step in unraveling and understanding geological evolution at any scale, from local to regional. In volcanic areas this is intrinsically more difficult than in sedimentary terrains because of the complicated/irregular geometry of volcanic rock bodies preserved in the geological record. The outcomes of mapping are strongly dependent on a number of objective and subjective factors such as the age of volcanism, degree of erosion, outcrop availability, map type and scale, researcher expertise/experience, and personal biases.

Previous Volcano Geology Workshops (i.e. Madeira and Etna/Aeolian Islands) were held in active/recent volcanic areas where fresh eruptive products are largely exposed and available to direct visual observation and sampling. There, the participants had the opportunity to gain insight into how the lithostratigraphic concept and methodology combined with remote sensing techniques are successfully applied to the mapping of well-exposed active/recent volcanic areas.

In many countries around the world, however, geologists are facing volcanic areas in which fieldwork and mapping are hindered by heavy vegetation/soil cover and, implicitly, poor exposure of the bedrocks. Many tropical-climate regions and most of Central/Eastern Europe host heavily forested volcanic areas. With the experience of past workshops in mind, we propose to broaden the perspective on volcano mapping in recent/active and well-exposed areas towards regions of ancient volcanic activity in poorly-exposed areas.

For this reason, the focus of the 4th CVG Workshop is to address the challenges of mapping in poorly-exposed volcanic areas, to discuss, illustrate and make progress in mapping approaches and methodology. An important objective of the workshop is to involve young and early career volcanologists in the problematic of volcano mapping with the help of experienced geologists. In addition, we use this opportunity to connect with other earth-science communities interested in fieldwork-based volcano research and mapping. For instance, the investigation of poorly-exposed volcanic areas may, and should, profit from geophysical methods and expertise; exploration geologists may be interested in gaining expertise in mapping in areas with dissected old volcanic edifices.

The Călimani-Gurghiu-Harghita volcanic range at the eastern rim of the Transylvanian Basin in Romania is the ideal site to illustrate and discuss all the above-mentioned issues within the framework of a fieldtrip-based CVG workshop. A previous IAVCEI-supported Workshop entitled "Volcaniclastic sequences around andesitic stratovolcanoes (East Carpathians, Romania)" was successfully held in the East Carpathians, Romania in 1996, jointly organized by the Commission on Explosive Volcanism and the Commission on Volcanogenic Sediments (Szakács & Seghedi, 1996). The Organizers of the 4th Volcano Geology Workshop take advantage of the experience accumulated during that Workshop.

WELCOME TO ALL WORKSHOP PARTICIPANTS!

2. Workshop concept

Following the tradition of the previous editions, the 4th International Volcano Geology Workshop is thought and proposed to be focused on mapping-related field activities in volcanic areas. The previous fieldtrip-based Volcano Geology Workshops (i.e. Madeira, 2014 and Etna/Aeolian Islands, 2016) were organized in active/recent volcanic areas where eruptive products are largely exposed and available to direct visual observation and sampling. However, geologists in many countries around the world share the common problem of performing fieldwork and mapping in areas with heavy vegetation and soil cover and, implicitly, limited exposure of the bedrocks, hence producing geological maps in such conditions poses a serious challenge.

The participants attending the pervious workshops learned how the lithostratigraphic concept and methodology – initiated, elaborated and proposed by Italian volcanologists – are successfully applied in the mapping of well-exposed active/recent volcanic areas. The lithostratigraphic approach to mapping is mainly based on the identification, ranking and mapping of unconformities frequently present in sequences of volcanic and related rocks. Those unconformities are, in fact, boundaries (i.e. contact surfaces) between distinguishable parts of the volcanic successions identified and described in the relevant literature as "Unconformity-Bounded Units" (UBUs, e.g., Branca et al. 2011). According to the ranks of the unconformities they are bounded by (given by their spatial extent or degree of regionality and by the extent of the repose times in volcano evolution), the UBUs are classified as different "synthemic units" – synthem, subsynthem, supersynthem – corresponding to stages of volcano evolution at different spatial/temporal scales. From the mapping point of view, this approach requires, as the first essential step, field-identification of unconformities using classical visual and remote-sensing methods. In well-exposed active/recent volcanic areas, many unconformities are visible at the surface and can easily be identified and mapped – at least partially. The next step is ranking the unconformities on which the definition of synthemic units depends. As we have seen during previous workshops held in active/recent volcanic areas, this is not a simple task and relies on a lot of complementary information (dating, petrology, biostratigraphy in some cases, etc.). Even so, the rank of particular unconformities was vividly debated and remained uncertain.

In the wide spectrum of exposure conditions that range from continuous to almost inexistent outcropping, the field conditions met in Central/Eastern Europe – similar to many other temperate-climate and tropical regions of the World – are closer to the no-exposure end-member.

In volcanic areas in Romania, for example, exposures are uneven because of the heavy soil and vegetation cover: continuous outcrops (100x m long) along some major valleys alternate with few and small (1x to 10 x m) outcrops along smaller tributaries and ridges and with large (km^2-scale) areas lacking any exposure. Exposed contacts between rock bodies or formations are thus extremely rare or absent. In such circumstances, correlation between established cartographic entities is largely based on interpolation and extrapolation,

sometimes across large outcrop-free areas. The researcher's experience and personal bias play an important role in the outcome of the mapping. Remote sensing techniques are hardly applicable because of pronounced erosion, weathering, and soil/vegetation coverage. Topographic features are sometimes relevant – in particular, where rocks of contrasting hardness are in contact – and can be used in tracing geologic boundaries on map. Post-volcanic deformation, more and more developed as we go back in time, is another problem.

In such circumstances, it seems inevitable that the lithostratigraphic approach and methodology used in mapping – successful in well-exposed areas – have to be adapted to new perspectives and/or completed with new methodologies. One significant issue, for instance is the fact that in poorly exposed areas discontinuities identified in outcrops are absent or rarely present, thus their correlation and ranking is nearly impossible. Hence, they cannot be used as objective features to systematize and order lithostratigraphic entities such as synthemic units. Instead, discontinuities will eventually emerge as interpreted features at the end of the mapping process, after all fieldwork information is processed. In such cases, the volcanologist has to deal with interpreted discontinuities instead of observed ones and define UBUs accordingly. Therefore, the accuracy and relevance of the resulted maps will be poorer and incorporate more subjectivity than in the case of maps realized in well exposed active/recent volcanic areas.

For all these reasons, maps representing ancient and poorly exposed volcanic areas look quite different from those obtained for recent/active volcanoes. The question is how to overcome or, at least, diminish the inaccuracies, and how to improve the reliability of the map units and boundaries.

One possible way to improve map accuracy and reliability in poorly-exposed volcanic areas is to replace the unconformities as major lithostratigraphic markers with a more diverse spectrum of significant features, which mark major events in volcano evolution. For instance, instead of identifying and tracking unconformities in the field, features/formations resulted from major volcanic events (i.e. "master-events", as defined and conceptualized by Szakács & Canon-Tapia (2010), such as sector collapse, caldera formation, abrupt petrographic/petrochemical changes, etc., are to be considered as major milestones of volcano evolution. Debris avalanche deposits (DADs), for instance, have the advantage of being more easily mappable due to their large volumes and wide dispersal areas. In addition, they are frequent in volcanic areas dominated by large composite volcanoes such as the Miocene-Pleistocene Călimani-Gurghiu-Harghita range in the East Carpathians, Romania. Calderas and products of caldera-forming eruptions also are large-scale features in many volcanic areas. However, in the case of small volcanoes, which did not undergo such major destructive or eruption events, this approach is less effective. Due to their small size, and generally less complex structure, such volcanoes can be mapped by combining outcrop observation with topography and geophysics within the lithosomatic approach, which defines volcanic edifices (or definable parts of them) – i.e. "lithosomes" – as the basic lithostratigraphic, hence map units.

A possible complementary approach in defining map units in volcanic areas could be that originating in the volcanic facies concept, which helps systematizing volcanological information as a function of dispersal areas of volcanic products with respect to their sources. Defining the spatial position of a certain formation of volcanic rocks or of a volcanic sequence with respect to their source area(s) is a crucial step not only in the understanding of volcanic structures/edifices and evolution but is extremely useful in mineral exploration and other practical activities as well.

Relying on the decades-long experience gained in mapping ancient volcanic areas in Romania, and learning from the expertise accumulated by others in active/recent volcanic areas, we suggest that a flexible combination of the UBU-based lithostratigraphic approach (in accordance with the level of exposure and age of volcanism) with the "master-event"-based approach and the facies-based approach might significantly improve results in mapping volcanic terrains. Each of these three approaches has to be considered in terms of map units and corresponding legend symbols. To develop such a combined system of map symbolistics, as part of Guidelines in volcano mapping, could be a major and attractive task of the IAVCEI Commission on Volcano Geology.

In the light of the discussion sketched above, a number of questions arise and should be addressed during the 4th Volcano Geology Workshop, such as (but not restricted to):

- whether, to what extent, and how the UBU-based lithostratigraphic approach is applicable in poorly-exposed and/or extinct/old volcanic areas;
- what kind of map units – petrographic/petrochemical, lithological, facies, etc. – should be defined and used during different stages of mapping activities;
- what is the significance of "formation" as a lithostratigraphic unit, and how can it be objectively defined, recognized and mapped in poorly-exposed volcanic areas (for instance, may one define a "formation" based on a single outcrop occurrence ?);
- whether and how the volcanic facies concept can be involved and integrated with the lithostratigraphic approach in mapping activities in poorly-exposed areas;
- how and to what extent topographic features can be used in defining and separating map units in old volcanic areas still preserving such features;
- whether and which kind of geophysical information can be used and integrated in the definition of map units in poorly-exposed volcanic areas.

3. Facies architecture and volcano evolution: a general conceptual approach

While the volcano facies concept helps understanding and describing the structure of volcanic edifices – either active/recent or old – according to the spatial distribution of the volcanic products with respect to their sources, the "master-event" concept helps understanding and

describing the long-term evolution of volcanoes in time according to size-ranked constructive and destructive volcanic events.

3.1. Volcanic facies

The lithostratigraphic approach in the study and mapping of volcanic areas can be improved and completed by integration of the volcanic facies concept, in particular in the investigation of ancient volcanic areas where volcanic rock assemblages are partly eroded, buried or disconnected from their source volcanoes. Interpreting volcanic successions in terms of volcanic facies may help correctly locating their actual position in the framework of volcanic edifices, inferring the identity and position of the eruption centers they belong to and, in general, reconstructing evolution histories of volcanic terrains.

Facies models, those of stratovolcanoes in particular, were devised for individual edifices by considering a central source of eruptive material distributed in an axial-symmetric centrifugal pattern around it. Three or four concentric volcanic facies have been defined and ordered from center to periphery. There are various nomenclatures used to name different volcanic facies. Williams & McBirney (1979) in their Volcanology textbook, for example, use the facies names central, proximal and distal. Vessel & Davies (1981), in turn, use a fourfold facies nomenclature for the Fuego volcano, Guatemala: central, proximal, medial, and distal. Davidson & Da Silva (2000) use „association", instead of „facies" and distinguish main vent, cone-building, ring-plain, and satellite vent associations at composite volcanoes. The lithological content of each volcanic facies can be characterized by a particular assemblage of rocks (effusive, intrusive and volcaniclastic in nature). Based on the Vessel and Davies classification, here we adopt the following facies terminology:

- **Central facies:** the central summit part of the volcanic edifice with its vent and crater system, summit domes, and near-surface intrusions; fumaroles and related alteration of the rocks. At old, dissected volcanoes, can be identified as a "volcanic core-complex" including exhumed shallow intrusions and their related hydrothermal alteration zones;

- **Proximal facies** - or cone or flank facies - defined on morphological grounds, as corresponding to the volcanic cone, extended from the crater rims down to the flat-lying volcaniclastic aprons;

- **Medial facies** - or volcaniclastic fan or ring-plain facies – corresponds to the gentle-sloping low-lying contiguous part of the volcano surrounding the proximal facies;

- **Distal facies** - or alluvial or fluvial facies - includes all recognizable volcanic deposits occurring beyond the outer limits of the contiguous volcaniclastic apron; it is controlled by the fluvial system surrounding the volcano, and typically occurs in discontinuous patches. Distal pyroclastic fall deposits (i.e. tuffs) belong to this facies as well.

At active/recent volcanoes, these facies also correspond to well-defined topographic features of the edifices. The ideal axial-symmetrical facies distribution at simple isolated cone-shaped

volcanoes built on flat topography (such as Mount Egmont in New Zealand) may be distorted to bilateral or asymmetrical facies distribution by various factors such as inclined or rugged basement topography, multiple vents, close spacing of edifices, interference of volcanic material sourced from neighboring volcanoes, etc. leading to more complex facies architectures. Processes like facies merging, facies juxtaposition and facies superposition can be related to facies interference at the junction of two or more neighboring volcanoes (Szakács, 2008). According to spacing, size, maturity, eruptive history, and relative age of the neighboring volcanoes, a whole spectrum of facies interference/combination patterns may result. By careful field mapping combined with lithostratigraphic studies and complementary (e.g. geophysical and geochronologic) data, rock assemblages belonging to particular volcanoes in a closely spaced group can be identified and characterized. Then, the pattern of facies interference can be understood even in old volcanic terrains where no relevant topographic features are preserved.

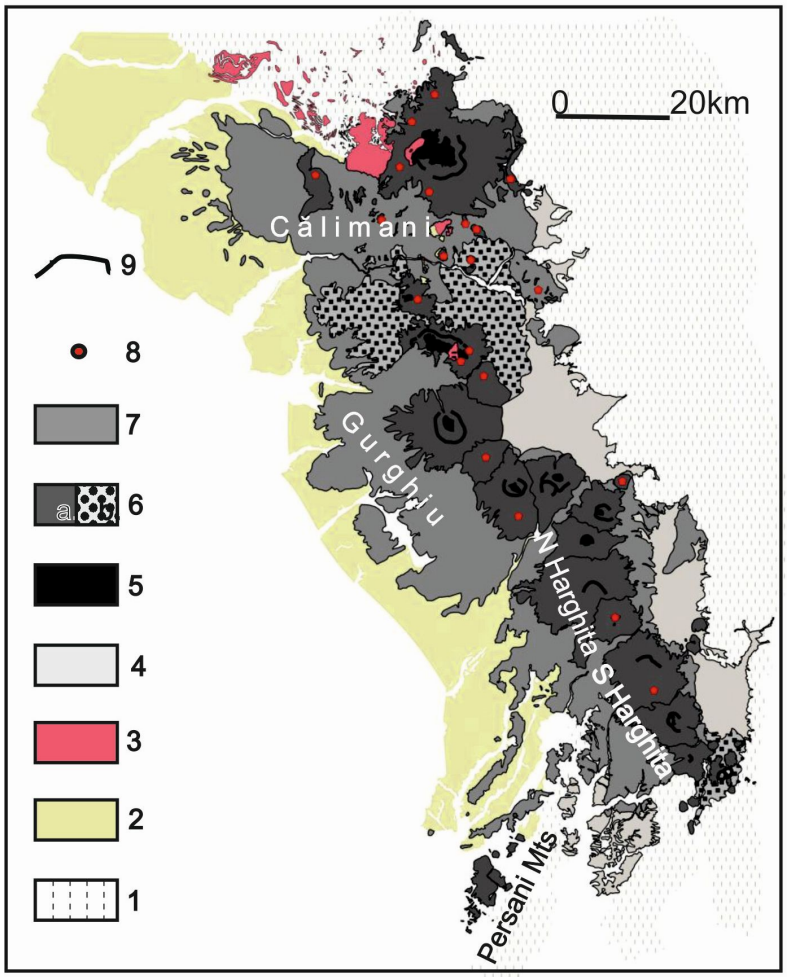

Fig. 1. Simplified volcanic facies map of the Călimani-Gurghiu-Harghita volcanic range (acc. to Szakács & Seghedi, 1995, updated). Legend: 1. East Carpathian basement; 2. Transylvanian Basin formations; 3. Subvolcanic intrusions; 4. Intra-mountain Basins; Volcanic edifice: 5. Central facies; 6. Proximal facies: a. dominantly effusive; b. dominantly explosive; 7. Medial-distal facies; 8. Volcanic center; 9. caldera/crater rim

The closely spaced Miocene composite volcanoes from the East Carpathians, Romania (Fig. 1) are representative examples of facies interfingering, juxtaposition and superposition in various combinations. Whereas the proximal cone facies of composite volcanoes in the Călimani, Gurghiu and Harghita Mts. are lava-dominated and form readily recognizable topographic features at the outer slopes of the individual edifices, their medial (ring-plain) facies, mostly composed of volcaniclastic deposits, are largely interfering with each other at their peripheries.

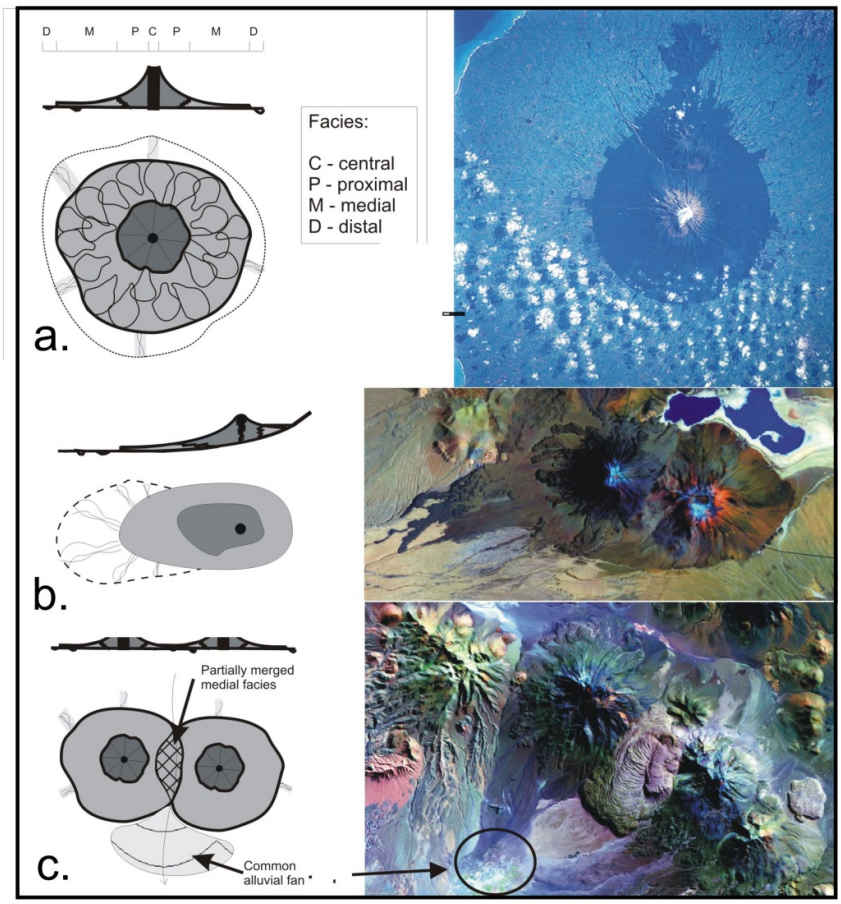

Fig. 2. a. Sketch of axial-symmetrical facies distribution at composite volcanoes (left) and example of Mt. Egmont (Taranaki) volcano in New Zealand (right);b. Sketch of distorted facies distribution at composite volcanoes built on monocline topography (left) and example from the Andes (Licancabur volcano, Chile, on the left of the picture) (right); c. Sketch of facies interaction (facies merging) of closely spaced volcanoes (left) and example from the Central Andes (Paniri and Leon volcanoes)(right; the facies merging area is shown by arrow and circle)

Where magma compositions are sensibly different, petrographic and geochronologic investigation may help identifying the sources of the volcaniclastic formations even if they are otherwise very similar. Adjoining debris avalanche deposits, for example, found tens of km away from their respective source edifices could be distinguished from each other based on clast compositions and ages. Since the volcanic activity migrated along the Călimani-Gurghiu-Harghita volcanic range, medial facies volcaniclastics, sometimes of the same type and of similar composition, but belonging to different volcanoes can be seen in stratigraphic superposition. A typical case is that of the ring-plain facies-dominated western peripheries of the South Harghita Mts., where volcaniclastic formations of neighboring volcanoes are underlain by farther-travelled volcaniclastics originated from the slightly older North-Harghita volcanoes. Here, the different sources have been distinguished from each other based on geochronological and petrographic/petrochemical studies. In contrast, ring-plain volcaniclastic deposits around a group of coeval and compositionally similar volcanoes in the southern Gurghiu Mts., could not be yet assigned to their respective source volcanoes. Recent studies of Miocene composite volcanoes in the CGH range found that their medial facies are volumetrically dominated by debris avalanche deposits and related debris-flow deposits, whereas primary pyroclastics are much less contributing to this facies.

Various types of facies distribution and interaction are illustrated and exemplified in Fig. 2a, b, c and 20. The volcanic facies approach to volcano mapping, a tool complementing the lithostratigraphic approach, can easily be applied to other type of volcanoes, such as shield volcanoes and even monogenetic volcanoes. In old, buried and eroded volcanic terrains it could be useful in mineral exploration given that mineralization often prefer and are limited to certain volcanic facies.

The relevance of the volcanic facies concept to mapping. If the exposure of volcanic products and features is uneven, the reconstruction of volcanic evolution and resulting geologic map will be inhomogeneous in terms of accuracy and reliability. Small map areas accurately representing the field reality (such as in the case of the well exposed Mureş Valley in CGH) are commonly separated by large map portions that feature mostly extrapolated and interpolated boundaries and formations due to the scarcity or lack of outcrops. One way to overcome such situations is to systematize all outcrop information in terms of volcanic facies belonging to known (or unknown) eruptive centers. Such an approach is not always easy to apply, especially if no clear criteria are available to distinguish between source areas, for example because of petrographic and geochemical monotony. This is the case of the group of closely spaced southern Gurghiu volcanoes of the CGH range with indistinguishable petrographic features, whose medial facies products cannot be reliably linked to their actual volcano source. Nevertheless, representing volcanic facies features (central, proximal, medial and distal) on a volcanological map is useful to illustrate the distribution pattern of primary and reworked eruptive products around volcanic centers. The significance of the facies representation on maps increases with the increasing age and erosion of the volcanic sequences resulting in areas with volcanic products disconnected from their sources. The proper identification of various facies is a fundamental step in interpreting volcanic formations as potential hosts of ore bodies in ancient volcanic terrains. At broader scales –

such that of the whole CGH range (Fig. 1) – volcanic facies maps represent a coherent, synthetic and homogenous view of the volcanic activity and the distribution of its products relative to various eruptive centers. As such, volcanic facies maps may, and should, provide a complementary view to cartographic representations based on the lithostratigraphic approach. Moreover, we can envisage map representations that combine the lithostratigraphic and facies-based approaches. For instance, a map unit defined as "merged medial facies volcaniclastics" can effectively increase the value of a volcanological map of the CGH range in areas where indistinguishable medial-facies sequences occur around closely-spaced and petrographically similar volcanoes, such as those in the Southern Gurghiu Mts. The K-Ar age of a basaltic andesite megablock identified at Rupea, far away from the continuous volcanic area (see also the description of Stop 1.1.), has been interpreted as an erosional remnant of a debris avalanche deposit (Szakács & Seghedi, 2000). This allowed us to consider it a relict of distal-facies volcaniclastic deposits derived from the collapsed Vârghiş volcano, which precludes the possibility that it represents medial facies products of the closer-located South-Harghita volcanoes. More examples are given in section 5.2 of this guide.

3.2. The "master-event" concept in reconstructing volcano evolution

Reconstruction of the evolution of inactive and ancient composite volcanoes relies on the available geological record of events occurring along their history. Inherently, the geological record is incomplete and frequently only partially available to observation for various reasons, including the poor exposure of volcanic products. To rationalize the description and characterization of long-term volcanic evolution the concept of "master event" was proposed (Szakács & Canon-Tapia, 2010) in order to pinpoint those major events whose geological record is prominent and available to observation. The following presentation of the "master event" concept is a summary adapted from Szakács & Canon-Tapia (2010).

Volcanic evolution can be conceptually viewed as a succession of eruptive and non-eruptive events. The initial and final eruptive events mark the "birth" and the "death" of a volcano. However, the volcano does not disappear after its last eruption; it can be subjected to subsequent non-eruptive events. Thus, to better characterize the physical existence of a volcano, in addition to distinguishing between eruptive and non-eruptive events we also should distinguish between its active stage from its extinct (post-eruptive) stage.

Fig. 3 shows a conceptual model of a possible volcano evolution along the time axis as a succession of discrete events marked by solid circles (eruptive events), and open circles (non-eruptive events). Events can be either discrete or non-discrete at the scale of volcano evolution. For instance, eruptions generally can be considered discrete events. Edifice failure and sector collapse also are discrete events, whereas long-lasting volcano-spreading and erosion are non-discrete events whose start and end cannot be accurately defined in time. Short periods of anomalously high-intensity erosion might be considered, however, discrete events.

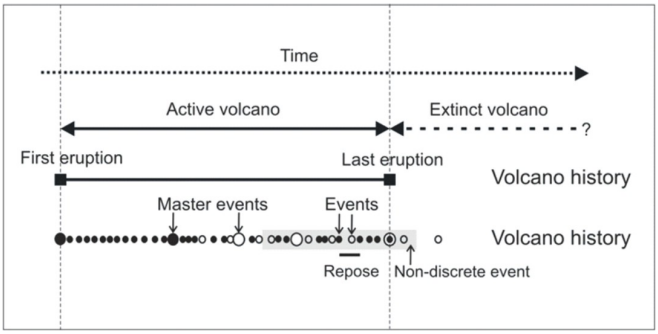

Fig. 3. Conceptual sketch illustrating the "master event" concept in volcano evolution (acc. to Szakács & Canon-Tapia, 2010). See explanation in text.

Another distinction between events takes into account the size and importance of each event. Some events such as caldera formation or volcanic-edifice failure are remarkable not only because of their amplitude but also due to their large-scale consequences for the future evolution of a volcano. Eruptive style and behavior of the volcano usually change after the occurrence of such large-size events. By their deep influence on the entire volcanic system and its environment, these types of events constitute milestones in volcano evolution. As such, they deserve to be clearly distinguished from "common" events. For this reason, the term "master event" was introduced to name them appropriately.

Notably, "non-events" can also be viewed as master events. Long-term periods of quiescence may result in such a degree of continuous erosion that significant changes occur to both the volcanic edifice and the subsurface parts of a volcanic system. In these cases, the long quiescence that commonly would be considered a "non-event" exerts such a strong influence on subsequent volcano behavior that it becomes a "master event". Therefore, neither all of the master events are discrete, nor all of the non-discrete events are common in the sense given above.

In summary, volcano evolution can be viewed as a succession of eruptive and non-eruptive events, some of which are discrete, others being non-discrete; all of these are punctuated by a few "master events" amidst a background of common events.

Ideally, the volcano researcher should identify and date all events occurring during volcano evolution in order to reconstruct the complete volcanic history. In practice, because not all events, especially those of small-scale, leave behind a recognizable geological record, any attempt to fully reconstruct volcano evolution is unrealistic. The situation is even worse if we consider the problems associated with geochronologic techniques and their accuracy. Radiometric dating techniques used for old volcanic rocks (in the range of 0.1 to slightly over1 Ma) may imply analytical errors larger than the time gaps between eruptions, hence many events, including large ones, may be lost from the record because of poor dating resolution. The volcanic record could also become highly inhomogeneous also because various segments of the volcanic history are represented by products variably available for observation.

Due to these limitations, we are commonly limited to reconstruct merely the "master-event-history" of a volcano. Although probably incomplete relative to the whole evolution of a volcano as illustrated in Fig. 3, this master-event history should be sufficient to allow segmentation of the volcanic evolution into a number of well-defined evolutionary stages. In principle, each of these stages will be characterized by a predominant eruptive behavior of the volcano that is characteristic for that stage. Thus, even if the complete record of the history of events within each stage is incomplete, the geological record might provide a reliable characterization of the style and intensity of volcanic activity between consecutive evolutionary stages.

3.3. The relevance of the master event concept in volcano mapping. Introducing MEBU

In poorly-exposed volcanic areas where unconformities are very rare or absent in outcrops, the UBU-based lithostratigraphic approach seeking to define synthemic units is hardly applicable. Products and features resulted from "master events" are, however, inevitably and prominently present in the geologic record. Therefore, these features and products should be the first-order entities to be identified, mapped, characterized, and dated. Then, volcanic products resulted from the "background activity" of volcanoes, found in between time-marker "master event" features, can be defined as synthemic units. In fact, the "master event" concept applied to mapping is fully compatible with the lithostratigraphic approach. The events in volcano history which result in major (say, 1st or 2nd-order) unconformities can be easily viewed as "master events" since they mark major changes in volcano evolution. Major unconformities in volcano sequences are thus just one sort of "master event" features. One may even envisage a ranking of "master events" which reflects the regional extent of their influence. Therefore, the "master event" approach just broadens the applicability field of the now classical UBU-based lithostratigraphic approach. We may even propose to replace UBU (i.e. Unconformity-Bounded Unit) with MEBU (i.e. Master-Event Bounded Unit), UBU being one particular type of MEBU. Similarly to unconformities, "master-event" features – such as debris avalanche deposits and collapse-related topographic features (a major unconformity!), calderas and caldera-forming products, large-volume Plinian deposits, long-lasting or intense erosion stages – can be used to define synthemic units, because they generate unconformities. Those unconformities might not be available to direct observation in poorly-exposed areas and thus are not mappable. Adopting the MEBU-based lithostratigraphy relying on the "master-event" concept has the advantage of being applicable in a consistent manner to any volcanic area regardless of its age and degree of exposure.

We used radiometrically dated "master-events" to mark the major evolutionary stages of a number of composite volcanoes in the CGH volcanic range as presented in section 5.2.

4.Regional geological and volcanological framework of the Carpathian-Pannonian region with emphasis on the Romanian territory

The Neogene/Quaternary volcanism in Romania is part of the much broader sub-alkaline/alkaline magmatism that accompanies the Carpathian orogenic belt and covers

various sedimentary basins of the Carpathian-Pannonian region (e.g. Pannonian and Transylvanian Basin systems) (Fig. 4).

From a geodynamic point of view, the post-Miocene evolution of the CPR was controlled by the long-term diachronous northward motion of Africa and its Adria Block promontory, causing convergence and related post-collisional tectonic and volcanic events (e.g. Harangi et al., 2006). Inside the Carpathian–Moesian realm, the lithospheric block motion is considered to be driven by the retreat of a west-dipping European lithospheric slab (e.g. Royden, 1988) and the push of Adria (e.g. Ratschbacher et al., 1991; Rosenbaum et al., 2004), resulting in various translation movements, strike–slip accommodations and diachronous extensional rotation (e.g., core complex type, see Fig 4). As a result, the crust broke up and was squeezed into the available space (e.g., Csontos, 1995; Fodor et al., 1999; Márton et al., 2000; Márton and Fodor, 2003; Horváth et al., 2006). A generally accepted model for the geodynamic processes in the CPR during Miocene-Quaternary times does not yet exist. Only a limited number of the existing models are explicitly considering the relationships between the tectonic evolution and magmatism (e.g. Seghedi et al., 1998, 2004a; Harangi et al, 2001;Konečný et al., 2002; Harangi et al., 2006;Pécskay et al., 2006; Harangi & Lenkey, 2007; Kovács & Szabó, 2008; Seghedi & Downes, 2011).

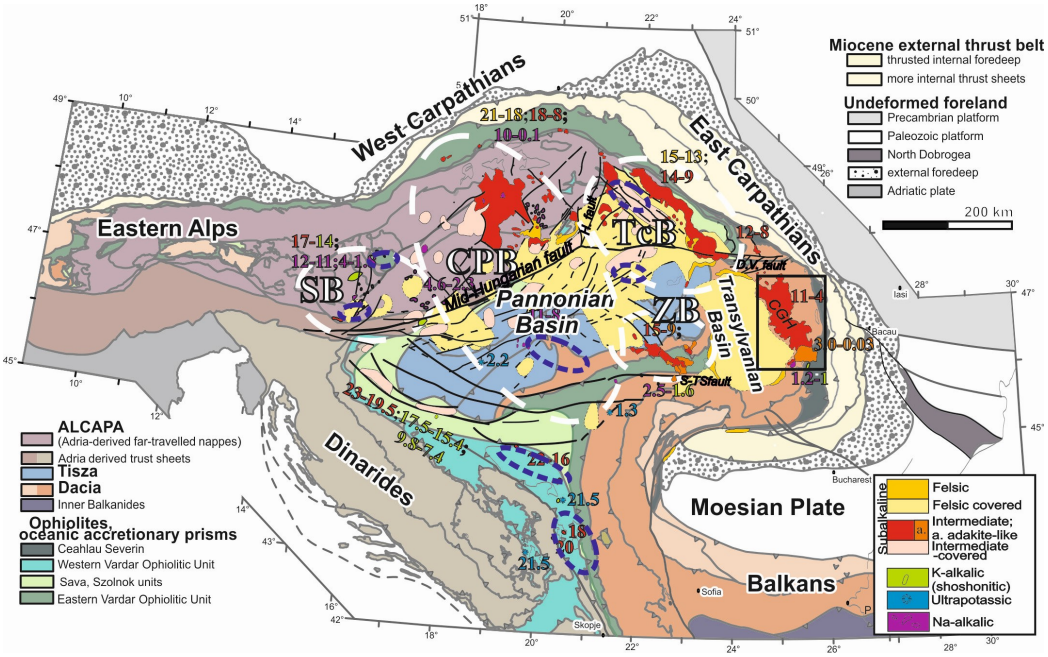

Fig. 4. Sketch map of the Carpathian–Pannonian region and surroundings (acc. Seghedi et al., 2013, with modifications). The regions where volcanism has developed volcanic edifices are encircled with a white dashed line: SB, Styrian Basin; CPB, Central Pannonian Basin; TcB, Transcarpathian Basin; ZB, Zărand Basin and Apuseni Mountains belonging to the main Pannonian basin system. Northern (Subvolcanic zone) and Eastern part of Transylvanian Basin: CGH, Călimani-Gurghiu-Harghita range (in the frame). Time intervals of volcanic activity for each region are given. Lower–middle crust metamorphic core complexes are outlined by blue dashed lines.

The East Carpathian fold-and-thrust belt is assumed to be finalized by oblique docking of the Tisza–Dacia block to the curved shape of the East European and Moesian blocks during Mid-Miocene times (e.g. Usztaszewski et al., 2008). The termination of outward-verging thrusting and nappe emplacement over the European foreland ended at ca. 11 Ma (Fig. 1; Mațenco & Bertotti, 2000).

There are four main petrologic groups in the Carpathian Pannonian Region (CPR), based on their variation in the SiO_2 versus Na_2O+K_2O diagram (Fig. 5): (1) calc-alkaline, (2) Na-alkalic, (3) K-alkalic and (4) ultra-potassic. All of these groups are represented on the Romanian territory. According to age, petrographic, geochemical and volcanological features, four main categories of Neogene-Quaternary volcanic activity can be distinguished: (1) Miocene felsic sub-alkaline explosive volcanism, (2) Miocene to Pleistocene intermediate sub-alkaline volcanism, (3) Pliocene K-alkalic volcanism, (4) Pliocene/Pleistocene Na-alkalic basaltic volcanism and (4) Pleistocene ultra-potassic volcanism (see Figs. 4 and 6).

Andesite-dominated sub-alkaline volcanic forms (e.g., composite volcanoes, shield volcanoes, domes and dome complexes, generated in subaerial or subaqueous conditions) occur in several discontinuous areas along the Eastern Carpathians (1) the Oaş-Gutâi segment in the Transcarpathian Basin, (2) the Toroiaga-Ţibles-Rodna-Bârgău segment, in the northern part of the Transylvanian Basin, and (3) the Călimani-Gurghiu-Harghita (CGH) segment, in the eastern part of the Transylvanian Basin (e.g., Seghedi et al., 2004a; Seghedi & Downes, 2011).

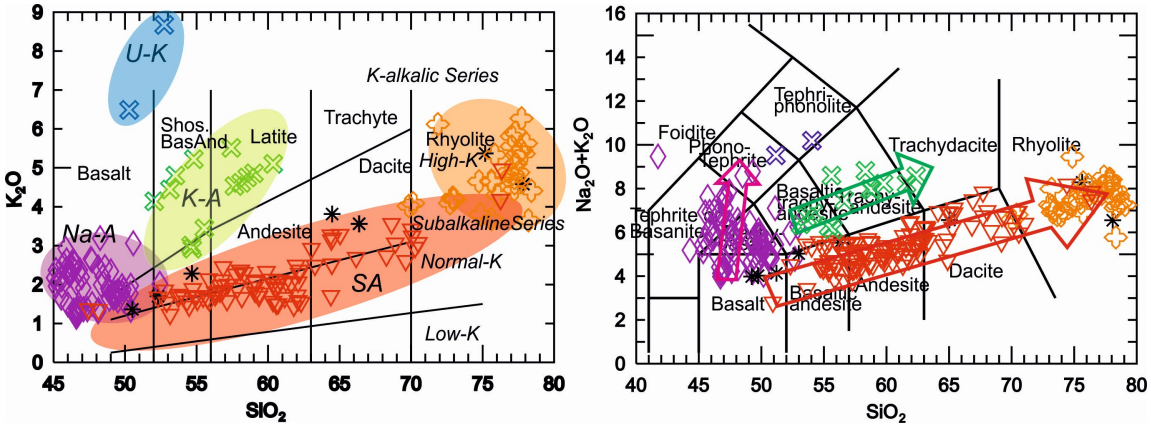

Fig. 5. SiO_2 vs. K_2O plot and SiO_2 vs. $Na_2O + K_2O$ for the volcanic rocks in the Carpathian–Pannonian region (acc. Seghedi & Downes, 2011).

Few km southwards from the South Harghita Mts. two small K-alkalic (shoshonitic) bodies occur at Bixad (Murgul Mic Hill) and Malnaş (Luget Hill) (Seghedi et al., 1987). Further ~40 km to the west, in the Perşani Mountains there is a field of basaltic volcanoes of Na-alkalic composition (e.g. Seghedi et al, 2016 and references therein).

In the southern part of the Apuseni Mts., there is a medium-size volcanic province with a subalkaline to alkaline character belonging mainly to the Zărand Basin developed in the eastern part of the Pannonian Basin. An isolated K-alkalic body at Uroi in the southern Apuseni Mts. (Roşu et al., 2004) is petrographically and geochemically similar to the East Carpathian shoshonites. The exotic Gătaia lamproite shield volcano and the Lucareţ Na-alkalic basaltic volcano are isolated in the south-western part of Romania (Downes et al., 1995; Seghedi et al., 2008; Tschegg et al., 2010).

The first time-space evolution model of the Neogene/Quaternary volcanism in the Carpathian-Pannonian region and Romania was presented by Pécskay et al. (1995a, b) and updated later by Pécskay et al. (2006). Since then, the geochronological data-base has been continuously extended with new thermo-luminescence, radiocarbon, K/Ar, $^{40}Ar/^{39}Ar$ and zircon radiometric data (Vinkler et al., 2007,Pécskay et al., 2009; Harangi et al., 2010, 2015; Seghedi et al., 2008, 2010; Szakács et al., 2012, 2015; Panaiotu et al., 2013; de Leeuw et al., 2013; Kovacs et al., 2013; Karátson et al., 2013, 2016; Fedele et al., 2016; Molnar et al., submitted).

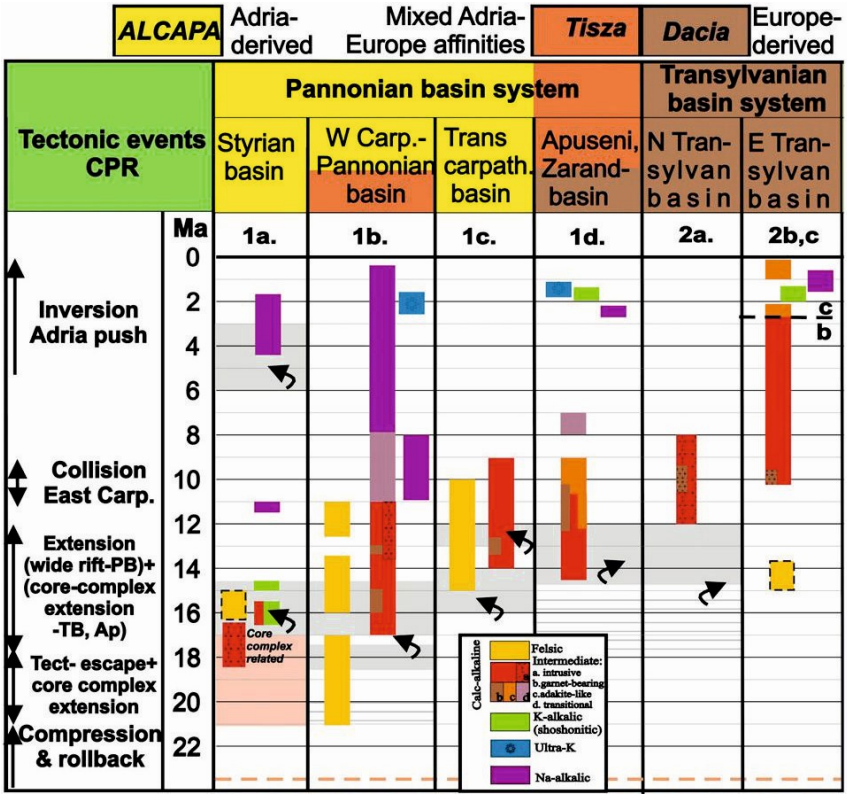

Fig. 6. Simplified spatial and temporal evolution of the of Miocene–Quaternary magmatism in the CPR, showing tectonic events and major block rotations events (arrows), (simplified after Seghedi & Downes, 2011) suggesting its relationship to the different tectonic blocks (AlCaPa, Tisza- Dacia) and sedimentary basins (Pannonian and Transylvanian systems).

Whereas the earliest Neogene volcanics in Romania are ~ 15 Ma old (Gutâi Mts. and Transylvanian Basin), most of the magmatic evolution of the area occurred between ca. 14

Ma in the Apuseni and Gutâi Mts. and less than 0.03 Main the South Harghita Mts. (Fig. 6), showing an overall eastward migration of the volcanism. The most important age progression occurring along the volcanic range characterizes the volcanic activity in the eastern part of the Transylvanian Basin, specifically in the CGH range in the 10.2-0.03 Ma interval (Fig. 6). K-alkali volcanism in the South Harghita (ca 1.4 Ma) and Apuseni Mts. (1.6 Ma) are almost coeval. The ultrapotassic lavas at Gătaia were generated at 1.3 Ma.

Products of large-scale felsic explosive volcanic activity (1) consist of up to 116 meters thick primary and reworked rhyolitic tuff sequences which are distributed over wide areas in the Transylvanian Basin and in the external Carpathian Miocene Molasse basins (Fig 4). Their origin is actually unknown, but closer-to-the-source lithologies, such as coarser volcaniclastics and ignimbrites, are encountered in Northwestern Transylvania, suggesting the western part of the Gutâi Mts. as one of the likely source areas (Szakács et al., 2012). The sub-alkaline volcanism (2) is characterized by various volcanic forms (e.g., Szakács & Seghedi, 1995, 2000; Lexa et al., 2010). The Pliocene K-alkalic volcanism (3) has generated only domes (e.g. Seghedi et al, 1987). The Pliocene/Pleistocene Na-alkalic basaltic volcanism (4) is represented by maars, scoria cones and associated lavas (e.g. Seghedi et al., 2016); the lonely ultrapotassic lavas (5) erupted from a small-sized shield volcano (e.g. Lexa et al., 2010).

5.The Călimani-Gurghiu-Harghita (CGH) volcanic range: geodynamic aspects, general features and volcanological characteristics

5.1 Geodynamic aspects

The CGH is a typical post-collisional volcanic range as it developed after the stacking of the collision-related East Carpathian nappe system (Mațenco & Bertotti, 2000). After collision and the step-by-step propagation of the CGH volcanism parallel with the orogen, the plate boundaries more or less sealed. The CGH magmatism was assumed to be associated with asthenosphere upwelling, explained by progressive break-off of an assumed Miocene subducted slab (e.g., Mason et al., 1998; Seghedi et al., 1998), as suggested by the present high heat flow coinciding exclusively with the volcanic area (Tari et al., 1999; Demetrescu et al., 2001). The along-range migration of the volcanism between ~10 and 0.03 Ma (Pécskay et al., 1995b, 2006) has been suggested to be a consequence of progressive slab detachment following an oblique subduction stage (Mason et al., 1998; Seghedi et al., 1998; Wortel & Spakman, 2000). The petrological variations observed along the CGH range (Szakács et al., 1993, Seghedi et al., 2004a, 2005a, b) have been explained by differences in foreland rheology between the East European and Scythian Platforms in the north and the southern part Moesian Platform in the south, separated by the Trotuş fault (Cloetingh et al., 2004 and references therein) (Fig. 7).

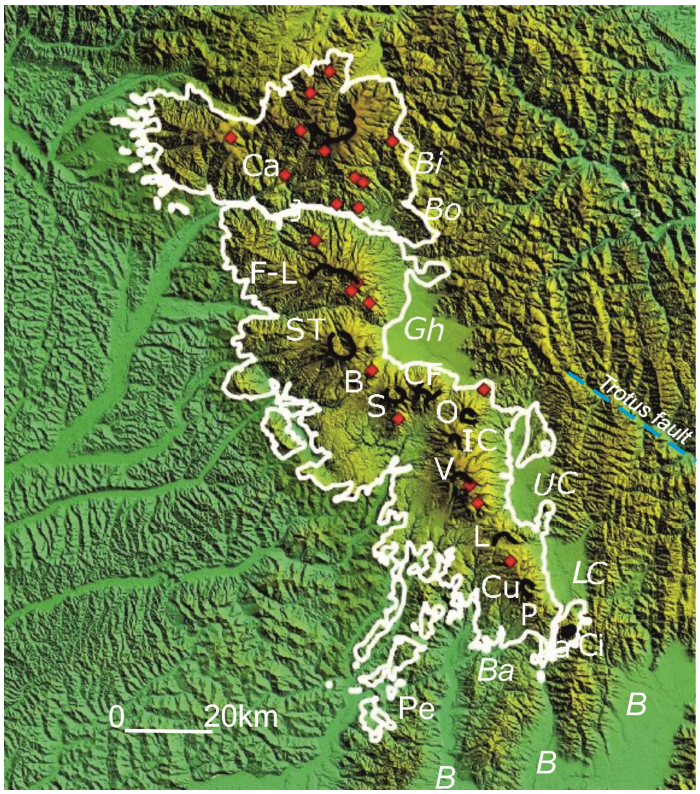

Fig. 7. 3D topographic map of CGH: Ca, Călimani; F-L, Fâncel-Lăpuşna; ST, Seaca-Tătarca; B, Borzont; S, Şumuleu; CF, Ciumani-Fierăstraie; O, Ostoroş; IC, Ivo-Cocoizaş; V, Vârghiş; L, Luci-Lazu; Cu, Cucu; P, Pilişca; Ci, Ciomadul and Pe, Perşani basaltic volcanic field; intra-mountain sedimentary basins: Bi, Bilbor; Bo, Borsec; Gh, Gheorgheni; UC, Upper Ciuc; LC, Lower Ciuc; B, Braşov; Ba, Baraolt.

In the north, the oblique collision has been accommodated by orogenic exhumation of about 6 km (Gröger et al., 2008), whereas in the south it was associated with minor uplift (Sanders et al., 1999) and foreland subsidence enabling the accumulation of up to 6 km thick Quaternary sediments in the Focșani Basin (Tărăpoancă et al., 2003).

5.2 General features

CGH is the southernmost and youngest, ca. 160 km long segment of the East Carpathian Miocene-Pleistocene volcanic range. It is geographically subdivided in four sub-segments corresponding to the Călimani, Gurghiu, North Harghita and South Harghita Mountains (Fig. 1 and 7). The volcanic history lasted ca. 10 Ma, from Pannonian to Upper Pleistocene, the earliest activity occurring in the northern part and the latest one at the southern end of the range. The CGH range is an assembly of adjacent or partially overlapping axial composite volcanoes surrounded by well-developed peripheral volcaniclastic aprons.

Most of the CGH products occur at the boundary between two major structural units;: the Eastern Carpathians and the Transylvanian Basin, being underline by a ca. 30 km thick crust (Dererova et al., 2006). The South Harghita makes an exception: unlike the other subsegments, it crosscuts the Carpathian accretionary prism lying over a ca. 40 km thick crust (e.g., Szakács et al., 1993).

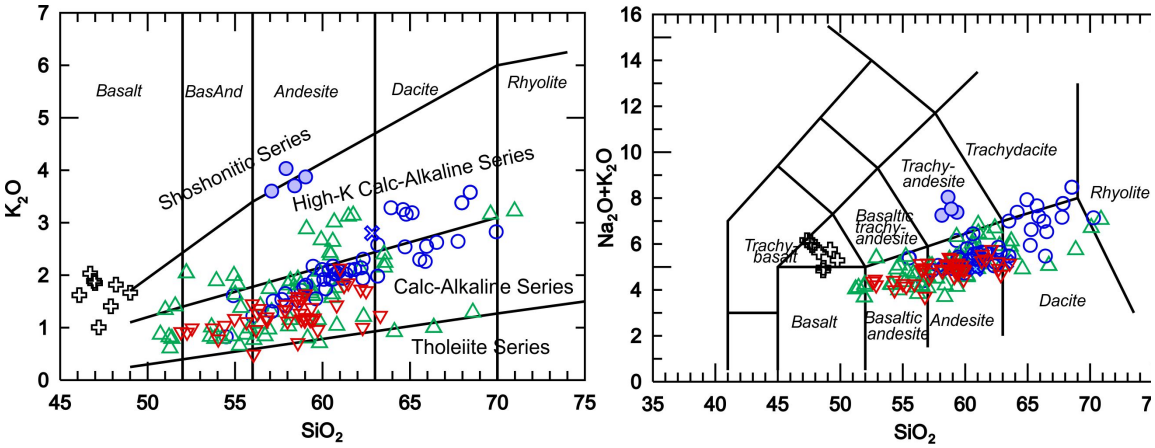

Fig. 8. SiO_2 vs. K_2O and Na_2O+K_2O plots for the CGH volcanic rocks. Symbols: green triangles, Călimani; red triangles, Gurghiu; open blue circles, Harghita; solid blue circles, K-trachytes (shoshonites); black crosses, Perşani Mts. Na-alkalic basalts.

Most rocks fall in the basaltic andesites to dacites range, andesites being the most common petro-type (two-pyroxene and two-pyroxene-hornblende-plagioclase-phyric andesites are the main varieties). Aphyric andesites and dacites, as well as biotite-bearing andesite and dacite are less voluminous. Rare garnet-bearing andesites occur in the Călimani, Gurghiu and North Harghita Mts. In the South Harghita Mts., in addition to the mentioned petro-types, there is also a large volume of amphibole-biotite-pyroxene-plagioclase-phyric dacites. A complex mineralogy, including olivine, pyroxene, amphibole, biotite and quartz characterizes the K-alkalic rocks (shoshonites) at the southern extreme of the South Harghita Mts.

In the classical K_2O vs. SiO_2 and $Na_2O + K_2O$ vs. SiO_2 diagrams (Le Bas et al., 1986; Peccerillo & Taylor, 1976)the volcanic rocks of CGH correspond to subalkaline and K-alkalic series showing typical trends from mafic (basalts) to felsic (rhyolites) (Fig. 8). The Na-alkalic basalts from the Perşani Mts. are also plotted for comparison. The rocks from the Călimani Mts. show a distinctly larger compositional dispersion than those from the Gurghiu and Harghita Mts.

Primitive mantle-normalized trace element spectra indicate many similarities among the different volcanic areas, especially the Călimani and Gurghiu Ms. (Fig. 9). Harghita Mts. rocks (especially South Harghita) are characterized by somewhat higher LILE (Rb, Ba, Th), LREE, and Sr and slightly lower HREE concentrations.

Petrogenetic studies pointed out the subduction-related mantle origin of the CGH magmas (Rădulescu, 1973; Peltz et al. 1984; Mason et al., 1995, 1996; Seghedi et al, 2004a). Minor volume lower crust-derived rocks were suggested in the Călimani Mts., exemplified by the Drăgoiasa dacite-rhyolite formation (Seghedi et al., 1995, 2005).

In the South Harghita Mts. two distinct petrochemical types, a subalkaline and a K-alkalic occur. Here the subalkaline type is geochemically different from the subalkaline magmas of the older Călimani-Gurghiu-North Harghita range by having higher Ba (1000–2000 ppm) and

Sr (1000–1600 ppm) and lower Y (5–15 ppm) and B (10–30 ppm) concentrations suggesting an adakite-like character (Mason et al., 1996, 1998; Seghedi et al., 1987; Szakács et al., 1993; Vinkler et al., 2007; Gméling et al., 2007). Seghedi et al., (2011) suggested that the adakite-like calk-alkaline volcanism is sourced in a metasomatized lithosphere heated during the horizontal asthenospheric flow around the steepening Vrancea block. For the K-alkalic (shoshonitic) magmas an upper lithospheric origin was proposed.

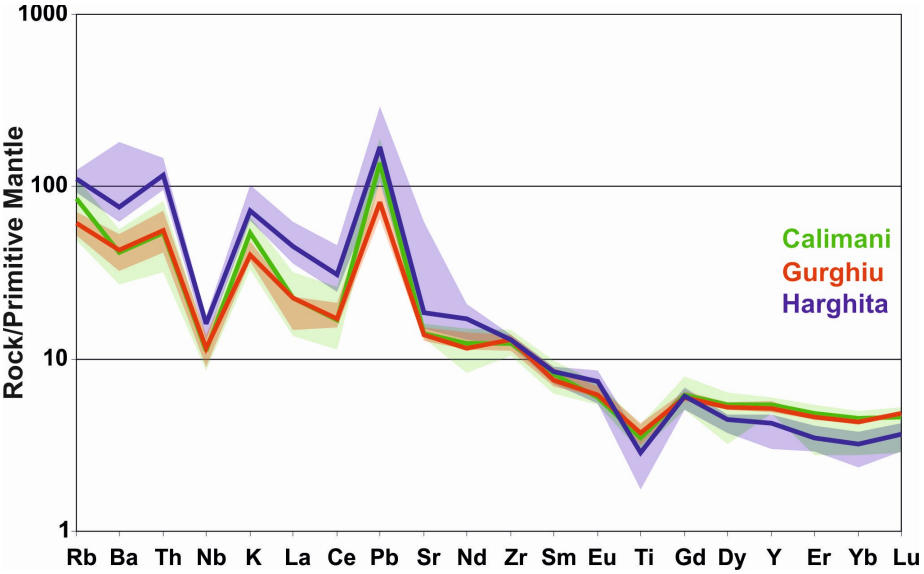

Fig. 9. Trace element spectra of the Călimani-Gurghiu-Harghita range normalized to primitive mantle values (Sun & Donough, 1989). Median values and IQR=0.25-0.75 intervals are shown for each volcanic area.

Major petrogenetic processes responsible for the observed petrographic and petrochemical features include fractional crystallization, crustal assimilation and magma mixing operating in crustal magma chambers at multiple levels (e.g., Mason et al., 1995, 1996; Seghedi et al., 2004a, 2005; Kiss et al., 2014).

The 10.2-9.3 Ma Călimani Mts. magmatism consisted of both intrusive processes (a continuation of the "subvolcanic zone" in the north) and isolated incipient volcanic activity (Pécskay et al., 1995a, 2006; Szakács & Seghedi, 1996; Seghedi et al., 2005b). It probably represents the transition from a mostly intrusive to a dominantly extrusive magmatism, and constitutes the first major event in the volcanic evolution of the CGH range (Fig. 10), and may coincide with the change in the regional tectonic regime marked by the initiation of normal and strike-slip faulting in the area (e.g. Fielitz & Seghedi, 2005). Some of the oldest volcanic rocks, such as the Drăgoiasa dacites and rhyolites occurring at the eastern periphery of the Călimani Mts. (ca. 9.3-8.7 Ma, Peltz et al., 1987; Pécskay et al., 1995a) formed in this period. Radiometric ages of some lava flows and clasts found in debris avalanche deposits belonging to the Rusca-Tihu volcano (9.3-10.2 Ma) suggest that the initiation of this volcano was roughly coeval with the end of subvolcanic intrusions (Seghedi et al., 2005b).

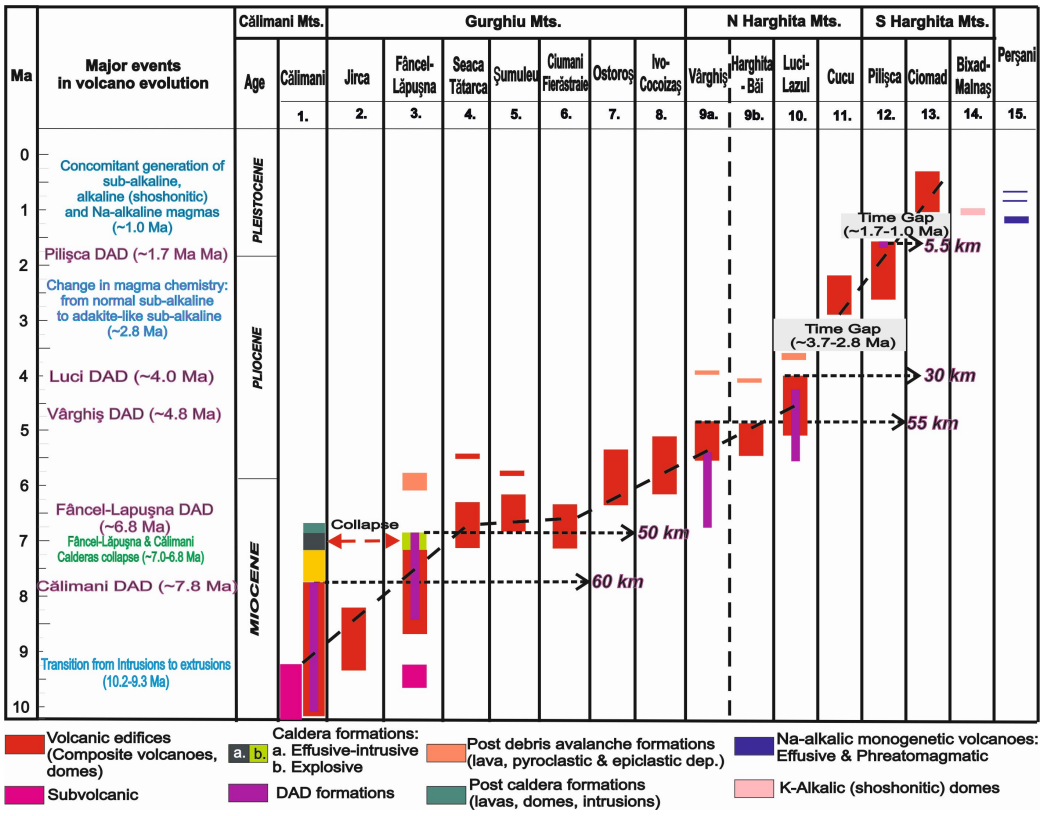

Fig. 10 Simplified time sequence of the main volcanic edifices and major events in the evolution of the Călimani-Gurghiu-Harghita range (DAD runout distances are shown by dashed arrows).

Volcanic activity continued up to 6.8 Ma in both the Călimani Mts. and the northern Gurghiu Mts. (Fâncel-Lăpuşna and Jirca volcanoes). In the rest of the Gurghiu Mts. eruptions lasted ca. 1 Ma longer than in the Călimani Mts. The latest activity in the Gurghiu Mts. overlaps with the earliest eruptions in the North Harghita Mts. where volcanism continued for ca. 2.4 Ma (6.3-3.9 Ma) (Seghedi et al., 2004b; Pécskay et al., 2006). K-Ar dating of the Vârghiş volcano and the associated Harghita-Băi volcano of the North Harghita Mts. indicate a <1 Ma-long activity (5.5-4.8 Ma) although an isolated lava flow formed later at 3.9 Ma (Pécskay et al., 2006). The K-Ar dated Rupea basaltic andesite mega-block, attributed to the Vârghiş volcano is 6.8 Ma old, suggesting a much longer duration for the volcano lifespan.

K-Ar geochronology on the Luci-Lazu volcano of the northernmost South Harghita Mts. suggest ~1 Ma duration (5.1-4.0 Ma). Following a period of waning activity of almost 1 Ma, eruptions continued in the rest of South Harghita with a distinct southward migration between ca. 3 Ma and less than 0.2 Ma (Pécskay et al., 2006). Near the southern terminus of the CGH range, the Ciomadul volcano is the youngest volcano of the Carpathian-Pannonian Region featuring dome-forming, phreatomagmatic and Plinian eruptions in the 1Ma-<0.03 Ma interval (Szakács et al., 2015). Its last eruption took place around 35-27 ka ago (Moriya et al.,

1996;Vinkler et al., 2007; Harangi et al., 2010, 2015; Karátson et al., 2013, 2016). The K-Ar dating of both shoshonite bodies yielded a controversial age interval: 2.4 Ma for Murgul Mic (Bixad) and 2.2 Ma, 1.45 Ma, and 1.3 Ma for Luget (Malnaş) (Peltz et al, 1987; Michailova et al., 1983). In contrast, the newest (U-Th)/He zircon ages of 907 ka and 942 ka obtained on the Murgul Mic and Luget rock samples, respectively, suggest much younger emplacement (Molnar et al, submitted).

5.3 Volcanological characteristics

Composite volcanoes associated with isolated domes, and dome complexes are the dominant volcanic structures in the CGH. In the Gurghiu and Harghita Mts. the composite volcanoes display typical, mostly symmetrical, cone-shape morphologies. They are aligned in a row of closely spaced, adjoining or partially overlapping edifices of which size tends to decrease toward the south (Szakács et al., 1997). Most composite volcanoes are medium-sized (with 1500 to 1000 m relative heights) and moderately eroded in the north, and better preserved toward the south. Their current central areas consist of erosion-enlarged depressions hosting unroofed shallow intrusions in some cases, most of which are associated with various hydrothermal alteration products (propylitic and argillic, as the dominant types). The oldest and largest edifices (Călimani Caldera in the Călimani Mts. and Fâncel-Lăpuşna in the Gurghiu Mts.) are the most complex by reaching the caldera stage of their evolution. Both calderas formed in the 6.8-7.0 Ma period, yet their collapse was caused by different types of volcanic activity: by effusive eruption of high-volume andesitic magma in the Călimani and by a series of Plinian eruptions in the Fâncel-Lăpuşna volcano that generated the Fâncel-Lăpuşna Volcaniclastic Formation (Szakács & Seghedi, 1996). In both cases post-caldera effusive and intrusive rocks were generated.

The cone area of the composite volcanoes (attributed to the proximal facies) consist of thick piles of basaltic-andesite and andesite lava flows sometimes associated with andesite and dacite lava domes or dome complexes; scarce interbedded pyroclastic deposits (pyroclastic flow, fall or block and ash flow types) have been also found. The southernmost Ciomadul volcano (South Harghita Mts.) is an exception as it consists entirely of a central group of extrusive domes surrounded by a number of isolated peripheral domes; here, late stage phreatomagmatic and Plinian eruptions ended the volcanic activity (Szakács et al., 2015). The Murgul Mic and Luget shoshonites form two small-size dome-like bodies near to an older andesitic dome (Murgul Mare). Whether they were emplaced as shallow intrusions or surface extrusions is still debated.

At the western side of CGH there is a largely developed peripheral ring-plane formed by adjoining and interfingered/merged volcaniclastic aprons (medial facies) (Fig. 11). Most of

the volcaniclastic formations have been identified as debris-avalanche deposits (DADs). The Rusca-Tihu DAD in the Călimani Mts. and Vârghiş DAD in North Harghita have been recognized first, and were interpreted as results of large-scale edifice-failure events occurring at their respective source volcanoes (Szakács & Seghedi, 2000). Recently, DADs were also identified at other Gurghiu and Harghita Mts. volcanoes such as Fâncel-Lăpuşna, Luci (northern part of the Luci-Lazu volcanic edifice) and Pilişca (Seghedi et al., in prep).

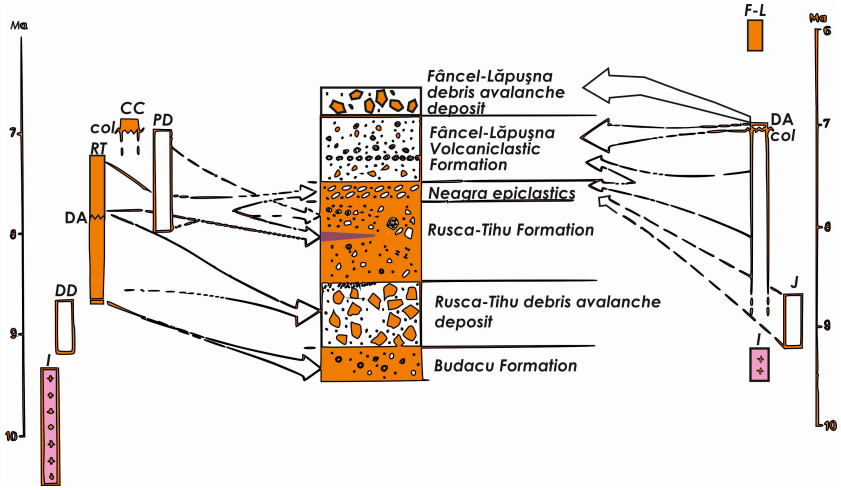

Fig. 11. Evolution of volcanism in the contact area (Mureş Valley) between the Călimani and Fâncel-Lăpuşna volcanic structures, based on the depositional record shown in the synthetic lithological column. Abbreviations: I, Old Intrusions; DD, Drăgoiasa dacites-rhyolites; RT, Rusca-Tihu Volcano; CC, Călimani Caldera volcano; PD, peripheral domes; F-L, Fâncel-Lăpuşna volcano; col, collapse and caldera forming event; DA, debris avalanche event (improved after Szakács & Seghedi, 1996).

The peripheral volcaniclastic aprons of the medial facies consist, in addition to debris avalanche breccias, of a complex lithological assemblage of mostly reworked volcanic material assembled in syn- and inter-volcanic volcaniclastic sequences (debris flow, hyperconcentrated flood flow and fluvio-lacustrine deposits and rare primary pyroclastics of both fall and flow origin). The depositional environments changed from terrestrial to subaqueous. In some places, e.g., along the Mureş Valley area between the Călimani and Gurghiu Mts., the volcaniclastic sequences are built up of material originating from roughly contemporaneously active neighboring volcanoes (Fig. 20). This area is one of the fortunate cases where the major source areas (Călimani and northern Gurghiu) display specific petrographic-petrochemical signatures allowing recognition of their individual contribution to the common volcaniclastic pile.

Results of our most recent field studies in the Călimani-Gurghiu-Harghita range are synthesized in a new simplified volcanological map realized in Qgis (Fig. 12).

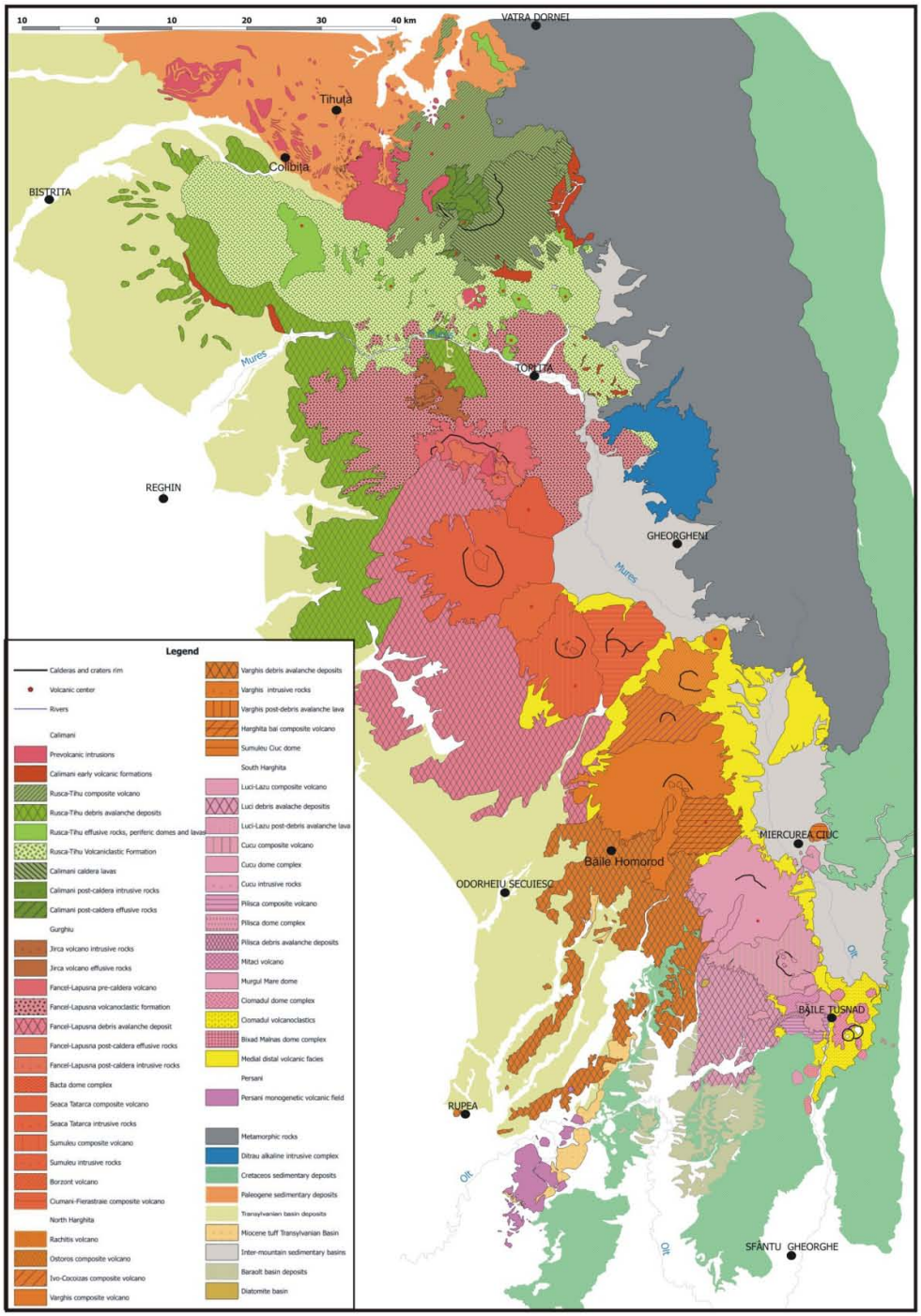

Fig. 12. Simplified volcanological map of the CGH range (acc. to Seghedi et al., in prep).

6. Daily Workshop Schedule

The Workshop fieldtrip itinerary including highlights of the daily routes and the accommodation sites are shown in Fig. 13.

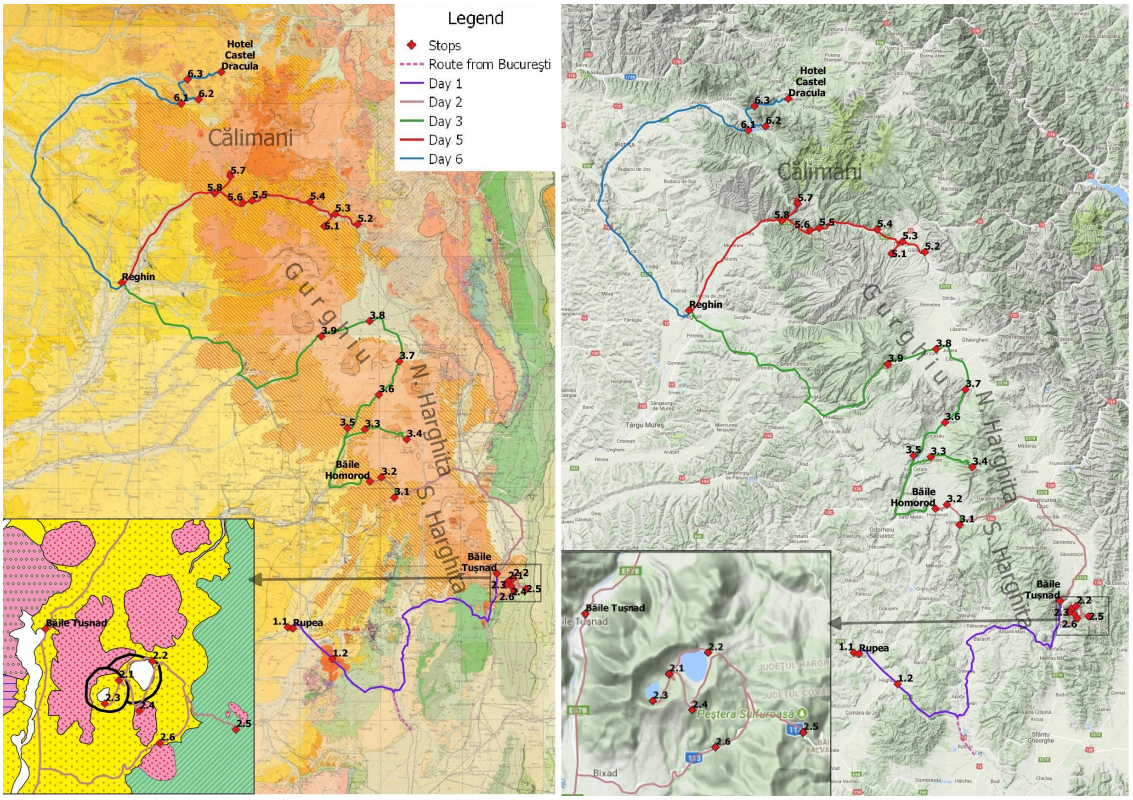

Fig 13. Workshop fieldtrip itinerary (daily driving routes with different colors) and the location of the stops. Inset: 2nd day stops in the Ciomadul volcano area.(left map after Geological map of Romania 1:200000, sheets Toplița, Odorhei, Târgu Mureș and Brașov, IGR)

Day 1 (October 8): Arrival and transfer to Băile Tușnad (Hotel O_3Zone); via Perșani Mts.

- Departure from Bucharest and Cluj-Napoca; travel to Rupea
- **Stop 1.1** Rupea Castle built on a large debris-avalanche block; box lunch
- **Stop 2.1** Quarries in the Perșani alkali basaltic volcanic field in the Bogata Valley
- Travel to Băile Tușnad; check in at Hotel O_3Zone
- Welcome speech and dinner

Day 2 (October 9): Fieldtrip in the South Harghita Mts. visiting the Ciomadul volcano and its environs

- Breakfast (Hotel O_3Zone, Băile Tușnad);
- Introduction to the Călimani-Gurghiu-Harghita volcanic range (Hotel O_3Zone conference room)

- **Stop 2.1** Ciomadul craters saddle; a short introduction to the Ciomadul volcano
- **Stop 2.2** N-Mohoș swamp outcropfeaturing explosive products of the phreatomagmatic Mohoș and the Plinian Sf. Ana craters
- **Stop 2.3** Sf. Ana crater, walking around the crater lake
- **Stop 2.4** Köves Ponk dome vista point; discussions; box lunch
- **Stop 2.5** Spectacular post-volcanic features at Bálványos
- **Stop 2.6** Debris flow and pyroclastic flow deposits of the Ciomadul volcano (roadside outcrop on the way back from Bálványos to Băile Tușnad)
- Travel to Băile Homorod via Băile Tușnad and Miercurea Ciuc; check in and dinner at Lobogó Panzió, Băile Homorod.

Day 3 (October 10): Fieldtrip in the North Harghita Mts. and southern Gurghiu Mts.

- Breakfast at Lobogó Panzió;
- **Stop3.1** Pre-debris-avalanche lavas (~5.4 Ma) at the Selters active quarry, Vârghiș Valley
- **Stop3.2** Căpâlnița vista point: a panoramic view on the Vârghiș volcano from the SW
- **Stop3.3** Block-and-ash-flow deposits of the Vârghiș volcano outcropping in the Ivo Valley
- **Stop3.4** Harghita Mădăraș ski resort area: panoramic view on the sector-collapse depression of the Vârghiș volcano; outcrop of pre-collapse lavas; box lunch
- **Stop 3.5** Debris avalanche deposits at the Zetea Dam; panoramic view on the southern part of the Gurghiu Mts.;
- **Stop 3.6** Quarry in andesite lavas belonging to the Ostoroș volcano
- **Stop 3.7** The Chilieni quarry carved in thick ponded lavas of the Ciumani-Fierăstraie volcano; panoramic view on the northernmost Harghita volcanoes, the Gheorgheni Basin and the fold-and-thrust belt of the East Carpathians
- **Stop 3.8** Vista point between Joseni and Borzont: panoramic view on the Gurghiu Mts.
- **Stop 3.9** Small quarry in Seaca-Tătarca lavas near the Bucin Pass
- Travel to Reghin via Bucin Pass-Praid-Sovata; check-in and dinner at Hotel Marion

Day 4 (October 11): Scientific session (Hotel Marion, Reghin)

- Breakfast
- Formal registration of participants
- Invited talks
- Lunch
- Oral presentations and poster session
- Discussions
- Dinner

Day 5 (October 12): Fieldtrip along the Mureș Gorges with focus on interfingering volcaniclastic sequences originating from the Călimani and Gurghiu eruption centers

- Breakfast (Hotel Marion, Reghin);

- **Stop 5.1** Toplița ski resort area; panoramic view on the Călimani Mts. and on the northernmost volcaniclastic deposits of the Fâncel-Lăpușna volcano (Gurghiu Mts.)
- **Stop 5.2** Sărmaș basalts in contact with post-debris avalanche Călimani volcaniclastic deposits
- **Stop 5.3** Reworked products of the Fâncel-Lăpușna formation (Gurghiu Mts.) near Toplița
- **Stop 5.4** Debris flow deposits of the Fâncel-Lăpușna formation at Ciobotani;
- **Stop 5.5** Primary Fâncel-Lăpușna block-and-ash-flow deposits at the Lunca Bradului bridge
- **Stop 5.6** Thick sequence of Rusca-Tihu basaltic andesite block-and-ash-flow deposits (Rusca-Tihu Formation) at Salard; box lunch
- **Stop 5.7** Thick sequence of post-debris avalanche volcaniclastics and lavas of the Rusca-Tihu formation at the Răstolița Dam
- **Stop 5.8** Debris avalanche deposit of Rusca-Tihu volcano at Răstolița (Iod road branch)
- Travel to Reghin and dinner (Hotel Marion)

Day 6 (October 13): Fieldtrip in the Northern Călimani Mts. and Bârgău Mts. area (AM) and final informal discussions (PM)

- Breakfast (Hotel Marion, Reghin);
- Travel to Colibița Dam via Bistrița-Prundu Bârgăului
- **Stop 6.1** Rusca-Tihu debris avalanche deposits near the Colibița Dam
- **Stop 6.2** The "great sill" at the Colibița quarry
- **Stop 6.3** Roadside outcrops of pre-volcanic sills intruded in flysch deposits; box lunch
- Travel to the Tihuța Pass, panoramic view of the beautiful landscape of the "Subvolcanic Zone" of the Bârgău and Țibleș Mts.; arrival to and check-in at the Hotel Dracula Castle
- Informal round-table discussions on the future activities of the IAVCEI Commission on Volcano Geology; proposals for the next VG Workshop
- Farewell dinner and "Dracula show"

Day 7 (October 14): Departure

7. Description of field stops

Day 1. Distal debris avalanche feature belonging to the Vârghis volcano (North Harghita Mts.); Perşani Mts. Na-alkalic basaltic volcanism

The location of stops is shown in Fig. 13. The volcanological map of the Perşani Mts. is shown in Fig.14.

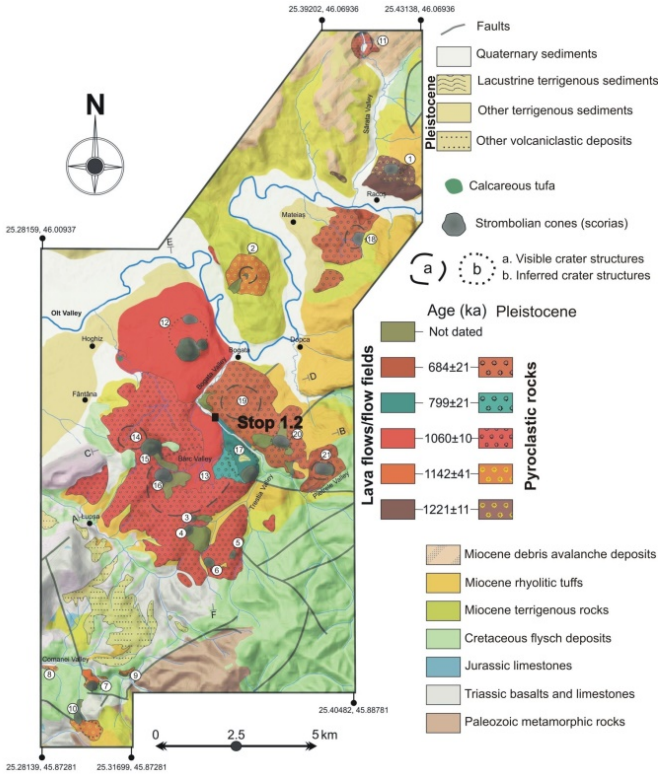

Fig. 14. Volcanological map of the Perşani Mts. volcanic field showing the location of stop 1.2 (modified after Seghedi et al, 2016)

Stop 1.1. Rupea Castle Hill.

Rupea Castle (Romanian: *Cetatea Rupea*, German: *Burg Reps*, Hungarian: *Kőhalmi vár*), located in the west of Rupea town, on a 120 m-high massive basalt (acc. to Wikipedia), is one of the oldest archaeological sites in Romania, the first signs of human settlements dating from the Paleolithic and early Neolithic. The first documentary attestation dates from 1324 when the Saxons revolted against King Charles I of Hungary and took refuge inside the citadel. According to archaeologists, the current castle was built on the ruins of a former Dacian defense fort conquered by the Romans. The name of the castle comes from Latin *rupes* meaning "stone". From the 10th century, the castle experienced a systematic expansion, so that in the 14th century it had a key strategic role, being the main linking point between Transylvania, Moldavia, and Wallachia. A popular legend in the area tells that Dacian king

Decebalus would commit suicide within the citadel, during the Second Dacian War (105–106), when the castle was known as Ramidava (Wikipedia).

Our initial research during the 1990^{s} has shown that the rocks are 6.8 Ma (K-Ar) basaltic andesites, probably sourced in the Harghita Mts. (Downes et al., 1995). László (2005) considered Rupea to be a peripheral volcanic structure. Our recent studies indicate that the Rupea castle was built on a huge, isolated debris avalanche block probably belonging to the Vârghiş DADs (see discussions in sections 3.1 and 5.2 of this Guide). Outcrops around the castle reveal several characteristics commonly found in debris avalanche blocks, such as slickensides with various orientations, petrographic heterogeneities, as well as diverse hydrothermal influences.

Stop 1.2. Perșani basalt quarries

This stop is dedicated to visiting a couple of quarries in the Perșani alkali basalt monogenetic volcanic field along the Bogata Valley. On our way to the quarries, we will spot the scoria cones of Măguricea (on the left side of the road) and Gruiu Mare (on the right).

The first quarry, located on the left bank of the Bogata Valley, is exposing a lava flow belonging to the 799 ka old tuff ring volcano named "636". The volcano debuted with a phreatomagmatic episode and finished with a lava flow that poured out of the initial edifice toward the NW (Fig 5b in Seghedi et al., 2016). The lavas show columnar joints and basal and upper clinker breccias. The lava is covered by a dm-thick soil and by deposits of the younger (684 ka), dominantly phreatomagmatic, Bogata volcano (Fig. 15). The phreatomagmatic successions involve alternating low angle bedded tuff and lapilli-tuff deposits rich in accidental lithic clasts and displaying either plane-parallel or cross-laminated bedding. Bomb sags from ballistically emplaced basement clasts in proximal facies as well as mantle xenoliths and amphibole xenocrysts are common.

The second quarry, located on the right side of the Bogata Valley, exposes a lava flow pouring out toward NW from the 1060 ka old Bârc maar volcano (~2.25 km across). The lavas are dense or slightly vesiculated, they peripherally show "sunburn" texture, and are among the richest in mantle xenoliths (up to dm-sized nodules dominated by spinel lherzolites. e.g. Vaselli et al., 1995).

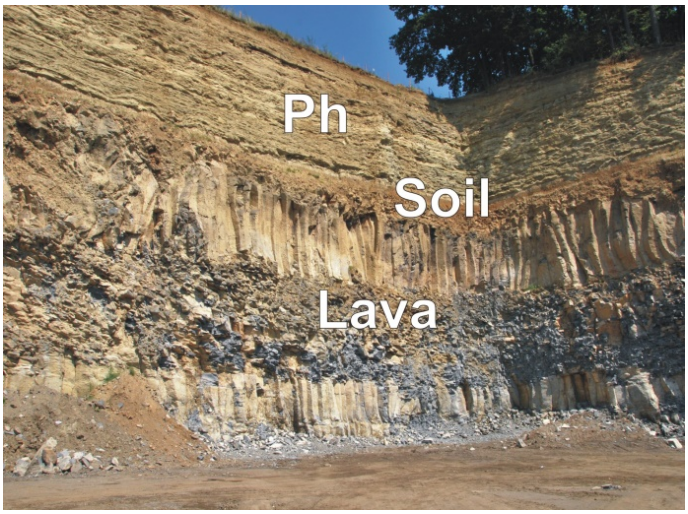

Fig 15. Basaltic lava of the "636" volcano showing columnar jointing at base and top of the flow unit and subhorizontal platy jointing in the central part, covered by soil and phreatomagmatic pyroclastic deposits of the Bogata volcano (acc. to Seghedi et al., 2016)

Day 2. Ciomadul volcano (South Harghita); post-volcanic phenomena

The day trip starts from Băile Tușnad, one of the most important and well-known tourist resorts of Romania, famous for its mineral water springs and mofette used in the cure of various diseases. Modern wellness centers, a balnear medical center, and a large number of hotels are located here to receive both tourists and people looking for health care. The country-wide known and appreciated "Tușnad" mineral water is bottled here. Băile Tușnad spa is located in-between the Pilișca volcano in the West and the Ciomadul volcano in the East, in the narrow, steep-sided North-South oriented gorges of the Olt Valley connecting the Lower Ciuc basin in the North with the Bârsa Basin (part of the Brașov Basin system) in the South.

On the way to the first stop we cross the gentle southern lower slopes of the Ciomadul volcano developed on medial facies volcaniclastic deposits (block-and-ash-flow deposits containing bread-crust blocks and debris flow deposits belonging to the dome-building stage and primary pyroclastic deposits and related debris flow deposits of the late explosive phase of volcano evolution (Szakács et al., 2015). After passing Bixad village the participants may enjoy – from the vans – a panoramic view of the volcano from the south with its higher left-side (western) part dominated by steep dome topography and its right-side (eastern) part showing the lower Mohoș crater rim with the Piscul Pietros (Köves Ponk) dome remnant as its highest point. The road continues in a long portion of forested area up to the Mohoș swamp and along its eastern margin, climbs to the crater rim at Piscul Pietros (site of Stop 2.4) and finally arrives in the saddle between the Mohoș and Sf. Ana craters (Fig. 16).

The location of the stops in the Ciomadul volcano area is displayed in Figs. 13 and 16.

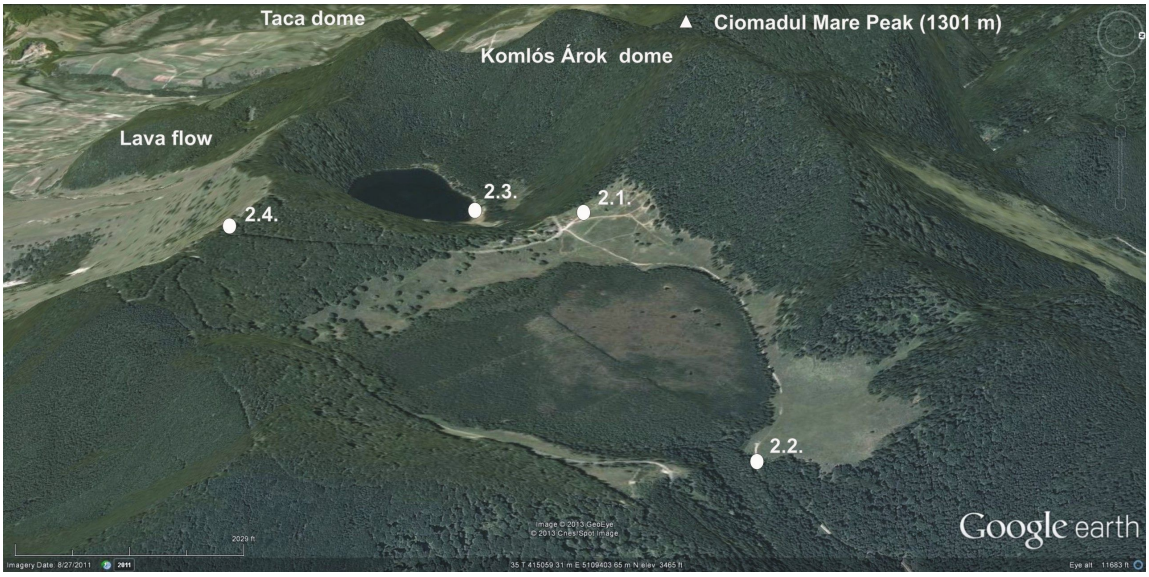

Fig. 16. Google Earth oblique view of the summit area of the Ciomadul volcano seen from the East, with its two craters hosting the Mohoş swamp (in the foreground) and the Sf. Ana Lake (behind). The road in the forest leading to the saddle between the two craters can be seen. Bixad village is in the far upper left corner of the image. Fieldtrip stop visible on the figure are marked.

Stop 2.1. Saddle between the Mohoş and Sf. Ana craters of the Ciomadul volcano. From here, the older Mohoş crater is visible in the east, whereas the younger Sf. Ana crater to the southwest is hidden. A short introduction to the structure and evolution of the Ciomadul volcano (Fig. 17) based on the information published in Szakács et al. (2015) completed with other recently published information (Harangi et al., 2015; Karátson et al., 2013, 2016) will be presented here.

The participants may observe and appreciate the fresh-looking volcanic morphology, the degree of vegetal coverage and scarcity of outcrops in the area.

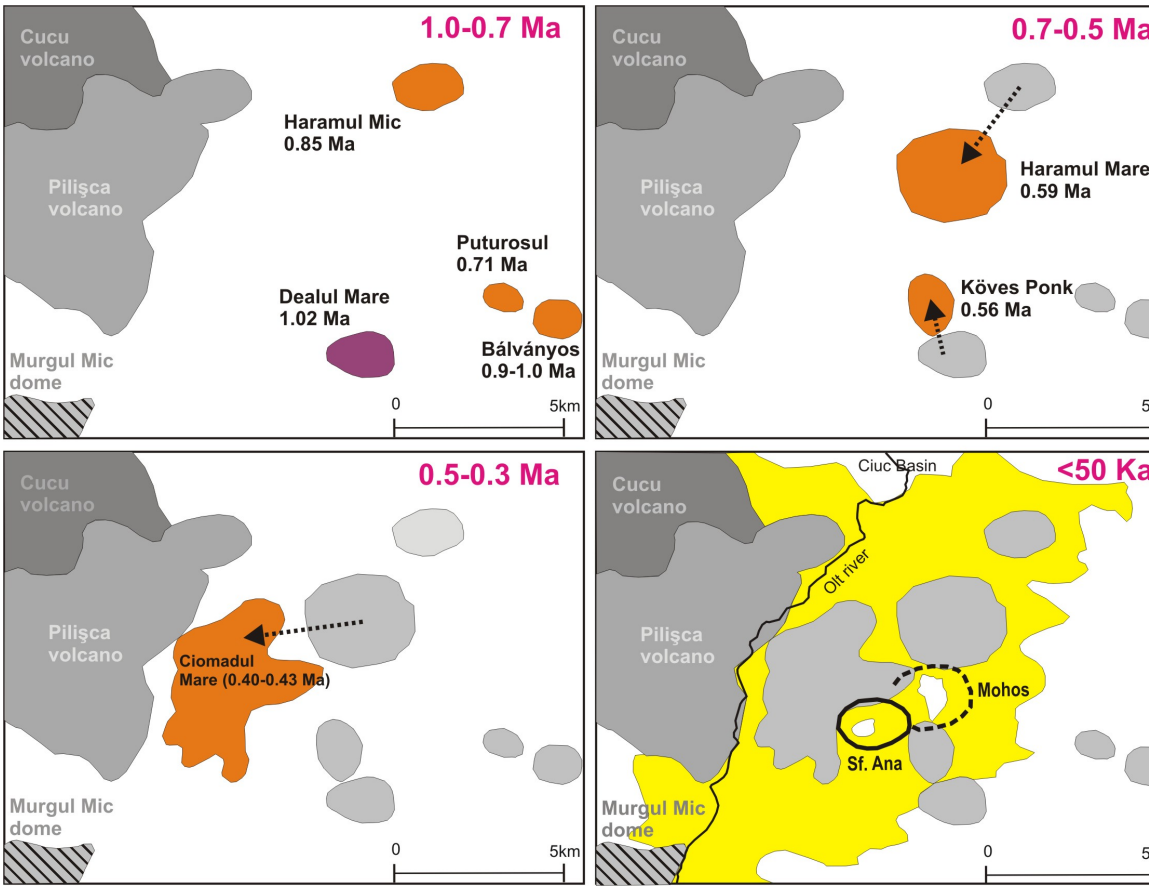

Fig. 17. Sketch of space-time evolution of the Ciomadul volcano (acc. to Szakács et al., 2015, Fig. 13). Legend: violet (andesite) and orange (dacite) show dome rock composition, and yellow stands for volcaniclastic rocks. Extinct volcanic features are shown in gray tones. Arrows show the direction of shift of volcanic activity from the previous phase.

Stop 2.2. Outcrop of pyroclastic deposits from the last two explosive eruptions of the Ciomadul volcano exposed at the north-eastern edge of the swamp where the Mohoş crater is breached to the east.

Phreatomagmatic deposits of the Mohoş eruption are covered by pumice-lapilli fall deposits of the latest Sf. Ana eruption (ca. 32 Ka). Inwards-dipping bedding of the phreatomagmatic deposits on the left-side of the outcrop indicates intra-crater setting near the crater rim (Fig 18).

The outcrop is described in more lithological details in Karátson et al. (2016) under the label MOH-VM1 and the deposits exposed here are interpreted as "pumiceous block-and-ash-flow" (upper part) and „pumiceous block-and-ash flow; subsequent (or partly coeval) py falls and py surges" (lower part) deposits (Table 1 in Karátson et al., 2016), both belonging - according to the authors - to the "Middle Plinian activity" of the "Proto-St. Ana crater".

Fig. 18. Picture of the outcrop at Stop 2.2. Note the inside-dipping (i.e., towards the right) attitude of the bedded volcaniclastic deposits in the left side of the picture in contrast to the horizontal layering in the right side.

The Mohoş crater is larger and shallower then the Sf. Ana crater (Fig. 16) and it hosts a peat-bog which is part of a nature reserve protected area. The maximum measured thickness of the peat-bog is 10.5 m. The actual swamp on top of the peat-bog hosts small free-surface lakes and a vegetation including rare protected species.

Stop 2.3. Sf. Ana crater interior and lake shore. The Sf. Ana Lake is hosted by the youngest Ciomadul crater forming a completely closed topographic depression (Fig. 16) that resulted from the most recent Plinian eruption. Its actual maximum depth is less than 7 m whereas some 100 years ago 13 m depths were measured, indicating gradual ongoing filling and eutrophication processes. There are no outcrops on the crater's heavily vegetated interior slopes. Minor CO_2 and SO_3 emanations and sulfate deposition are observed on the slopes, along the lake shore, and through the lake itself (bubbling).

There is a touristic vista point above the road descending to the lake, the only spot from which the entire lake can be spotted. An easy walk around the lake is planned if weather permits.

Stop 2.4. Piscul Pietros (Köves Ponk) vista point and outcrop on the southern rim of the Mohoş crater. Above the road and in a small abandoned and vegetation-invaded quarry below

the road, typical amphibole-biotite Ciomadul dacites are exposed. Here they represent the remnants of a dome disrupted by the phreatomagmatic eruption of the Mohoş crater. Different radiometric methods yielded different ages for the dome-forming rocks. According to the K-Ar dating (Szakács et al., 2015), the Köves Ponk dome was emplaced ca. 290 ka ago, whereas Harangi et al. (2015) reported much younger ages, of only 42.9 ka, which have been obtained by U–Th/He and U–Th geochronology methods on zircons.

From this point, a panoramic view opens towards the south. In the foreground, the Taca dome and its thick lava-flow extension as well as the lower slopes of the Ciomadul volcano in the front descending toward and beyond Bixad village, developed on medial-facies volcaniclastics, are visible. In the background the southernmost volcanic features of the Călimani-Gurghiu-Harghita range can be observed: the isolated Murgul Mare andesite dome (2.56 Ma K-Ar age), the Luget (1.3 to 2.2 Ma K-Ar age), and the Murgul Mic (2.4 Ma K-Ar age) shoshonite domes with large quarries carved in them.

Stop 2.5. Spectacular "postvolcanic" features at the site named "Apor lányok feredője" (in Hungarian, meaning "The bath of the Apor girls"). This is a spot where intense diffuse CO_2 emanations occur over a vegetation-barren elongated area percolating through the shallow water-table. Amongst the bubbling grounds, a number of smaller and larger wooden pools were reconstructed as used in old times by local people for curative purposes in the form of "feet-bath" and as "eye-water". The mineral water in these strongly bubbling pools contains native sulfur in the form of "sulfur-milk", which deposits and incrusts pool-wood and vegetation. It resulted from oxidation of H_2S, which accompanies the CO_2 as a minor component of the emanated gas. Where the CO_2 reaches the surface as a dry gas, it is termed "mofette". There are many mofettes in the area, part of them captured and arranged in so-called "gas-bath" facilities for curative purposes. One of the most famous of them – the Büdös (meaning "stinking" in Hungarian) – is hosted by an artificially enlarged natural cave formed by fumarolic alteration of the dome-forming dacite in the Puturosul Hill. The lower part of walls of the mofette is lined with yellow sulfur deposition. We may not have time to visit this mofette.

A general overview of the "postvolcanic" phenomenology in the CGH range is given by Szakács (2010). Vaselli et al. (2002) published geochemical and isotopic data on the CO_2 emanations in South Harghita. Quantitative estimates of diffuse soil CO_2 emissions in areas around the Ciomadul volcano, such as the "Apor lányok feredője", yielded values from 1.7×10^1 to 8.2×10^4 $g.m^{-2}.d^{-1}$ (Kis et al., 2017).

Stop 2.6. Roadside outcrop in Ciomadul volcaniclastic deposits of medial facies. At least three depositional units of lithoclast-rich debris-flow deposits, one on top of another from right to left in the outcrop, are unconformably covered by a pumice-bearing pyroclastic flow deposit in the left part of the exposure. The debris-flow deposits lacking pumice but including instead a number of marginally-cracked massive dacite blocks (suggesting cooling) are interpreted as belonging to the early dome-building stage of volcano evolution. The pumice-rich flow deposit hosts a large piece of charcoal at the leftmost part of the outcrop, which is dated at 29,500 ± 260 yr cal BC by radiocarbon method, and is interpreted as resulting from the last eruption of the Sf. Ana crater (Harangi et al., 2010).

Day 3. North Harghita Mts. (with focus on Vârghiș volcano) and southern Gurghiu Mts.

Starting from Băile Homorod (a small tourist resort with mineral water springs and a skiing area) we head eastwards for a few km passing Vlăhița town (south of the road, where iron ore – Fe oxides/hydroxides and carbonates – were mined and processed for centuries but exhausted in 1984) to reach the Vârghiş Valley and the first stop of the day downstream along the valley.

Stop 3.1. Pre-debris-avalanche lavas (ca 5.4 Ma) of Vârghiş volcano at the Selters quarry

Vârghiş is the largest composite volcanic edifice in the Harghita Mts. topped by the Harghita Mădăraş Peak at 1800 m a.s.l. (Fig. 19). Its proximal facies consists of thick stacks of lava flows consisting of amphibole-pyroxene andesites, pyroxene-amphibole andesites, two-pyroxene andesites, garnet-bearing andesites and aphyric andesites/dacites. The Harghita-Băi volcano is a satellite edifice located on the SSE flank of the Vârghiş edifice (Fig. 19). The medial facies of the Vârghiș volcano at its lower southern and south-western slopes is dominated by volcaniclastic deposits of debris-avalanche and debris-flow origin but a few lava tongues channelized by valleys also reach the volcano's ring-plain peripheries. One of them flew southwards along the present Vârghiş Valley. Near the spot called Selters (after the name of a group of mineral water springs) a small artisanal quarry was opened in order to exploit the andesite of the lava flow. Roadside outcrops and the active quarry expose a fresh light-grey medium-porphyric pyroxene-amphibole andesite with a very dense platy jointing system. The plates separated by the joints are only a few cm thick and easy to remove in larger pieces which are then used for paving various ground surfaces. The dense platy-jointing indicates a dynamic cooling regime of the lava flow interior controlled by intense shearing during consolidation, on a relatively gentle slope. The upper part of the lava flow is not exposed. The measured K-Ar radiometric age of the andesite lava – 5.4 Ma (Pécskay in

Seghedi et al, in preparation) – indicates that its emplacement occurred before the collapse of the Vârghiş edifice (at. ca 5 Ma, Szakács and Seghedi, 2000).

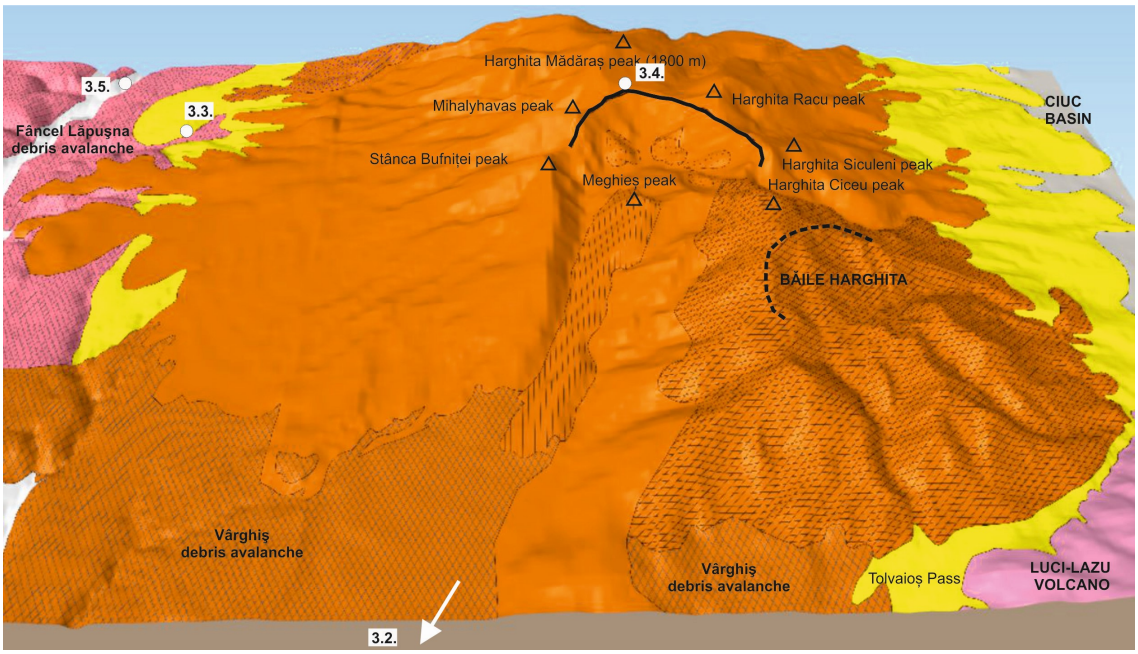

Fig. 19. 3D volcanological map of the central part of the Vârghiş volcano and its satellite volcano (Băile Harghita) with the major topographical features and the fieldtrip stops (3.2. to 3.5.) marked. Colors: central and proximal facies in red, medial facies and in yellow and Vârghiş DAD in red.

To reach the next stops, we drive back to the west, heading towards Odorheiu Secuiesc.

Stop 3.2. Căpâlnița vista point

Located on the medial-facies area of Vârghiş volcano – traditionally coined "volcanic plateau" because of its almost flat, gently dipping topography and its relatively high elevation to the Transylvanian Basin to the West – this stop offers a beautiful panoramic view on the topography of the Vârghiş volcano. The geomorphological difference between the proximal and medial facies of the volcano can be fully appreciated from here.
A particular aspect of the medial-facies ring-plain topography will be discussed here: the topographic and structural plateau surface dips inwards (i.e. towards the volcano center) instead of dipping outwards (i.e. towards the ring-plain periphery). According to Szakács and Krézsek (2006) this is the topographic response of volcano spreading processes experienced by many CGH edifices, including Vârghiş.
A lava flow front belonging to another lava tongue heading down into the volcaniclastics-dominated ring-plain is also visible in the foreground.

From Căpâlnița we first follow the road to Odorheiu Secuiesc, and descend from the "volcanic plateau" toward the Miocene sediments (pre-volcanic basement) of the

Transylvanian Basin. Then, we turn north at Bradești and head for Gheorgheni along the Târnava Mare Valley and across the Liban Pass. At Subcetate, we leave the main road for the Ivo Valley to reach Stop 3.3.

Stop 3.3. Block-and-ash-flow deposits of the Vârghiș volcano exposed in the Ivo Valley

A manmade exposure (small quarry) located at the right side of the valley offers one of the very few outcrops of Vârghiş volcano medial-facies volcaniclastics at its western peripheries. It is a coarse non-sorted matrix-rich monomictic breccia with mostly angular-subangular cm- to dm-sized andesite clasts, some of which show polygonal shapes and radial peripheral jointing. The deposit is penetrated by meters-long and dm-wide degassing pipes, which stop at the upper boundary of the deposit (Fig. 20).

Fig. 20. Picture of the Ivo Valley exposure (Stop 3.3.) showing block-and-ash-flow deposits with degassing pipes covered by a debris flow deposit

These features are diagnostic of hot-state emplacement of the volcanic material and the deposit is interpreted as resulting from a block-and-ash-flow originated at the Vârghiş volcano located east of the spot. A debris-flow depositional unit covers the block-and-ash-flow deposit in the uppermost part of the exposure.

Leaving the visited outcrop, we follow the Ivo Valley upstream, then deviate along its left-side tributary (Filio Valley) for the high-mountain Harghita Mădăraş tourist and winter-sports resort area.

Stop 3.4. Edge of the central debris-avalanche depression of the Vârghiş volcano below the Harghita Mădăraş summit

Here, from the hotel platform/parking area, we can contemplate from above the central-facies area of the Vârghiș volcano hosted by the large southward-opened horseshoe-shaped depression resulted from the large-scale ca. 5 Ma edifice-failure event and related debris avalanche. The depression below us contains exhumed shallow intrusive bodies and a large area of pervasive hydrothermal alterations (propylitic to advance-argillic type). The tailing-dump of a former exploration adit can also be seen in the depression. The depression is surrounded by a series of summits along the semicircular crest, named, from south to north – from right to left from our viewpoint – after 4 consecutive villages in the Middle and Upper Ciuc Basins: Harghita Ciceu, Harghita Siculeni, Harghita Racu and Harghita Mădăraș (hidden behind us). The effusive center of post-edifice-failure lava flows Meghieş inside the debris-avalanche depression can also be seen from here (Fig. 18).
A small-sized outcrop of dark-colored porphyric two-pyroxene pre-failure andesite lava, belonging to the proximal (cone) facies is also visible close to our viewing point.

We return to the main road connecting Odorheiu Secuiesc and Gheorgheni towns and continue upstream the Târnava Mare Valley until we arrive to the Zetea Dam.

Stop 3.5. Debris avalanche deposits at the Zetea Dam and panoramic view on the southern part of the Gurghiu Mts.

The large-scale works related to the construction of the dam opened several new exposures of volcaniclastic deposits in the area belonging to medial facies of neighboring volcanoes. Here, most of the volcaniclastics consist of debris avalanche deposits. Typical DAD features including coarse chaotic polymictic breccias, heterogeneous breccia matrix, jig-saw-fit textures of clasts, soft-sediment deformation of matrix portions can be observed in outcrops at the western end of the dam. The deposits in this area were first interpreted as parts of the Rusca-Tihu DAD originating in the Călimani Mts. (Szakács and Seghedi, 2000). The most recent detailed investigations suggest, however, that they belong to the Fâncel-Lăpuşna volcano (northern Gurghiu Mts.) (Seghedi et al., in prep.). From the dam a panoramic view is opened to the North and West including the southern sides of the Şumuleu and Ciumani-Fierăstraie volcanoes (Southern Gurghiu Mts.) whose proximal and medial facies topography can be observed.

From here, our route follows the eastern lake-contour road, then the Şicasău Valley (left-side tributary of the Târnava Mare Valley).

Stop 3.6. Quarry in andesite lavas of the Ostoroș volcano at Şicasău (time-permitting, optional)

For the sake of completeness, products of another North-Harghita volcano (Ostoroş) are intended to be observed in a quarry at the eastern side of the Şicasău Valley. The blocky-jointed porphyric pyroxene andesites belong to the volcano's proximal facies lavas.

After traversing the Liban Pass, the geographic boundary between the Gurghiu Mts. and the North Harghita Mts., and starting descending towards the Gheorgheni Basin, we stop on the roadside at the upper edge of the Chilieni andesite quarry, one of the largest of its kind in Romania.

Stop 3.7. Thick ponded lavas of the Ciumani-Fierăstraie volcano at the Chilieni quarry; panoramic view on the North Harghita volcanoes, Gheorgheni Basin, and the East Carpathians

The quarry extracts andesite for road-constructions and other technical purposes owing to its hardness, thickness (more than 80 m), and relatively good homogeneity. It is a massive grey porphyric pyroxene-amphibole andesite forming the internal part of a thick lava flow. It is rich in upper crustal xenoliths. Blocky to columnar jointing prevails. Because of its thickness, this rock body was previously interpreted (e.g. on the Voşlobeni sheet of the 1:50.000 scale map, (Peltz in Mureşan et al., 1986) as a very wide (more than 100 m!) dyke. However, the joint system seen in the quarry is inconsistent with such an interpretation and points to a thick body of lava ponded in a topographic depression. Its spatial position suggests that the lava flow originated in the nearby Ciumani-Fierăstraie volcano located to the North of the quarry and belongs to the proximal facies of that volcano.
Our stop is a frequently visited touristic vista point from which a panoramic eastward view opens over the quarry and surrounding landscape. Two of the northernmost Harghita volcanoes are visible from here: the effusive Răchitiş monogenetic shield volcano and the Ostoroş composite volcano. In the middle ground, the Quaternary flat-bottomed Gheorgheni Basin is lying below us, whereas the East Carpathian fold-and-thrust belt's Giurgeu Mts. segment can be seen in the background plan. Crystalline limestone/marble quarries belonging to those mountains can be spotted close to Voşlăbeni village in the east direction. An explanatory panel containing a brief description of the quarry and the volcanic origin of its

rocks, as well as the names of the landforms and geographic features visible from the spot can be found at the vista point terrace.

From the quarry, we continue to descend in the Gheorgheni Basin, turn north and then north-west heading for the Bucin Pass.

Stop 3.8. Panoramic view on the Gurghiu Mts. from the southern part of the Gheorgheni Basin between Joseni and Borzont

We stop at a roadside spot to contemplate the topographic features of the Gurghiu volcanoes, which from left to right are: Ciumani-Fierăstraie composite volcano, Şumuleu composite volcano (partially hidden behind Ciumani-Fierăstraie), Borzont monogenetic effusive volcano, Seaca-Tătarca shield-looking composite volcano, Bacta dome cluster, and Fâncel-Lăpuşna caldera-hosting composite volcano. The volcano morphologies are dominated by a relatively steep proximal facies topography. The medial-facies low-lying parts of the edifices are in general less developed on their eastern side than on their western side (i.e. towards the Transylvanian Basin). This asymmetry of facies distribution is due to the westward dipping basement topography, as explained in section 3.1 of this guide. In addition, we can observe the extremely poor exposure of this eastern ring-plain area.

We continue driving across the Bucin Pass separating the Seaca-Tătarca volcano (to the North) from the Şumuleu volcano (to the South) and connecting the Gheorgheni Basin with the Transylvanian Basin via Praid and Sovata.

Stop 3.9. Small quarry exposing proximal-facies Seaca-Tătarca lavas close to the Bucin Pass (time-permitting, optional)

A small roadside quarry exposes two-pyroxene andesites showing mostly blocky jointing belonging to the nearby Seaca-Tătarca volcano of which crater rim is nearby (Fig. 7). Here, the proximal lava-dominated cone facies of the two closely spaced neighboring volcanoes Seaca-Tătarca and Şumuleu meet and interact with each another. Because of the poor exposures in the area, and due to the petrographic and chemical similarities, the spatial relationships between the lavas belonging to the two volcanoes are very difficult to decipher.
Leaving the last stop of the day and crossing the Bucin Pass, we drive through Praid located on Transylvanian Basin sediments, famous for its centuries-old mine exploiting a more than 1500 m high salt diapir, and Sovata, an Europe-wide famous tourist resort and spa with a heliothermic salt lake and salt outcropping at surface. We continue our travel to Reghin by traversing a hilly landscape formed on Miocene sedimentary formations of the Transylvanian Basin.

DAY 5. Interfingering Călimani and Gurghiu Mts. medial-facies volcaniclastics along the Mureș Valley

The description of the outcrops is based on the actualized information found in the 1996 IAVCEI Workshop Guide (Szakács & Seghedi, 1996). The fieldtrip stops are shown in Fig. 21.

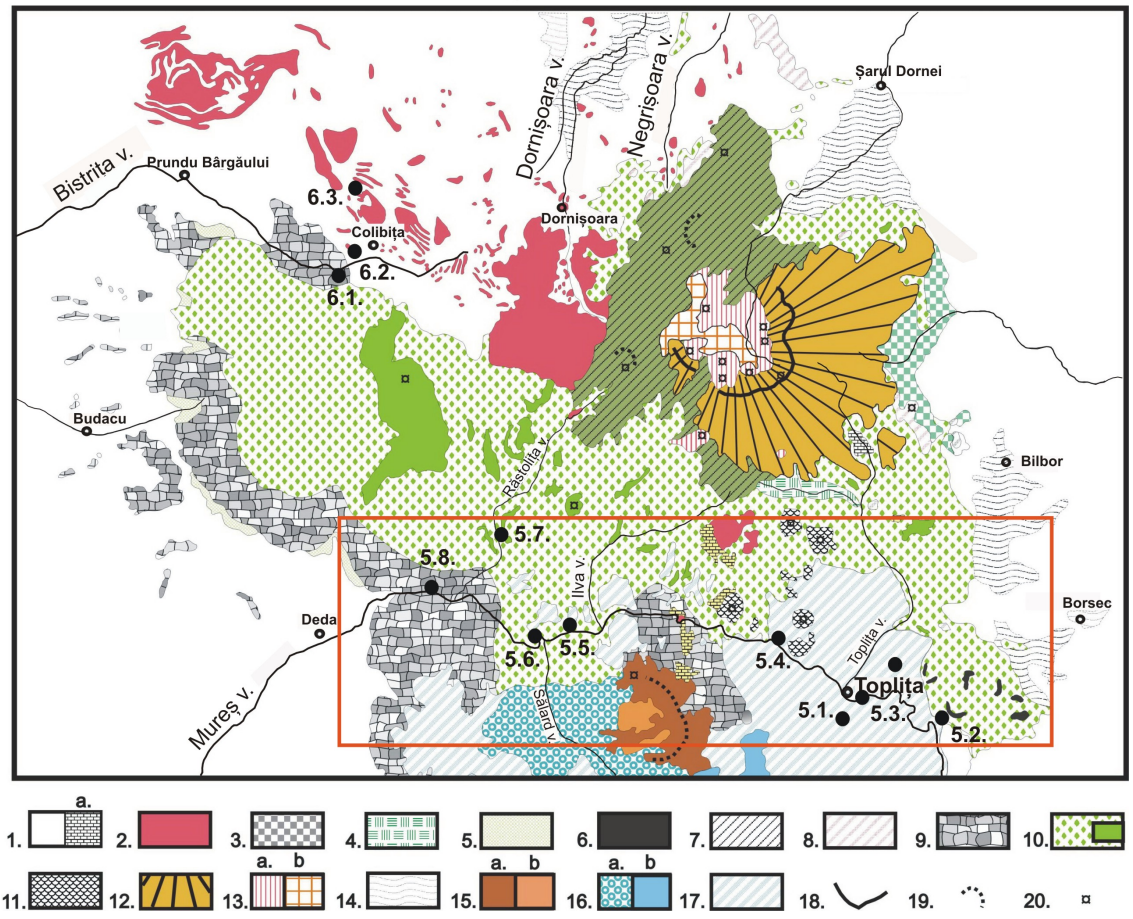

Fig. 21. Geological map of the Călimani Mts. and northern part of the Gurghiu Mts. (acc. to Seghedi et al., 2005b, with modifications) with location of fieldtrip stops of days 5 (5.1. to 5.8.) and 6 (6.1. to 6.3.). Legend 1. Prevolcanic basement a. inside the volcanic area, 2. Prevolcanic intrusions, 3. Drăgoiasa formation (dacite, rhyolite), 4. Lomaș formation (Low-K andesite and dacite), 5. Budacu formation (andesite), 6. Sărmaș basalt lavas, 7. Rusca-Tihu composite volcano (basaltic andesite, andesite), 8. Aphyric andesite lavas, 9. Rusca-Tihu debris avalanche deposit, 10. Rusca-Tihu Volcaniclastic formation (andesite, basaltic andesite), 11. Peripheral domes (andesite, dacite), 12. Călimani Caldera lava flows (andesite), 13. Post-Călimani-caldera rocks: a. monzodiorite, diorite, b. andesite, dacite, 14. Upper Miocene intra-mountain basins, 15. Jirca volcano: a. andesite, b. diorite, 16. Fâncel-Lăpușna precaldera rocks: a. volcaniclastics, b. lavas (andesite, basaltic andesite), 17. Fâncel-Lăpușna Volcaniclastic formation (andesite, dacite), 18. Morphological caldera rim, 19. Morphological crater rim, 20. Eruption center (vent).

From Reghin we follow the Mureș Valley upstream to Toplița.

Stop 5.1. Panoramic view on the Călimani Mts. from the Topliţa ski resort area

Topliţa is another well-known tourist resort and spa in Romania. It hosts thermal water springs, two thermal water pools, and a wellness center besides a popular ski and winter sports area.

The panoramic vista point, located at the upper end of the ski grounds near the Baciu Pension, offers an excellent visual perspective of the Călimani Mts. with its lower (southern) slopes, the Mureş Valley and its tributaries, the town of Topliţa and the northern lower slopes of the northern Gurghiu Mts. Fâncel-Lăpuşna volcano in the front of us (Fig. 22). A large number of volcanic features belonging to both the Călimani and Gurghiu Mts. can be seen from this point. These include the remnants of the collapsed Rusca-Tihu volcano and the Călimani caldera rim with the Pietricelul dome in the background, peripheral domes and the Sărmaş basalt occurrence area in the middle ground, and Fâncel-Lăpuşna caldera-forming eruption products and their landforms in the foreground. A short introduction to the volcanic history of the Călimani Mts. and northern Gurghiu Mts. volcanoes will be presented – based on the information published in Seghedi et al. (2004b, 2005b). Features related to medial facies interfingering of Călimani and Gurghiu volcanic products will be illustrated and explained – based on information published in Szakács and Seghedi (1996).

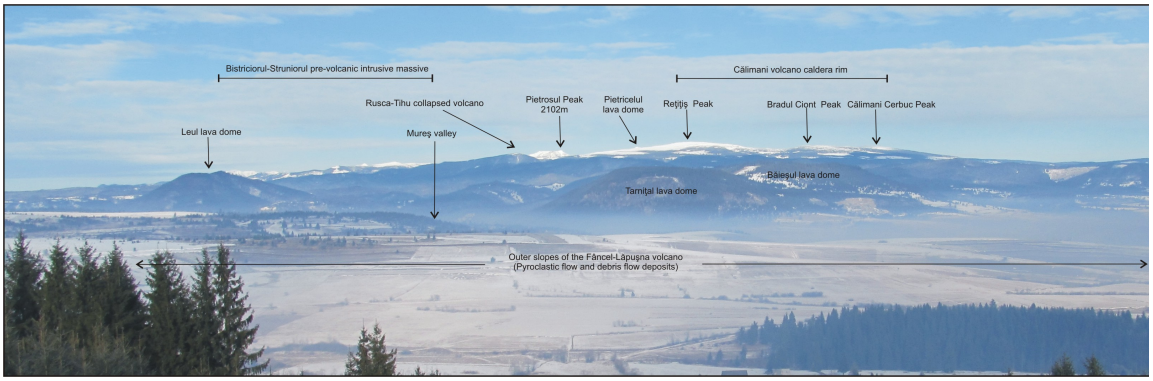

Fig. 22. General panoramic view of the Călimani Mts. and of the lower northern slopes (medial facies) of the Fâncel-Lăpuşna volcano (Gurghiu Mts.) as seen from the Topliţa ski resort area

Stop 5.2. The Sărmaş basalts, Rusca-Tihu Formation, and Fâncel-Lăpuşna Formation

An abandoned roadside quarry east of Gălauţaş locality exposes lavas of the subalkaline Sărmaş basalts. The Sărmaş basalts are the most mafic rocks besides some Rusca-Tihu volcano products, and belong to a small shield-like effusive volcano, the only monogenetic basaltic edifice in the whole CGH range. Its products are largely covered by later volcaniclastic deposits. The basaltic lavas are exposed in a number of isolated small outcrop areas where erosion removed the covering deposits, mostly along deeply incised valleys, and provide an example for mapping of a covered volcano. They appear as aphyric dark-grey colored rocks, massive to slightly porous in the lower part, and autobrecciated and clinkery towards the top. These outcrops occur within a limited area and are helpful in outlining the Sărmaş shield volcano while mapping. The 8.3-8.5 Ma K-Ar age of the Sărmaş basalts (Seghedi et al., 2005b) places them among the earliest stages of evolution of the Călimani Mts. volcanism.

A ~300 m long roadside outcrop west from the quarry reveals the contact between the Sărmaş basalt and the overlying debris-flow deposits containing mainly basaltic andesite lithoclasts derived from the Rusca-Tihu volcano. Downstream, the exposed succession is continued by polymictic debris flow deposits covering the monomictic basaltic andesite debris flow deposits. The polymictic nature of the sequence is marked by the gradual transition between a bottom dominated by basaltic andesite lithoclasts and a top rich in amphibole andesite lithoclasts sourced in the Fâncel-Lăpuşna volcano, all being hosted in a well-developed fine volcaniclastic matrix. These mixed-clast deposits pass upwards into a thick sequence of amphibole andesite dominated volcaniclastics of a mostly epiclastic origin, which contains coarser, non-bedded debris flows and finer, laminated fluvial deposits rich in pumice clasts locally concentrated in lenticular bodies. Polymictic conglomeratic epiclastics are frequent in the upper part of the exposed sequence. We interpret this sequence as belonging to the Fâncel-Lăpuşna Formation (Szakács & Seghedi, 1996) generated during and shortly after the caldera-forming eruption of the Fâncel-Lăpuşna volcano. It covers the volcaniclastic deposits of the Rusca-Tihu Formation (Szakács & Seghedi, 1996) which, in turn, covers the Sărmaş basalts.

Stop 5.3. Reworked products of the Fâncel-Lăpușna Formation (Gurghiu Mts.) at Toplița

A more than 20 m thick sequence of the Fâncel-Lăpușna Formation is discontinuously exposed on the hillside. Following a lithoclast-rich debris flow unit, numerous beds of pumice-dominated epiclastics form a well-stratified sequence at the lower part of the exposure. Low-angle cross-laminated pumiceous sandy fluvial epiclastic deposits alternate with pumice- and lithoclast-rich debris flow deposits and with pumice-rich, lithoclast-poor non-bedded volcaniclastics with prominent pumice concentration zones suggesting a primary

or slightly reworked pumice-and-ash-flow origin. Logs and opalized branch fragments can be found in the basal debris flow deposits (e.g., Szakács & Seghedi, 1996). The upper part of the hillside outcrop shows again coarse polymictic debris flow deposits variable in thickness and with lateral transition to finer-grained textures. The sequence is capped by coarse Quaternary terrace deposits including large (meter-sized) exhumed blocks dotting the hilltop.

Detailed lithological columns of the Topliţa hillside Fâncel-Lăpuşna Formation volcaniclastic sequence can be found in Szakács and Seghedi (1996, Fig. 22).

A beautiful 360° panoramic view can be enjoyed from the flat hilltop. The Fâncel-Lăpuşna volcanic edifice dominates the south, but its gently sloping medial-facies topography extends far northwards across the Mureş valley in a topographic depression. Geomorphological features of the southern Călimani Mts. can be observed in the west.

Stop 5.4. Debris flow deposits of the Fâncel-Lăpuşna Formation at Ciobotani

A sequence of lithoclast-dominated polymictic debris-flow units are exposed at the confluence of the Mureş Valley with Valea Pietrii tributary. Local channeling features and lenses of stream-flow deposits can be observed within the pile of epiclastic depositional units. The boundary between debris flow units is diffuse in places making difficult to define individual depositional entities. Lateral variability in clast size and of clast-matrix ratio is characteristic for most depositional units. A meters-sized lump of reworked sandy tuff resembles a large block engulfed in one of the debris flow units. Marginally cracked lithic blocks are also found. The amphibole andesite composition of most lithic clasts and the presence of pumice clasts, concentrated at certain levels, indicate that the volcanic material of this sequence originated from the Fâncel-Lăpuşna volcano and it belongs to the Fâncel-Lăpuşna Formation.

Stop 5.5. Pyroclastic pumice-and-ash-flow deposits of the Fâncel-Lăpuşna Formation at Lunca Bradului

Two pumice-bearing pyroclastic flow units can be identified in the outcrop. The lower one, with its upper 3 m exposed, is pinkish in color suggesting thermal oxidation, and displays normal grading of the lithics and reverse grading of the pumice clasts. The overlying unit is ca. 11 m thick, massive, grey-colored, excepting for its thermally oxidized pinkish uppermost 1.5 m, and is capped by a fine white ash horizon of ca. 10 cm. Here, too, the lithic clasts show reverse grading. The pyroclastic deposits are covered by a flow unit of which basal 50 cm are exposed in the top of the outcrop.

Stop 5.6. Thick sequence of Rusca-Tihu basaltic andesite block-and-ash-flow deposits of the Rusca-Tihu Formation at Sălard

Over 50 m high spectacular rock cliffs in the extremely steep northern valley-side expose a thick sequence of meters-thick depositional units of medium to coarse monomictic matrix-supported breccias, frequently with undulated erosional basal contacts and finer tops. Almost all lithic blocks are dark-colored basaltic andesites, many of them pyroxene-phyric, a characteristic feature of the Rusca-Tihu volcano products. In the interior of many of the depositional units, the lithic clasts and the matrix are sintered together lending the deposit a hard-rock appearance. The units frequently show rough normal grading of the lithic clasts. Several depositional units host mostly sub-horizontal, meters-long and decimeters-diameter tree-log holes (named "tree-caves" by speleologists). The sequence is interpreted as a succession of block-and-ash-flow deposits belonging to the Rusca-Tihu Formation generated by the post-edifice failure (i.e. post-debris avalanche) activity of the Rusca-Tihu volcano in the Călimani Mts.

Stop 5.7. Thick sequence of post-debris-avalanche Rusca-Tihu formation volcaniclastics and lavas at the Răstolița Dam

Dam construction works exposed a ca. 200 m thick section of the Rusca-Tihu Formation along a serpentine road. This is the thickest continuous exposure of volcanic formations in the whole CGH range. It allows to study and better understand the internal structure of the medial-facies of composite volcanoes in the CGH range and, possibly, elsewhere.

The description below is an updated interpretation of the exposure, presented in Szakács and Seghedi (1996, fig. 26).

The exposed pile of volcanic rocks includes phreatomagmatic fall deposits, pyroclastic flow deposits, epiclastic deposits, and lavas. At the lower part of the exposure, an erosional unconformity surface steeply dipping at the very base of the outcrop separates well-bedded pyroclastic deposits in the bottom and a sequence of coarse matrix-supported breccias of debris flow and of block-and-ash-flow origin in the top (Fig. 23). Since the unconformable erosional surface is highly irregular, with portions subparallel to the exposed surface, the spatial relationships between the phreatomagmatic sequence below and the coarse breccias sequence above repeat several times as we are climbing upwards along the serpentine road, revealing various aspects of the contact, from steep angular unconformities to flat near-conformities.

Fig. 23. Unconformity separating bedded phreatomagmatic deposits (below) and debris-flow deposits (above) at the base of the Răstolița Dam exposure

Pumice-rich and pumice-poor levels alternate in the lower sequence. The pumice-rich parts of the sequence contain pumice lapilli levels of probably fall origin, and matrix-supported levels of probably pyroclastic flow origin. The juvenile component of the pumice-poor phreatomagmatic parts of the sequence is represented by rare dark-colored basaltic andesite clasts, sometimes with cauliflower-like shapes (Fig. 24b). Impact sags with or without massive basaltic andesite blocks within them are often visible (Fig. 24a).

The upper sequence, above the unconformity is composed of meters-thick matrix-supported breccias units often with erosional bases resembling the block-and-ash-flow units in the Mureş Valley. However, parts of the breccias are epiclastic in origin, with a channelized base and agglomeration of coarse lithic clasts in the channels. Breccia depositional units of debris flow origin are more frequent in the upper part of the sequence.

Fig. 24. a. Impact sag in subhorizontal phreatomagmatic deposits; b. Juvenile basaltic andesite clast in phreatomagmatic deposits at the Răstolița Dam exposure

The volcaniclastic pile described above is topped by a 30-35 m thick pyroxene andesite lava flow with autoclastic breccias at the base and on the top and platy jointing in the middle. The debris flow deposits just below the lava are thermally altered (to brick-red) (Fig. 25). Another phreatomagmatic sequence with debris flow intercalations overlies the lavas as seen in the uppermost part of the exposure. A 4 m thick massive silt-mudstone bed with silicified plant fragments and curved vertical cracks can also be observed in this sequence.

Fig. 25. Contact between andesite lava flow (above) and thermally influenced (pinkish) matrix-supported debris flow deposits (below) at the upper part of the Răstolița dam exposure

This thick exposure illustrate the complicated internal architecture of the medial facies part of an andesitic composite volcano, mostly composed of volcaniclastic deposits but also containing far-reaching lava flows. The volumetric contribution of the lava flows in the medial-facies lithology is less than 10%.

If the whole sequence is attributed to the post-debris avalanche Rusca-Tihu Formation, then it can be subdivided in at least four different members. Because the uniqueness of the exposure, no correlation is possible with parts of the same Formation recognized in small outcrops elsewhere, excepting for the lava flow member of the formation correlated across the Răstolița Valley (see Fig. 21).

Stop 5.8. Debris avalanche deposit of the Rusca-Tihu volcano at Răstolița (Iod road branch) (time permitting, optional)

Typical DAD features can be observed at this roadside outcrop including heterogeneous chaotic breccia, matrix heterogeneities, adjoining irregular monomictic and polymictic breccia portions, jig-saw fit texture of cracked and slightly dispersed lithoclasts, lack of bedding, large thickness, and unsorted clasts. The characteristic presence of pyroxene-phyric basaltic andesite clasts is the diagnostic feature for the origin of the DAD in the Rusca-Tihu volcano. Internal shear zones and fractures in the deposit suggest emplacement-related deformation of the huge inertial body of the avalanche moving by a plug-flow mechanism. Measuring shear-zone directions is a possible tool of determining flow direction, potentially pointing towards the source.

Day 6. Rusca-Tihu debris avalanche deposits and pre-volcanic intrusions

Our journey from Reghin to the Colibiţa Dam follows the road to Bistrița, and then toward Prundu Bârgăului. After leaving Bistrița, we arrive to the boundary between the Bârgău and Călimani Mts. On the left we will observe the impressive high-mountain morphology of the Heniu Hill, one of the largest eroded intrusive laccolithes surrounded by a plethora of sills and dykes of the Bârgău Mts. (Fig. 21). At Prundu Bârgăului, our trip will leave the main road toward the Colibiţa artificial lake up to its dam system.

Stop 6.1. Rusca-Tihu debris avalanche deposits

The first stop of the day targets large outcrops opened by the dam system in the debris avalanche deposits of the Rusca-Tihu volcano belonging to an avalanche lobe directed to the west. The deposits are represented by massive breccia dominated by basaltic andesites and are showing a heterogeneous matrix as well as jig-saw-fit textures of the clasts. The unusual aspect of this debris avalanche is related to the presence of several dykes of pyroxene-amphibole andesitic composition. The 1-5 m wide, mostly vertical dykes are strongly disturbed along their length (Fig. 26). The dominant vertical dyke position suggests that the main plug-type movement of the debris avalanche involved sliding and moving around a vertical axis rather than rolling.

Fig. 26. Debris avalanche deposit including a dyke at the Colibiţa Dam.

Stop 6.2. We continue the trip along the northern side of the Colibiţa Lake up to a large active quarry that opens one of the thickest sills of the Bârgău Mts.

Fig. 27. Large sill at the northern side of the Colibiţa Lake (upper part of the exposure where it was heavily quarried) in contact with sub-horizontal sedimentary deposits below it.

The more than 50 m thick sill pierces a sequence of the so-called Paleogene Trans-Carpathian Flysch consisting of dm-thick sandstone and marl strata in a subhorizontal position (Fig. 27). The only obvious contact feature is a sub-metric hornfels zone discontinuously affecting the host sedimentary rocks.

On the other side of the lake, volcanic and volcaniclastic deposits of the Călimani Mts., represented by Rusca Tihu debris avalanche and volcaniclastic formations are exposed.

Here we turn back and follow a road to the main road between Bistriţa and Piatra Fântânele, traversing Paleogene sediments penetrated by sills and dykes up to our last destination

Stop 6.3. Sill in Paleogene sediments in a roadside outcrop at the exit of Bistrița Bârgăului

At our last stop, we are going to visit a roadside outcrop of a sill system intruded in Paleogene flysch deposits (Fig. 28). The sills are connected to a laccolite intrusion at depth. The contacts are sharp and clearly follow the sediment bedding, rarely cutting it. An obvious cooling joint system is observable perpendicular to the sedimentary stratification. The magmatic rocks are andesites and belong to the Low-K group (Fedele et al., 2016).

Fig. 28. Sill at Valea Străjii showing perpendicular cooling jointing against sub-horizontal bedding of the host sedimentary beds above.

We continue our journey along the western side of the Tihuța Pass while enjoying the beautiful landscape of the "Subvolcanic Zone" of the Bârgău Mts., resulted from the longstanding (since ~9 Ma) differential erosion of the more resistant intrusive rocks and their softer sedimentary host. We will finally arrive and check-in at the Hotel Dracula Castle, itself located on the top of a small, shallow intrusive body unroofed by erosion.

Acknowledgments

We wish to thank Antoneta Seghedi, Angela Neață, Crișan Demetrescu and Marian Munteanu for their support. We also thank the support of PN-II-IDPCE-2012-4-0137 grant of the Ministry of Education and Scientific Research, CNCS-UEFISCDI during the last years field work**.**

References

Branca, S., Coltelli, M., Groppelli, G., 2011. Geological evolution of a complex basaltic volcano: Mount Etna, Italy. Ital.J.Geosci. (Boll.Soc.Geol.It.), Vol. 130, No. 3 (2011), pp. 306-317.

Cloetingh, S.A.P.L., Burov, E., Maţenco, L., Toussaint, G., Bertotti, G., Andriessen, P.A.M., Wortel, R., Spakman, W., 2004. Thermo-mechanical controls on the mode of continental collision in the SE Carpathians (Romania). Earth and Planet. Sci. Lett. 218, 57–76.

Csontos, L., 1995. Tertiary tectonic evolution of the Intra-Carpathian area: a review. Acta Vulcanologica 7, 1–13.

de Leeuw, A., Filipescu, S., Maţenco, L., Krijgsman W., Kuiper, K., Stoica M., 2013. Paleomagnetic and chronostratigraphic constraints on the Middle to Late Miocene evolution of the Transylvanian Basin (Romania): Implications for Central Paratethys stratigraphy and emplacement of the Tisza–Dacia plate. Global and Planetary Change 103, 82–98

Demetrescu, C., Nielsen, S.B., Enea, M., Şerban, D.Z., Polonic, G., Andreescu, M., Pop, A., Balling, N., 2001. Lithosphere thermal structure and evolution of the Transylvanian Depression — insights from new geothermal measurements and modelling results. Physics of the Earth and Planetary Interiors 126, 249–267.

Davidson, J. and Da Silva, S., 2000. Composite volcanoes. In Sigurdsson H., Houghton B.F., McNutt S.R., Rymer H. and Stix J. eds. Encyclopedia of Volcanoes. Acedemkic Press, San Diego, p. 663-681.

Downes, H., Seghedi I., Szakács, A., Dobosi G., James, D.E., Vaselli O., Rigby, I.J., Ingram, J.A., Rex, D., Pécskay Z., 1995**.** Petrology and geochemistry of Late Tertiary/ Quaternary mafic alkaline volcanism in Romania. Lithos, 35, 65-81.

Fedele, L., Seghedi, I., Chung, S-L., Laiena, F., Lin, Te-H., Morra, V. Lustrino, M., 2016. Post-collisional magmatism in the Late Miocene Rodna-Bârgău district (East Carpathians, Romania): geochemical constraints and petrogenetic models. Lithos266–267, 367–382.

Fielitz, W. and Seghedi, I., 2005. Late Miocene–Quaternary volcanism, tectonics and drainage system evolution in the East Carpathians, Romania. Tectonophysics 410, 111–136.

Fodor, L., Csontos, L., Bada, G., Györfy, I., Benkovics, L., 1999. Tertiary tectonic evolution of the Pannonian Basin system and neighboring orogens: a new synthesis of paleostress data. Geological Society London Special Publications 156, 295–334.

Gméling, K., Kasztovszky, Z., Szentmiklósi, L., Révay, Z., Harangi, S., 2007. Boron concentration measurements by prompt gamma activation analysis: application on Miocene–Quaternary volcanics of the Carpathian–Pannonian Region. Journal of Radioanalytical and Nuclear Chemistry 271, 397–403.

Gröger, H.R., Fugenschuh, B., Tischler, M., Schmid, S.M., Foeken, J.P.T., 2008. Tertiary cooling and exhumation history in the Maramures area (internal eastern Carpathians, northernRomania): thermochronology and structural data. Geological Society London Special Publications 298, 169–195.

Harangi, S., 2001. Neogene to Quaternary volcanism of the Carpathian-Pannonian Region – A review, Acta Geologica Hungarica, 44(2-3), 223-258.

Harangi, S., Downes, H., Seghedi, I., 2006. Tertiary–Quaternary subduction processes and related magmatism in Europe. In: Gee, D.G., Stephenson, R.A. (Eds.), European Lithosphere Dynamics. Geological Society London Memoirs, 32, pp. 167–190.

Harangi, S., and Lenkey L., 2007. Genesis of the Neogene to Quaternary volcanism in the Carpathian-Pannonian region: Role of subduction, extension, and mantle plume, in Special Paper 418: Cenozoic Volcanism in the Mediterranean Area, edited by L. Beccaluva, G. Bianchini and M. Wilson, pp. 67-92.

Harangi, S., Molnár, M., Vinkler, A.P., Kiss, B., Jull, A.J.T., Leonard, A.E., 2010. Radiocarbon dating of the last volcanic eruptions of Ciomadul volcano, Southeast Carpathians, eastern–central Europe. Radiocarbon 52, 1498–1507.

Harangi, S., Lukács, R., Schmitt, A.K., Dunkl, I., Molnár, K., Kiss, B., Seghedi, I., Novothny, Á., Molnár, B., 2015. Constraints on the timing of Quaternary volcanism and duration of magma residence at Ciomadul volcano, east–central Europe, from combined U–Th/ He and U–Th zircon geochronology. J. Volcanol. Geotherm. Res. 301, 66–80.

Horváth, F., Bada, G., Szafián, P., Tari, G., Ádám. A., 2006. Formation and deformation of the Pannonian Basin: constraints from observational data, in European Lithosphere Dynamics, edited by D. G. Gee and R. Stephenson, , The Geol. Soc.of London Memoirs, pp. 191-206.

Karátson, D., Telbisz, T., Harangi, S., Magyari, E., Dunkl, I., Kiss, B., Jánosi, C., Veres, D., Braun, M., Fodor, E., Biró, T., Kósik, S., von Eynatten, H., Lin, D., 2013. Morphometrical and geochronological constraints on the youngest eruptive activity in East-Central Europe at the Ciomadul (Csomád) lava dome complex, East Carpathians. J. Volcanol. Geotherm. Res. 255, 43–56.

Karátson, D., Wulf S., Veres D., Magyari E.K.,Gertisser R., Timar-Gabor A., Novothny Á., Telbisz, T., Z. Szalai Z., Anechitei-Deacu V., Appelt O., Bormann M., Jánosi C., K. Hubay K., Schäbitz F., 2016. The latest explosive eruptions of Ciomadul (Csomád) volcano, East Carpathians — A tephrostratigraphic approach for the 51–29 ka BP time interval. J. Volcanol. Geotherm. Res. 319, 29–51

Kiss, B., Harangi, S., Ntaflos, T., Mason, P.R.D., Pál-Molnár, E., 2014. Amphibole perspective to unravel pre-eruptive processes and conditions in volcanic plumbing systems beneath intermediate arc volcanoes: a case study from Ciomadul volcano (SE Carpathians). Contrib. Mineral. Petrol. 167, 986. http://dx.doi.org/10.1007/s00410-014-0986-6.

Kis, B. M., Ionescu, A., Cardellini, C., Harangi S., Baciu, C., Caracusi, A., Vivieros, F., 2017. Quantification of carbon dioxide emissions of Ciomadul, the youngest volcano of the Carpathian-Pannonian Region (Eastern-Central Europe, Romania). Journal of Volcanology and Geothermal Research, 341, 119–130.

Konečný, V., Kováč, M., Lexa, J., Šefara, J., 2002. Neogene evolution of the Carpatho-Pannonian region: an interplay of subduction and back-arc diapiric uprise in the mantle. EGS Special Publication Series 1, 165–194.

Kovács, I., and Szabó, C., 2008. Middle Miocene volcanism in the vicinity of the Middle Hungarian zone: Evidence for an inherited enriched mantle source, Journal of Geodynamics, 45(1), 1-17.

László A., 2005. The post-Late Pontian paleogeographic evolution of the south Harghita Mountains area and adjacent basins. Studia Universitas Babeş-Bolyai 50, 27-40.

LeBas, M.J., LeMaitre, R.W., Streckeisen, A., Zanettin, B., 1986. A chemical classification of volcanic rocks based on the total alkali silica diagram. Journal of Petrology 27, 745–750.

Lexa, J., Seghedi, I., Németh, K., Szakács, A., Konečný, V., Pécskay, Z., Fülöp, A., Kovacs, M., 2010. Neogene–Quaternary volcanic forms in the Carpathian–Pannonian Region: a review. Central European Journal of Geosciences 2 (3), 207–270.

Mason, P., Downes, H., Seghedi, I., Szakács, A., Thirlwall, M.F., 1995. Low-pressure evolution of magmas from the Călimani, Gurghiu and Harghita Mountains. Acta Vulcanologica 7, 43–53.

Mason, P., Downes, H., Thirlwall, M.F., Seghedi, I., Szakács, A., Lowry, D., Mattey, D., 1996. Crustal assimilation as a major petrogenetic process in the East Carpathian Neogene and Quaternary continental margin arc. Romania. J. Petrology 37, 927–959.

Mason, P.R.D., Seghedi, I., Szakács, A., Downes, H., 1998. Magmatic constraints on geodynamic models of subduction in the Eastern Carpathians, Romania. Tectonophysics 297, 157–176.

Márton, E., Kuhlemann, J., Frisch, W., Dunkl, I., 2000. Miocene rotations in the Eastern Alps—palaeomagnetic results from intramontane basin sediments. Tectonophysics 323, 163–182.

Márton, E., Fodor, L., 2003. Tertiary paleomagnetic results and structural analysis from the Transdanubian Range (Hungary): rotational desintegration of the Alcapa unit. Tectonophysics 363, 201–224.

Maţenco, L. and Bertotti, G., 2000. Tertiary tectonic evolution of the external East Carpathians (Romania). Tectonophysics 316, 255–286.

Michailova, N., Glevasskaya, A, Tsykora, V., Neştianu, T., Romanescu, D., 1983. New paleomagnetic data for the Calimani Gurghiu Harghita Mountains in the Romanian Carpathians. An. lnst. Geol. Geofiz., LXIII, 101-113.

Molnár, K., Lukács R., Harangi, S., Dunkl, I., Schmitd, A. K., Kiss, B., Garamhegyi, T., Seghedi, I., (submitted) The onset of the volcanism in the Ciomadul Lava Dome Field: eruption chronology and magma type variation. Journal of Volcanology and Geothermal Research.

Moriya, I., Okuno, M., Nakamura, T., Ono, K., Szakács, A., Seghedi, I., 1996. Radiocarbon ages of charcoal fragments from the pumice flow deposits of the last eruption of Ciomadul Volcano, Romania. Summaries of Research using AMS at Nagoya University VII, 255-257.

Mureşan, M., Mureşan, G., Kräutner, H., Kräutner, F., Peltz, S., Szakács, A., Seghedi, I., Bandrabur, T., 1986. Geological map of Romania, sc, 1: 50 000, Sheet Voşlăbeni, Geological Institute of Romania

Panaiotu, C.G., Jicha, B.R., Singer, B.S., Ţugui,A., Seghedi, I., Panaiotu,A.G., Necula, C., 2013. $^{40}Ar/^{39}Ar$ chronology and paleomagnetism of Quaternary basaltic lavas from the Perşani Mountains (East Carpathians). Phys. of the Earth and Planet. Interiors 221, 1–14.

Peccerillo, A., Taylor, S.R., 1976. Geochemistry of Eocene Calc-Alkaline Volcanic-Rocks from Kastamonu Area, Northern Turkey, Contributions to Mineralogy and Petrology, 58, 63-81.

Pécskay, Z., Lexa, J., Szakács, A., Balogh, K., Seghedi, I., Konečny, V., Kovacs, M., Marton, E., Széky-Fux, V., Póka, T., Gyarmaty, P., Edelstein, O., Roşu, E., Žec, B., 1995a. Space and time distribution of Neogene–Quaternary volcanism in the Carpatho–Pannonian Region. Acta Vulcanologica 7, 15–29.

Pécskay, Z., Edelstein, O., Seghedi, I., Szakács, A., Kovacs, M., Crihan, M., Bernad, A., 1995b. K–Ar datings of the Neogene–Quaternary calc-alkaline volcanic rocks in Romania. Acta Vulcanologica 7, 53–63.

Pécskay, Z., Lexa, J., Szakács, A., Seghedi, I., Balogh, K., Konečný, V., Zelenka, T., Kovacs, M., Póka, T., Fülöp, A., Márton, E., Panaiotu, C., Cvetković, V., 2006. Geochronology of Neogene–Quaternary magmatism in the Carpathian arc and Intra-Carpathian area: a review. Geologica Carpathica 57, 511–530.

Pécskay Z., Seghedi I., Kovacs M., Szakács A., Fülöp A., 2009. Geochronology of the Neogene calc-alkaline intrusive magmatism in the "Subvolcanic Zone" of the Eastern Carpathians (Romania). Geologica Carpathica 60, 2,181-190.

Peltz, S., Grabari, G., Stoian, M., Tănăsescu, A., Vâjdea, E., 1984. REE, Rb, Sr and K Distribution in Volcanic Rocks from the East Carpathians (Călimani-Harghita and Perşani Mts). Petrogenetic Significance. In: Symp.: Magm. molasse-form. epoch rel. end. mineraliz., (1982). Geol. Úst. D. Stura, Bratislava, p. 47-58.

Peltz, S., Vâjdea, E., Balogh, K., Pécskay, Z., 1987. Contributions to the Chronological Study of the Volcanic Processes in the Călimani and Harghita Mountains (East Carpathians, Romania); D. S. Inst. Geol. Geofiz., Bucureşti, 72–73/1, (1985; 1986), p. 323–338

Rădulescu, D.P., 1973. Considerations on the Origin of Magmas of the Neozoic Subsequent Volcanism in the East Carpathians-Simp. Int. Vulc. An. Inst. Geol., Bucureşti , XLI, 69-76.

Ratschbacher, L., Frisch, W., Linzer, H.-G., Merle, O., 1991. Lateral extrusion in the Eastern Alps; Part 2, Structural analysis. Tectonics 10, 257–271.

Rosenbaum, G., Lister, G.S., Duboz, C., 2004. The Mesozoic and Cenozoic motion of Adria (central Mediterranean): a review of constraints and limitations. Geodinamica Acta 17, 125–139.

Royden, L.H., 1988. Late Cenozoic tectonics of the Pannonian Basin system. In: Royden, L.H., Horváth, F. (Eds.), The Pannonian Basin. A Study in Basin Evolution, AAPG Memoir 45. The AAPG and the Hungarian Geological Society, Tulsa, Budapest, pp. 27–48.

Sanders, C.A.E., Andriessen, P.A.M., Cloetingh, S.A.P.L., 1999. Life cycle of the East Carpathian orogen: erosion history of a doubly vergent critical wedge assessed by fission track thermochronology. J. Geophys. Res. 104 (B12), 29, 095–29, 112.

Seghedi, I., Szakács, A., Udrescu, C., Stoian, M., Grabari, G., 1987. Trace element geochemistry of the South Harghita volcanics (East Carpathians). Calc-alkaline and shoshonitic association. D.S.Inst.Geol.Geofiz., 72-73/1, 381-397, Bucureşti.

Seghedi, I., Szakács, A., Mason, P.R.D., 1995. Petrogenesis and magmatic evolutions in the East Carpathians Neogene volcanic arc (Romania). Acta Volcanologica 7 (2), 135–145.

Seghedi, I., Balintoni, I., Szakács, A., 1998. Interplay of tectonics and Neogene postcollisional magmatism in the Intracarpathian area. Lithos 45, 483–499.

Seghedi, I., Downes, H., Szakács, A., Mason, P.R.D., Thirlwall, M.F., Roşu, E., Pécskay, Z., Marton, E., Panaiotu, C., 2004a. Neogene–Quaternary magmatism and geodynamics in the Carpathian–Pannonian region: a synthesis. Lithos 72, 117–146.

Seghedi, I., Szakács, A., Snelling, N., Pécskay, Z. 2004b**.** Evolution of the Neogene Gurghiu Mountains volcanic range (Eastern Carpathians, Romania), based on K-Ar geochronology. Geologica Carpathica 55, 4, 325-332

Seghedi, I., Downes, H., Harangi, S., Mason, P.R.D., Pécskay, Z., 2005a. Geochemical response of magmas to Neogene–Quaternary continental collision in the Carpathian–Pannonian region: a review. Tectonophysics 410, 485–499.

Seghedi, I., Szakács, A., Pécskay, Z., Mason, P. R. D., 2005b. Eruptive history and age of magmatic processes in the Călimani volcanic structure (Romania). Geologica Carpathica 56, 67-75.

Seghedi, I., Ntaflos, T., Pécskay, Z., 2008. The Gătaia Pleistocene lamproite: a new occurrence at the southeastern edge of the Pannonian Basin, Romania. Geological Society London Special Publication 293, 83–100.

Seghedi, I., Szakács, A., Roşu, E., Pécskay Z., Gméling, K., 2010. Note on the evolution of a Miocene composite volcano in an extensional setting, Zărand Basin (Apuseni Mts., Romania). Central European Journal of Geosciences, 2, 3, 321-328.

Seghedi, I., Maţenco, L., Downes, H., Mason, P.R.D., Szakács, A., Pécskay, Z., 2011. Tectonic significance of changes in post-subduction Pliocene–Quaternary magmatism in the south east part of the Carpathian–Pannonian Region. Tectonophysics 502, 146–157.

Seghedi, I. and Downes, H., 2011. Geochemistry and tectonic development of Cenozoic magmatism in the Carpathian–Pannonian region. Gondwana Research 20, 655–672.

Seghedi, I., Ersoy, Y. E., Helvacı, C., 2013. Miocene–Quaternary volcanism and geodynamic evolution in the Pannonian Basin and the Menderes Massif: A comparative study. Lithos 180–181, 25–42.

Seghedi, I., Popa, R.-G., Panaiotu, C.G., Szakács, A., Pécskay, Z., 2016. Short-lived eruptive episodes during the construction of a Na-alkalic basaltic field (Perşani Mountains, SE Transylvania, Romania). Bulletin of Volcanology 78:69, DOI 10.1007/s00445-016-1063-y.

Seghedi I., Szakács, A., Pécskay, Z., Mirea V., Luffi P., The significance of debris avalanche deposits in the architecture of the Călimani-Gurghiu-Harghita volcanic range (Eastern Transylvania, Romania). In preparation.

Szakács, A., Seghedi, I., Pécskay, Z., 1993. Pecularities of South Harghita Mts. as terminal segment of the Carpathian Neogene to Quaternary volcanic chain. Rev. Roum. Geologie 37, 21–36.

Szakács, A. and Seghedi, I., 1995. The Călimani–Gurghiu–Harghita volcanic chain, East Carpathians, Romania: volcanological features. Acta Vulcanologica 7 (2), 145–153.

Szakács A. and Seghedi I., 1996. Volcaniclastic sequences around andesitic stratovolcanoes, East Carpathians, Romania, Workshop guide, of the IAVCEI, CEV and CVS commisions. Rom. Jour. of Petrology, 77, supplement 1, 55p.

Szakács, A., Ioane, D., Seghedi, I., Rogobete, M., Pécskay, Z., 1997. Rates of migration of volcanic activity and magma output along the Călimani-Gurghiu-Harghita volcanic range, East Carpathians, Romania. Przglad Geologiczny 45, 10/2: 1106

Szakács, A. and Seghedi, I., 2000. Large volume volcanic debris avalanche in the East Carpathians, Romania. In Volcaniclastic rocks, from magma to sediments, H. Leyrit and C. Montenat (edt), Ed. Gordon Breach Science Publishers, 131-151.

Szakács, A. and Krézsek, Cs., 2006. Volcano-basement interactions in the Eastern Carpathians: Explaining unusual tectonic features in the Eastern Transylvanian Basin, Romania. J.Volcanol. Geotherm.Res., 158, 6-20.

Szakács, A., 2008. Volcanic facies revisited. Application to areas of closely-spaced composite volcanoes. IAVCEI General Assembly, Reykjavik, Iceland, 17-22 August 2008, Abstracts., p. 83

Szakács, A. and Canon-Tapia, E., 2010. Some challenging new perspectives of volcanology. In Canon-Tapia, E. and Szakács, A, eds., What is a Volcano? Geological Society of America Special Paper 470, 123-140

Szakács, A., Pécskay, Z., Silye, L., Balogh, K., Vlad D., Fülöp, A., 2012. On the age of the Dej Tuff, Transylvanian Basin (Romania). Geologica Carpathica 63, 2, 139-148.

Szakács, A., Seghedi, I., Pécskay, Z., Mirea, V., 2015. Eruptive history of a low-frequency and low-output rate Pleistocene volcano, Ciomadul, South Harghita Mts., Romania. Bull. Volcanol. 77, 12. http://dx.doi.org/10.1007/s00445-014-0894-7.

Sun, S. and McDonough, W.F., 1989. Chemical and isotopic systematics of oceanic basalts: implications for mantle compositions and processes. Geological Society Special Publication 42, 313–345.

Tari, G., Dovenyi, P., Dunkl, I., Horváth, F., Lenkey, L., Stefanescu, M., Szafian, P., Toth, T., 1999. Lithospheric structure of the Pannonian basin derived from seismic, gravityand geothermal data. In: Durand, B., Jolivet, L., Horváth, F., Serrane, M. (Eds.), The Mediterranean Basins: extension within the Alpine Orogen: Geol. Soc. London Spec. Publ., 156, pp. 215–250.

Tărăpoancă, M., Bertotti, G., Maţenco, L., Dinu, C., Cloetingh, S., 2003. Architecture of the Focşani depression: A 13 km deep basin in the Carpathians bend zone (Romania). Tectonics 22, 1074.

Tschegg, C., Ntaflos, T., Kiraly, F., Harangi, S., 2010.High temperature corrosion of olivine phenocrysts in Pliocene basalts from Banat, Romania.Austrian Journal of Earth Sciences Volume 103/1, 101-110.

Ustaszewski, K., Schmid, S., Fügenschuh, B., Tischler, M., Kissling, E., Spakman,W., 2008. A map-view restoration of the Alpine–Carpathian–Dinaridic system for the Early Miocene. Swiss Journal of Geosciences 101, 273–294.

Vaselli, O., Downes, H.,Thirlwall, M., Dobosi, G., Coradossi, N., Seghedi, I., Szakács, A., Vanucci, R., 1995.Ultramafic xenoliths in Plio-Pleistocene alkali basalts from the Eastern Transylvanian Basin: Depleted mantle enriched by vein metasomatism. Journal of Petrology, 36, 1, 23-53.

Vessel, R.K. and Davies, D.K., 1981. Nonmarine sedimentation on an active fore arc basin. Soc. Econ. Paleont. Mineral. Publ., 31, 31-45.

Vinkler, A.P., Harangi, S., Ntaflos, T., Szakács, A., 2007. Petrology and geochemistry of pumices from the Ciomadul volcano (Eastern Carpathians) - implication for petrogenetic processes (in Hungarian with an English abstract) Földtani Közlöny 137/1, 103–128.

Williams, H. and McBirney, A.R., 1979. Volcanology. Freeman, Cooper, and Co., San Francisco, 626 pp.

Wortel, M.J.R. and Spakman, W., 2000. Subduction and slab detachment in the Mediterranean–Carpathian region. Science 290, 1910–1917.

LIST OF PARTICIPANTS

Rigoberto Aguilar Contreras
Volcanological Observatory, INGEMMET, Perú
aguilar.contreras75@gmail.com

Guillermo Alvarado
Instituto Costarricense de Electricidad ICE, Costa Rica
galvaradoi@ice.go.cr

Tamás Bíró
University of Budapest ELTE, Hungary
tbiro.geogr@gmail.com

Tamara Carley
Lafayette College, U.S.A
carleyt@lafayette.edu

Stéphane Dibacto-Kamwa
University of Paris-Sud, France
stephane.dibacto-kamwa@u-psud.fr

Ingomar Fritz
Universalmuseum Joanneum, Geology & Paleontology, Graz, Austria
ingomar.fritz@a1.net

Alexandrina Fülöp
Canada/Romania
alexandrinafulop@yahoo.com

Nobuo Geshi
Institute of Earthquake and Volcano Geology, Geological Survey of Japan AIST, Japan
geshi-nob@aist.go.jp

Gabriel Grădinaru
University of Bucharest, Romania
gabriel.constantin95@gmail.com

Gianluca Groppelli
Istituto per la Dinamica dei Processi Ambientali
Dipartimento di Scienze della Terra, Milano, Italy
gianluca.groppelli@unimi.it

Moshe Inbar
University of Haifa, Israel
inbar@geo.haifa.ac.il

Jun'ichi Itoh
Institute of Earthquake and Volcano Geology, Geological Survey of Japan AIST, Japan
itoh-j@aist.go.jp

Georgi Ivanov
Dundee Precious Metals, Canada, Chelopech branch, Bulgaria
georgi.ivanov@dundeeprecious.com

Balázs Kiss
MTA-ELTE Volcanology Research Group, Budapest, Hungary
geobalazs@gmail.com

Marinel Kovacs
Technical University of Cluj-Napoca, North University Centre, Baia Mare, Romania
Romania, marinel.kovacs@cunbm.utcluj.ro

Péter Luffi
Institute of Geodynamics, Bucharest, Romania
peter.luffi@gmail.com

José Luis Macías Vázquez
Instituto de Geofísica, UNAM, Michoacán, México
macias@geofisica.unam.mx

Stefan Metodiev
Dundee Precious Metals, Canada, Chelopech branch, Bulgaria
stefan.metodiev@dundeeprecious.com

Viorel Mirea
Institute of Geodynamics, Bucharest, Romania
vmirea@geodin.ro

Lyndsay Moore
Department of Earth and Planetary Sciences, University of Montreal, Quebec, Canada
lyndsay.moore@mail.mcgill.ca

Jan Mrlina
Institute of Geophysics ASCR Prague, Czech Republic
jan@ig.cas.cz

Károly Németh
Volcanic Risk Solutions, Massey University, Palmerston North, New Zealand
k.nemeth@massey.ac.nz

Ivan Strmbanovic
Dundee Precious Metals, Canada, Bor branch, Serbia
ivan.strmbanovic@dundeeprecious.com

Claudia Pellicioli
The University of Milan, Italia
claudia.pellicioli@unimi.it

Zoltán Pécskay
Institute of Nuclear Research (ATOMKI), Debrecen, Hungary
zoltan.pecskay@gmail.com

Nino Popkhadze
Faculty of Exact and Natural Sciences Javakhishvili, Tbilisi State University, Armenia
nino_popkhadze@yahoo.com

Ioan Seghedi
Institute of Geodynamics, Bucharest, Romania
seghedi@geodin.ro

Alina Shevchenko
Institute of Volcanology and Seismology, Petropavlovsk-Kamchatsky, Russia
al.vic.shevchenko@gmail.com

Giovanni Sosa-Ceballos
National Autonomous University of Mexico, Mexico
giovannis@igeofisica.unam.mx

Alexandru Szakács
Institute of Geodynamics, Bucharest, Romania
szakacs@sapientia.ro

János Szepesi
MTA-ELTE Volcanology Research Group, Budapest, Hungary
szepeja@gmail.com

Olaf Tietz
Senckenberg Museum of Natural History, Görlitz, Germany
olaf.tietz@senckenberg.de

Ingrid Ukstins
Earth & Environmental Sciences, University of Iowa, U.S.A.
ingrid-peate@uiowa.edu

Mădălina Vişan
Institute of Geodynamics, Bucharest, Romania
danamadalina@yahoo.com

Mladen Zdravkovic
Dundee Precious Metals, Canada, Bor branch, Serbia
mladen.zdravkovic@dundeeprecious.com

Nikolay Zhivkov
Dundee Precious Metals, Canada, Chelopech branch, Bulgaria
nikolay.zhivkov@dundeeprecious.com

4th international Volcano Geology Workshop Transylvania, Romania 8-14 October 2017

Abstracts

.

Middle Miocene silicic phreatomagmatism at the Bükk Foreland Volcanic Area

Tamás Biró[1], Mátyás Hencz[1], Dávid Karátson[1], Emő Márton[2,] Zoltán Szalai[3] and Balázs Bradák[4]

[1] *Eötvös University, Department of Physical Geography, Budapest, Hungary – birotamas@caesar.elte.hu*
[2] *Mining and Geological Survey of Hungary, Paleomagnetic Laboratory, Budapest, Hungary*
[3] *Hungarian Academy of Sciences, Research Centrer for Astronomy and Earth Sciences, Geographical Institute, Budapest, Hungary*
[3] *Research Center for Inland Seas, Kobe University, Kobe, Japan*

Keywords: Bükk Foreland Volcanic Area, granulometry, phreatomagmatism.

The Bükk Foreland Volcanic Area (BFVA, North Hungary) is a 8 x 40 km large surficial outcrop of the Miocene, intrabasinal, Si-rich „Tuff Formations" at North Hungary, within the Carpatho-Pannonian Region (CPR). The several ten meters thick BFVA pyroclastic succession was subdivided into three main units. All main pyroclastic units consist mainly of pumiceous pyroclastic density current deposits with block-bearing, massive lapilli tuff facies (ignimbrites). Layered pyroclastic and epiclastic formations and accretionary lapilli-bearing phreatomagmatic units are rare and are observed only at the boundaries between the three main pyroclastic units (Capaccioni et al. 1995; Szakács et al. 1998; Lukács et al. 2007).

The succession between the Bogács Ignimbrite Unit (BIU; Middle Pyroclastic Unit) and Harsányi Ignimbrite Unit (HIU; Upper Pyroclastic Unit) at Tibolddaróc contains four epiclastic layers, few fall pyroclastits and a 15 m thick ash-flow deposit (Lukács et al. 2007), however the interpretations were only based on the field characteristics of the formations without detailed description and granulometrical analysis.

We found, that besides Tibolddaróc, the layered succession is exposed near Bogács and it is relatively well-preserved too. The Bogács and Tibolddaróc successions contain the same layers, thus can be correlated. Here, we present new detailed physical volcanological, ganulometrical and anisotropy of magnetic susceptibility (AMS) results from these localities to infer to the nature of the eruptional and depositional processes.

Between the BIU and the HIU a complex, layered succession was revealed, which is subdivided into four units (Unit I, II, III, IV) by three well-developed paleosoil horizons (Fig. 1). Unit II is the best preserved and most complex one, thus granulometrical and AMS investigations were focused on it. Only the uppermost 2.5 meters of Unit II was affected by weathering and soilification. Unit II contains at least 31 cm to 80 cm thick layers, which have constant thickness and preserved the undulation of the paleotopography (Fig. 2).

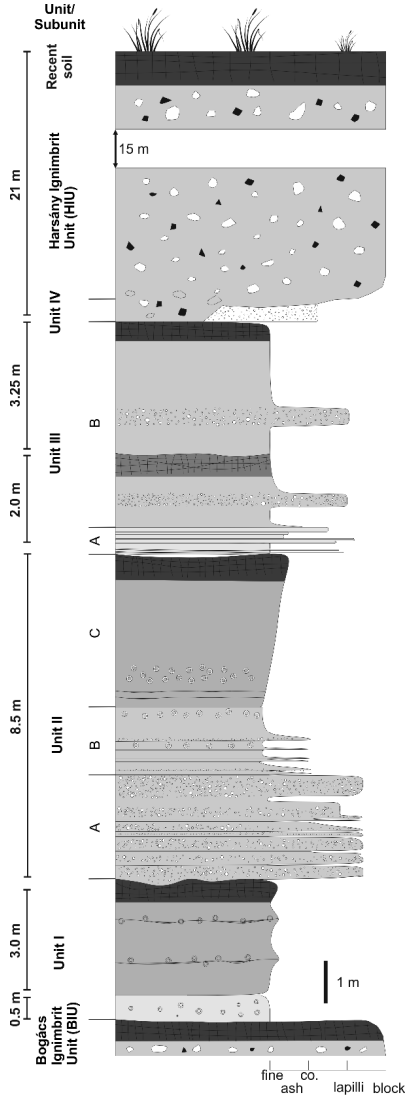

Fig. 1 – Generalized log between the Bogács Ignimbrit Unit (BIU, Middle Pyroclastic Unit) and the Harsány Ignimbrite Unit (HIU, Upper Pyroclastic Unit). The succession is subdivided by four paleosoil horizons (dark grey) and is dominated by cm to m thick fine and coarse tuff layers. The best preserved part of the succession is Unit II.

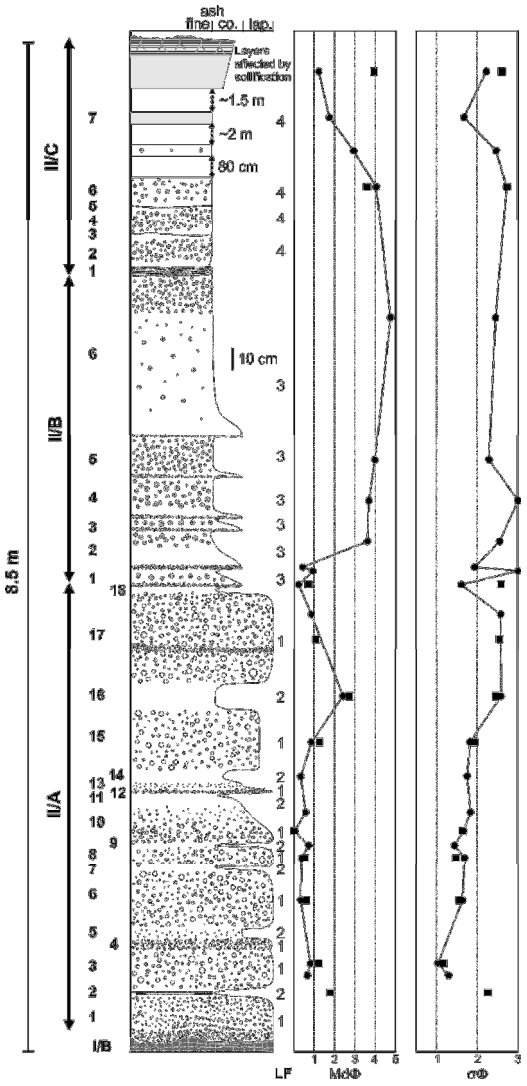

Fig. 2 – Detailed stratigraphical log with Mdϕ and σϕ values of Unit II. Unit II can be subdivided into Subunit A, B and C based on the granulometrical and grading features of the layers. LF - lithofacies

Erosional contacts (except the boundary between II/A/1 and 2) or weathering cannot be observed in Unit II, which imply a continuous deposition within a short period of time. Unit II can be subdivided into three subunits (A, B, C) based on the relative frequency of different lithofacies (LF). Four lithofacies can be discriminated based on internal structure, absence or prescence of accretionary lapilli, and amount of fine ash. While the Subunit A is dominated by LF1, which is relatively well sorted coarse tuff, without accretionary lapilli and internal gradation, Subunit B and C are dominated by LF3 and 4 which are characterized by normal gradation, high amount of fine ash and the prescence of accretionary lapilli. The uppermost 2.5 m of Unit II is weathered due to soil formation and did not preserve the original structure. This part is marked by II/C/7, which possibly contained several layers originally, which is supported by the decreasing Mdϕ and σϕ values (Fig. 2).

AMS results show very weak anisotropy. 45% of the investigated 53 samples show F-test values lower, than 3.48, which imply statistically significant isotropic magnetic fabric. Similarly, except two samples, all other samples show P (degree of anisotropy) < 1%, which are much lower, than in cross-bedded, accretionary lapilli-bearing deposits from phreatomagmatic, dilute base surges.

In Unit II the constant thickness of the layers, the lack of erosional lower contacts, internal cross stratification and pinch and swell structures and the normal grading in LF3 indicate fall origin or emplacement from dilute PDCs, where the depositional regime is dominated by vertical settling and the lack of lateral movement. The phreatomagmatic character is evident in Subunit B and C, from the abundant accretionary lapilli and the >40 wt.% of the finest (<63 μm) particles. The Mdϕ=3.5-5 and σϕ>2 values of layers in Subunit B are similar to the values from phreatoplinian PDC and fall deposits.

Our new results show that besides ignimbrite-forming PDC activity, pyroclastic fallout from powerful magmatic and phreatomagmatic eruptions were also occurred in the volcanic history of the BFVA. However, fall deposits are subordinate from a volumetrical point of view, but could be even more important with respect to the number of eruptions, than the ignimbrite-forming ones within the Si-rich, Miocene volcanism of the CPR.

Acknowledgements

The research was supported by OTKA K-115472, NF-101362 and K-105245 programs and by the ÚNKP-16-1 New National Excellence Program of the Ministry of Human Capacities.

References

Capaccioni, B., Corodannosi, N., Harangi, R., Harangi, Sz., Karátson, D., Sarocchi, D., Valentini, L., 1995. Early Miocene pyroclastic rocks of the Bükkalja Ignimbrite Field (North Hungary) - A preliminary stratigraphic report. Acta Vulcanol. VII, 119–124.

Lukács, R., Harangi, Sz., Ntaflos, T., Koller, F., Pécskay, Z., 2007. The characteristics of the Upper Rhyolite Tuff Horizon in the Bükkalja Volcanic Field: The Harsány ignimbrite unit – Bull. Hun. Geol. Soc., CXXXVII, 487–514. (In Hungarian with English abstract)

Szakács, A., Márton, E., Póka, T., Zelenka, T., Pécskay, Z., Seghedi, I., 1998. Miocene acidic explosive volcanism in the Bükk Foreland, Hungary: Identifying eruptive sequences and searching for source locations. Acta Geol. Hung., XLI, 413–435.

Altered, eroded, obscured by ice: A detrital zircon perspective into Iceland's rhyolitic history

Tamara L. Carley[1], Tenley J. Banik[2], Emma S. Sosa[1,3], Matthew A. Coble[4]
[1] *Lafayette College Department of Geology and Environmental Geosciences, Easton, PA, USA – carleyt@lafayette.edu*
[2] *Illinois State University Department of Geography, Geology, and the Environment, Normal, IL, USA*
[3] *California Institute of Technology Division of Geological and Planetary Sciences, Pasadena, CA, USA*
[4] *Department of Geological Sciences, Stanford University, Stanford, CA, USA*

Keywords: Iceland, rhyolite, detrital zircon

Despite its oceanic setting, Iceland has thick (25-40 km) and rhyolite-rich (10-13%) crust due to its unique location at the intersection of a hotspot and mid-ocean ridge. Although Iceland is ideal for investigating juvenile rhyolite petrogenesis and proto-continental nucleation, several environmental factors complicate studies of its rhyolites (Fig. 1). Obsidian is common at major central volcanoes, but these glassy black rocks are camouflaged in a landscape dominated by basalt. Hydrothermally altered rhyolitic lavas and tephras are easier to locate in this mafic landscape, but alteration complicates whole rock geochemical investigations. Repeated Plio-Pleistocene glacier advance and retreat caused significant erosion of rhyolites older than 0.8 M.y. Several currently active rhyolite-producing central volcanoes are partially obscured by glacial ice (e.g., Öræfajökull), while the rhyolitic records of other active volcanoes (e.g., Bárðarbunga, Kverkfjöll) are largely unknown due to near-total ice coverage. Investigations into these subglacial magmatic systems are especially critical in this era of climate change because deglaciation may trigger magma production and destabilization, thus increasing potential for eruption hazards.

In this study, we use zircon to investigate Iceland's elusive rhyolitic history because it is chemically resilient against the effects of hydrothermal alteration and physically durable during erosion. In a country-wide study of zircons from intrusive, extrusive, and detrital samples, trace element analyses reveal a globally distinctive geochemical signature (e.g., high Ti and M-HREE) reflective of unique petrogenetic conditions for Icelandic rhyolites (Carley et al. 2014, Grimes et al. 2015). Oxygen isotope ratios (median $\delta^{18}O$ +3.2 ‰; Carley et al. 2014) suggest hydrothermally altered crust plays a critical role in generation of Icelandic rhyolites.

Inspired by success of prior zircon-based studies of Icelandic rhyolites (Carley et al. 2011, 2014, 2017), we now focus on investigating potential rhyolites beneath Vatnajökull, an ice cap covering ~10% of Iceland. In support of our ultimate goal to

Fig. 1 – Examples of rhyolite in Iceland (Top Left): obsidian at Torfajökull volcano; (Top Right) altered rhyolite at Kerlingarfjöll volcano; (Bottom Left) Fjallsjökull glacier on Öræfajökull volcano's eastern flank; (Bottom Right) glacially carved valley with sparse rhyolitic tephra preserved.

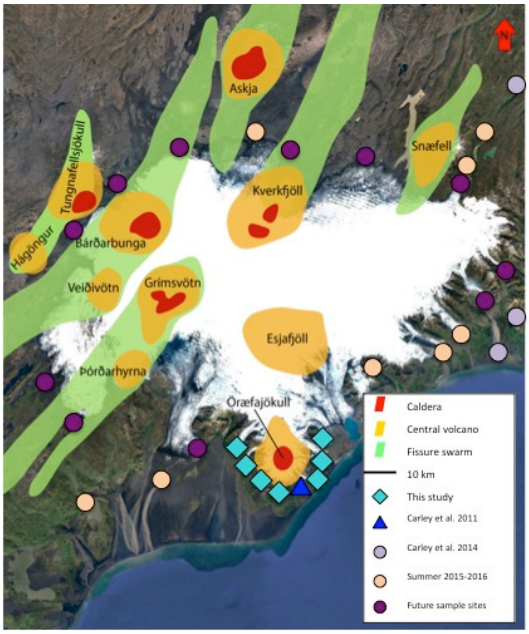

Fig. 2 – Google Earth view of the Vatnajökull ice cap in SE Iceland with existing and proposed sample sites indicated. Volcanic features adapted from Hannesdottir et al. (2013).

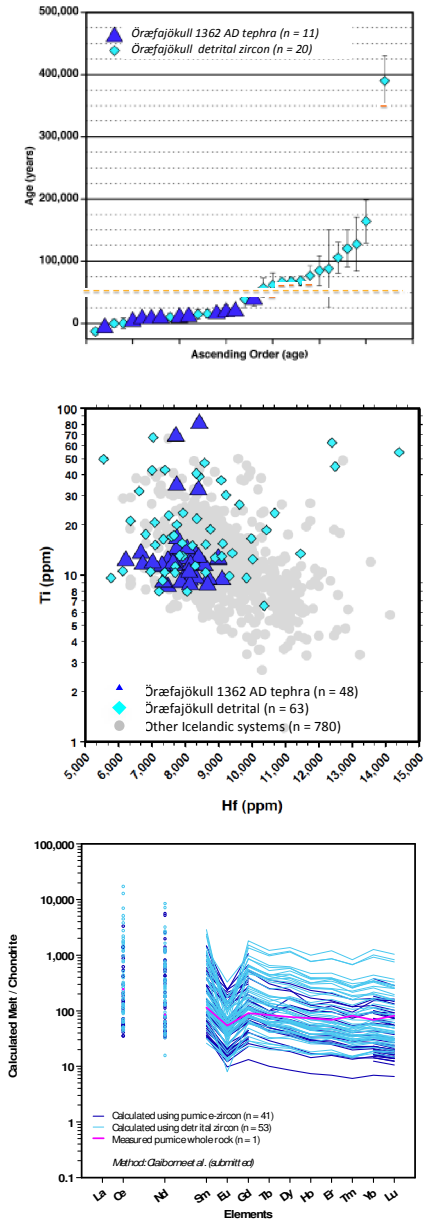

Fig. 3 – Data for Öræfajökull zircons from 1362 AD pumice (dark blue) and sediments (light blue) measured on SHRIMP-RG. (Top) U-Pb and U-Th ages for pumice (n = 11) and detrital (n = 20) zircon. (Middle) Ti vs Hf in pumice (n = 48) and detrital (n = 63) zircon in an Icelandic context (n = 780). (Bottom) Pumice (n = 41) and detrital (n = 53) zircon REE used to calculate melt compositions using methods of Claiborne et al. (in press), normalized to chondrite (McDonough and Sun, 1995).

identify and characterize previously unrecognized instances of subglacial rhyolites, we present a proof-of-concept study from Öræfajökull, a subglacial volcano on the southern margin of Vatnajökull (Fig. 2). We compare ages and trace elements from 1362 AD tephra zircon to those from detrital zircon sourced from 7 outlet glaciers (moraines, streams, proglacial lakes) around the accessible southern perimeter of Öræfajökull.

Data from 1362 AD tephra zircons suggests that zircon ages typically predate eruption by 1-10's ka (median ~12 ka; rarely > 100 ka; n = 11; Fig. 3). Tephra-derived zircons tend to be younger than detrital zircons (n = 20), which range continuously from ~0 to ~150 ka, and ages up to ~475 ka. Tephra-derived zircon trace elements (n = 48) form coherent trends within typical Icelandic compositional fields but have restricted and low Hf (5500-9000 ppm) and Ti (8-16 ppm), suggesting limited fractionation at moderate and restricted temperatures. Detrital zircon trace elements (n = 63) consistently follow and expand geochemical trends of the tephra zircon, revealing more diverse crystallization conditions (e.g., Hf to ~12500 ppm, Ti to ~30 ppm; n=63). When Ti-calibrated zircon-melt partition coefficients (Claiborne et al., in press) are used to calculate model melt values, both detrital and tephra zircon compositions yield REE/chondrite trends that resemble those of measured glass compositions from 1362 AD Öræfajökull pumice.

These Öræfajökull data suggest that zircons from glacially-derived sediments expand the magmatic history captured by the tephra record (Fig. 3). A large-scale study of rhyolites beneath Vatnajökull using sediments from its outlet glaciers is thus viable and warranted.

References

Carley, T.L., et al., 2011, Zircon from historic eruptions in Iceland: Reconstructing storage and evolution of silicic magmas: Mineralogy and Petrology, v. 102, no. 1–4, doi: 10.1007/s00710-011-0169-3.

Carley, T.L., et al., 2017, Detrital zircon resolve longevity and evolution of silicic magmatism in extinct volcanic centers: A case study from the East Fjords of Iceland: Geosphere, v. 13, no. 4, doi:10.1130/GES01467.1.

Carley, T.L.,et al., 2014, Iceland is not a magmatic analog for the Hadean: Evidence from the zircon record: Earth and Planetary Science Letters, v. 405, p. 85-97, doi: 10.1016/j.epsl.2014.08.015

Claiborne, L.L., et al., Zircon as a magma monitor: Robust partition coefficients from surface, rim, and glass measurements from natural systems: in Moser D, Corfu F, Darling J, Tait K, Reddy S (eds) Microstructural Geochronology; lattice to atom-scale records of planetary evolution, AGU Monograph Series (in press).

Grimes, C.B., et al., 2015, "Fingerprinting'' tectono-magmatic provenance using trace elements in igneous zircon: Contributions to Mineralogy and Petrology, v. 170, no. 5, p. 1–26, doi: 10.1007/s00410-015-1199-3.

Hannesdottir, H., et al., 2013, Vatnajokull National Park: Geology and Geodynamics: Northern Environmental Education Development, p. 39.

McDonough, W.F., and Sun, S. -s., 1995, The composition of the Earth: Chemical Geology, v. 120, no. 3–4, p. 223–253, doi: 10.1016/0009-2541(94)00140-4.

Reconstruction of the evolution and magma system of caldera-forming eruption from the geological and petrological analysis, an example of the Aira Caldera, Japan

Nobuo Geshi[1],

[1] *Geological Survey of Japan, AIST, Japan – geshi-nob@aist.go.jp*

Keywords: caldera volcano, magma system, .

Large-scale pyroclastic eruption empties a shallow magma chamber and results caldera collapse. One of the major questions about the caldera-forming eruption is the timing of collapse (onset and duration) during a large-scale pyroclastic eruption. the caldera-border faults cut the roof of magma chamber and the roof block starts subsiding into the magma chamber to form a collapse caldera at the onset of the caldera collapse. This process makes the significant pressure change within the magma chamber (e.g., Marti et al. 2000) which can be recorded in the erupted materials.

We have no real-time scientific observation of caldera-forming pyroclastic eruption except for two small examples of Pinatubo 1991 and Katmai 1912. Therefore, the geological investigation on the erupted materials is only the approach to reconstruct the dynamic process of caldera-forming eruption. Sequence of the eruption products of a caldera-forming eruption can record these magmatic process, evolution of the vent system, and the timing of caldera collapse.

An example from the 29 ka Aira Caldera, Kyushu Island Japan, presents the evolution of caldera-forming eruption (Geshi and Miyabuchi, 2016 and references therein). The eruption produced more than 400 km^3 of rhyolitic magma and formed the Aira caldera with ~ 15 km across. Homogeneous magma composition (~74-76 wt.% of SiO_2 throughout the eruption) suggests the extraction of magma from a single magma chamber, though minor contribution of additional mafic component is recognized.

The eruption started with a Plinian eruption from a single vent at the southern rim of the caldera. The total discharge volume of the pumice is ~40 km^3 (in DRE). The stratigraphy and upward-coarsening of grain-size of the fall-out deposit suggest the increase of magma flux during the Plinian phase up to ~10^8 kgs^{-1} at the end of the initial Plinian phase.

The increase of magma flux during the initial Plinian phase may be caused by the enlargement of the conduit by the mechanical erosion. The pumice fall deposit contains ~2 volume percent of lithic fragments of basement rock derived from the wall of the conduit. The abundance of lithic fragments in the pumice fall deposit indicates intense erosion of the conduit wall to increase the effective radius of conduit. Enlargement of the conduit radius encouraged the continuous extraction of magma from the decompressing magma chamber.

Decompression of magma chamber caused partial subsidence of the roof of magma chamber. The deformation of the chamber roof may allow the opening of ring conduit. This change of conduit shape as well as the location resulted in the change of eruption style from the initial Plinian eruption from single vent at the caldera margin to an ignimbrite overflow from multiple vents distributed inside the caldera. This process was recorded as the emplacement of a minor ignimbrite named Tsumaya pyroclastic flow. Distribution of the pyroclastic flow deposit suggests the shift of eruption site to the center of caldera.

Opening of new conduit system also enhanced the additional extraction of magma with higher flux, and resulted in the further decompression of the magma chamber. Finally, this resulted in the establishment of ring fault and collapse of the entire part of the roof of magma chamber. This catastrophic change triggered the eruption of the main ignimbrite (Ito ignimbrite). The volume of Ito ignimbrite is estimated as ~350 km^3 in DRE, which corresponds >90 % of the total volume of the erupted material of the eruption.

Evolution of the eruption style, site of the eruption, and the flux of magma are important parameters to understand the caldera-forming eruption. Therefore, the geological investigation of the caldera-forming eruption should target on the revealing of these parameter.

References

Marti, J., Folch, A., Neri, A., Macedonio G., 2000. Pressure evolution during explosive caldera forming eruptions. Earth Planet Sci Lett. 175, 275-287.

Geshi, N., Miyabuchi, Y. (2016) Conduit enlargement during the precursory Plinian eruption of Aira Caldera, Japan . Bulletin of Volcanology 78, 63

Morphological development of cinder cones

Moshe Inbar

Department of Geography and Environmental Studies, University of Haifa, Haifa, Israel – inbar@geo.haifa.ac.il

Keywords: cinder cones, morphometry, erosion

Cinder cones are the simplest and most common volcanic landforms in existence. It is probably the only landform on the globe with a distinct and defined initial date of formation, and lasting no more than a few million years. The progressive decrease of morphometric parameters with increasing of age is the basis for relative dating of cinder cones. Morphometric and morphological studies are efficient tools for determining ages of cinder cones and their morphological evolution.

There is no comprehensive inventory of the cones in the globe, but my estimation is about fifty thousand, around four thousand in Mexico, and five thousand in Kamchatka. The aim of this study is to analyze erosional processes affecting the degradation of the cinder cones under different climatic conditions.

Global examples: Degradation values for the Kamchatka peninsula are higher than for semiarid areas in the Southern Andes or the Golan Heights. Peaks of erosion occurred probably in the first stage of one or two years after the eruption, with the stripping of the fine ash material.

The study on about 800 cones of the Payun Matru Volcanic Field in the Southern Andes (Mendoza, Argentina) showed a good correlation between the old cones with a low ratio of height/diameter of cone and the more recent of Holocene times with a high ratio. Morphometric values of the 1988 erupted Navidad cone, close to the Lonquimay volcano in Chile, are similar to those of recent erupted cones.

Erosional processes on monogenetic volcanism determine their morphometric characteristics according to their climatic environment.

The evolution of landscape over time is a central aspect of geological, paleogeographical and geomorphological studies.

Fig. 1 - Kamchatka 1975 eruption in theTolbachik field

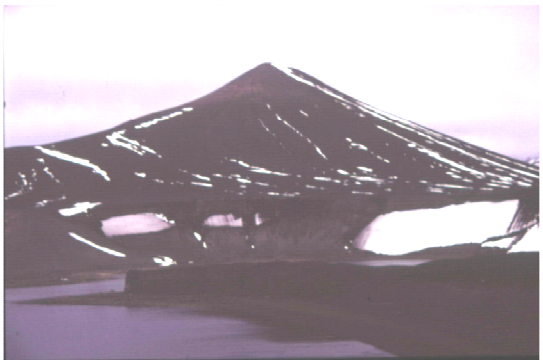

Fig. 2 - Antarctica- 1975 eruption in Deception Island

Fig. 3 – Paricutin - Mexico 1943-1952 eruption

Fig. 4 - Payun Matru volcanic field, Argentina

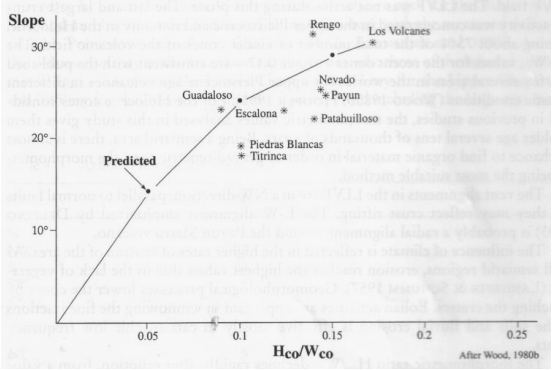

Fig. 5 - Cone slope values and Hco/Wco ratio values for cinder cones in the ACBP. Predicted curve is from weathering and mass wasting model by Wood (1982b)

References

Inbar, M., Lugo Hubp, J., Villers Ruiz, L., 1994: The geomorphological evolution of the Paricutin cone and lava flows, Mexico, 1943-1990. Geomorphology, 57-76.

Inbar, M. Inbar, M., Risso, C., 2001. A morphological and morphometric analysis of a high density cinder cone volcanic field- Payun Matru, south-central Andes, Argentina. Z. Geomorph. 45, 321-343.

Inbar, M., Gilichinsky, M., Melekestsev, I., Melnikov, D., 2011: Morphometric and morphological development of Holocene cinder cones: A field and remote sensing study in the Tolbachik volcanic field, Kamchatka. J. of Volcanology and Geothermal Research. V. 201, 301-311.

Geological maps of volcanoes in Japan; lessons from one example tested by eruption

Jun'ich Itoh[1], Nobuo Geshi[2]

[1] *Geological Survey of Japan, AIST, Japan – itoh-j@aist.go.jp*
[2] *Geological Survey of Japan, AIST, Japan – geshi-nob@aist.go.jp*

Keywords: mapping, pyroclastic flow, risk recognition

Geological Survey of Japan (GSJ) is a public organization in The National Institute of Advanced Industrial Science and Technology (AIST), a National Research and Development Agency under the Ministry of Economy, Trade and Industry (METI) of the government of Japan. GSJ has consistently provided geological information in Japan since its establishment in 1882.

More than 400 Quaternary volcanoes are distributed in Japan, excluding submarine volcanoes (Nakano et al., 2013). 111 of them are active volcano which have eruption history since 10 ka and/or continued vigorous fumarolic activity. GSJ published geological maps (printed matter and/or GIS data) of more than 40 active volcanoes in Japan since 1980, and established databases on the Web.

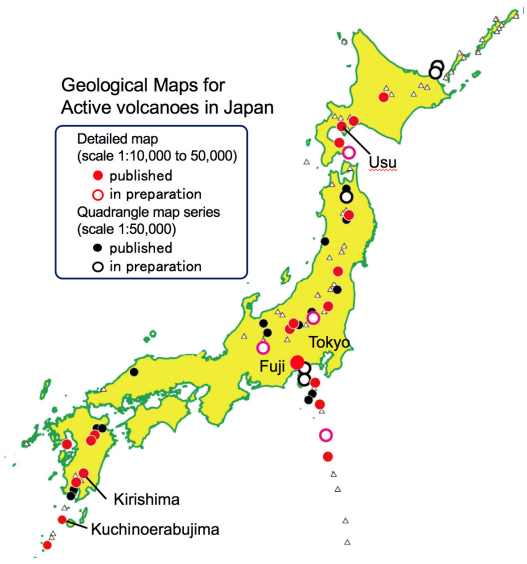

Fig. 1 Geological maps of Active Volcanoes in Japan, which are published and be preparing by GSJ

Japan is under warm and humid climate, volcanic products tends to be eroded by surface water, and covered by the development of soil and vegetation. For this reason, in the study of the eruption history based on field survey, trench survey is effective in addition to the observation of natural outcrop.

Fig. 2 Trench survey on the foot of active volcano

Volcano is one of the tourism resources, such as mountain climbing, tourists are likely to approach the crater and fumarolic area on active volcano. Even a small-scaled phreatic eruption, there is a risk that serious damage will occur to the climbers. In the case of the Ontake 2015 eruption, casualties occurred more than 60 climbers by phreatic eruption (ca. 10^9 kg, 10^5 DRE m^3; by Maeno et al. 2016). To reveal the history of such a small-scaled volcanic activity, there is a need for detailed geological survey in the vicinity area of the crater. And, to make correlation for phreatic deposits which have similar lithology, it is effective to compare the characteristics of mineral assemblage and/or eruption age for each deposits (ex. Itoh et al., 2014).

Geological maps are used for planning volcanic disaster prevention plans. The geological maps of Usu (Soya et al., 1981), Kirishima (Imura and Kobayashi, 2000), and Kuchinoerabujima (Geshi and Kobayashi, 2007) experienced eruption crisis resulted in the evacuation of inhabitants.

The geological survey of Kuchinoerabujima (it's means as Kuchinoerabu Island) for the publication of the geological map was performed in 2002-2005. During the field survey, some layers of block-and-ash flow deposit within 1000 years old were found in the flank of the main edifice. The grain components of the deposit suggest the phreato-magmatic – phreatic origin. Based on these geological evidences, the risk of the pyroclastic flow

in the volcano is recognized. In the surrounding area of the block-and-ash flow deposit, some ash layers associated with the minor eruption were also recognized but not identified in the map.

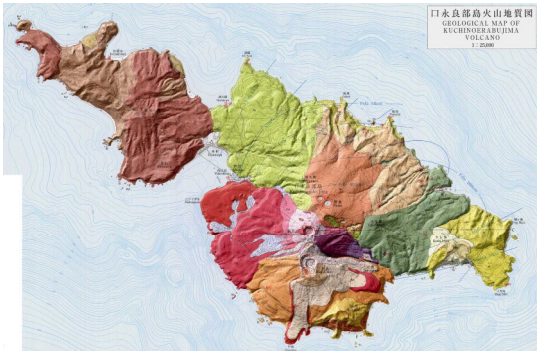

Fig. 3 Geological map of Kuchinoerabujima Volcano (after topographical shadow processing. Geshi & Kobayashi, 2016)

The 2014-2015 phreatomagmatic eruption in Kuchinoerabujima followed 34 years of hiatus (Geshi et al., 2016). The eruptions produced pyroclastic density current which threated the inhabited area. The pyroclastic density current formed block-and-ash flow deposits at the foot of the volcano. Their distribution coincides with that of the previous block-and-flow deposits mapped in the geological map. However, the diluted and high-velocity pyroclastic surge spread beyond the area of the block-and-ash flow deposit. Though the temperature of the sure is relatively low, below the ignition temperature of forest, one inhabitant entrained in the marginal portion of the flow was injured. The surge rests a very thin and easily eroded out. The deposit provides no clear sedimentary structure indicating the high-speed lateral flow.

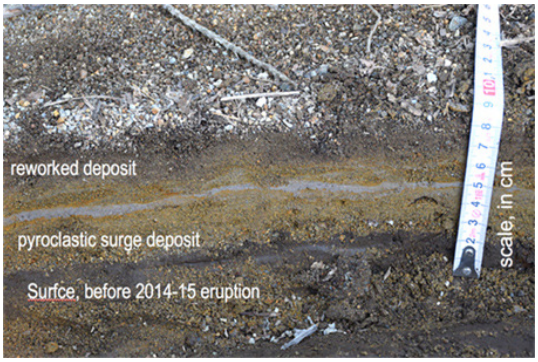

Fig. 4 Pyroclastic surge deposit, which was erupted 2014-2015 activitiy.

The reason why the geological map could not express the potential of the pyroclastic surge is the poor preservation and outcropping of the deposit and the difficulty to recognize the deposit as surge deposit. Some poorly-sorted ash layers with hydrothermally-altered ash were recognized in the soil layer, and some of them could be formed by surge, not fall-out. If the mapping of these "surge deposit" the geological map was more effective for the risk recognition and management.

The lesson from the eruption is 1) detailed geological investigation can reveal the unknown potential hazard of the volcano, 2) even the geologically-minor event can be hazardous, 3) horizontal extent of the events is difficult to detect only from the geological evidences, and we should combined the geological data and other methods such as numerical modeling or compiling of the examples over the world to figure out the entire view of the hazard.

References

Geshi, N. and Kobayashi, T. (2004) Kuchinoerabujima Volcano, Geological Map of Volcanoes no,14, GSJ

Geshi, N. et al. (2016) Phreatomagmatic Eruptions of 2014 and 2015 in Kuchinoerabujima Volcano Triggered by a Shallow Intrusion of Magma, Jour. Natural Disaster Science, 37(2), 67-78

Itoh, J. et al. (2014) Eruptive history of phreatic activity of Kuju Volcano during the recent 5,000 years, Bull. Volc. Soc. Jpn, 59, 241-254 (in Japanese)

Imura, R. and Kobayashi, T. (2001) Kirishima Volcano, Geological Map of Volcanoes no,11, GSJ

Nakano, S. et al. (2003) Volcanoes of Japan (3rd Edition), https://gbank.gsj.jp/volcano/Quat_Vol/act_map_e.html

Maeno, F. et al. (2016) Reconstruction of a phreatic eruption on 27 September 2014 at Ontake volcano, central Japan, based on proximal pyroclastic density current and fallout deposits. Earth Planets Space, 68: doi:10.1186/s40623-016-0449-6

Soya, T. et al. (1981) Usu Volcano, Geological Map of Volcanoes no.2, GSJ

The origin of the erupted magmas of the youngest volcano in the Carpathian-Pannonian Region (Ciomadul)

Balázs Kiss[1], Szabolcs Harangi[1], Theodoros Ntaflos[2], Christoph Hauzenberger[3] and Paul R. D. Mason[4]

[1] *MTA-ELTE Volcanology Research Group, Budapest, Hungary – balazskissgeo @gmail.com*
[2] *Department of Lithospheric Research, University of Vienna, Vienna, Austria*
[3] *Department of Earth Sciences Mineralogy & Petrology, University of Graz, Graz, Austria*
[3] *Department of Earth Sciences Mineralogy & Petrology, Utrecht University, Utrecht, Netherlands*

Keywords: dacite, mush column, petrogenesis.

Ciomadul lava dome complex is the youngest volcano in the Carpathian-Pannonian region and it was active in the late Pleistocene. The last eruption occurred only ~30 kyrs ago. The eruptions were fed by monotonous dacitic magmas with small compositional variation (SiO2=~63-69wt%) but there is no systematic change with time. The dacites are crystal-rich containing 25-30% phenocryst in rhyolitic glass. The dacites and the rhyolite glass show strong depletion in the MREE but no negative Eu-anomaly indicating the important role of amphibole fractionation during the magma evolution. The dacites have several textural evidence (e.g. coexisting quartz and olivine, resorption textures, multiple phenocryst populations) of open system evolution.

The erupted dacites contain abundant amphibole phenocrysts coexist with all of the rock forming minerals additionally amphiboles show large compositional variation (e.g. Al_2O_3: 6-15 wt%, Cr: 10-3000 ppm, Sr: 55-855 ppm, Eu/Eu*: 0.62-1.19) suggesting that they were crystallized at different conditions from different melts. Based on the calculations the studied amphiboles were crystallized from evolved rhyolite-dacite-andesite melts. Analysis of amphibole zoning indicates that single amphiboles are built up by different growth unites representing different melt components. Thermobarometry calculations based on amphibole crystals indicate that these melts were crystallized at ~750-1000°C and ~100-700 MPa.

Our results indicate that evolved melts R-D-A are captured in a trans-crustal storage zone and forming a magma mush column ~4-25 km below the volcano. This magma capture zone experienced incremental growth during continuous intrusion of evolved melts more probably originate from a lower crustal hot zone represented by incorporated olivine, cpx, opx, Cr-Spinel crystals. Fractional crystallization especially amphibole in the capture zone produce rhyolitic melts percolating upwards in the mush column. Eruption may occur when the migrating rhyolitic melts accumulate and melt/crystal ratio is high enough to mobilize some parts of the mush and produce mobile magma batches (i.e. the erupted dacites). This implies a relatively passive (i.e. not need the intrusion of fresh melts) process for the reactivation of the magma chamber and eruption initiation and also strengthen the idea of potential rejuvenation of the volcanic activity. Modell calculations suggest that the eruptions are fed by monotonous dacite magmas because rhyolitic melts buffer the composition of the erupted magma during the remobilization of dioritic mineral assemblage. This new petrogenetic model indicate that a complex magmatic plumbing system exists beneath the volcano. The deepest part experience basaltic input more probably at the crust-mantle boundary from the mantle. Differentiation processes in this basaltic hot zone produce evolved A-D-(R?) melts those are ascend into the upper crustal levels. The evolved melts crystallize in the lower-mid crustal levels and produce a vertically elongated amphibole sponge and rhyolite melts. Our model clearly indicates the important role of amphibole crystallization during the differentiation of Ciomadul's magmas and strengthens the amphibole sponge theory.

Facies architecture, alteration and mineralization at submarine felsic volcanic complexes: insights from the felsic centres of the Abitibi greenstone belt, Quebec, Canada

Lyndsay Moore[1], Réal Daigneault[2], Dominique Genna[3], Claude Pilote[4] and Claude Bernier[4], and John Stix[1]

[1] *Department of Earth and Planetary Sciences, McGill University, Montreal, Canada*
[2] *Centre d'études sur les ressources minérales, Université du Québec à Chicoutimi, Chicoutimi, Canada*
[3] *Consortium de recherche en exploration minérales (CONSOREM), Chicoutimi, Canada*
[4] *Falco Resources Ltd., Rouyn-Noranda, Canada*

Keywords: submarine, felsic complex, mineralization

Archean-aged sub-vertically- to vertically-dipping strata allow for the opportunity to study internal structures and organization of extrusive and intrusive volcanic facies of ancient submarine volcanic complexes. The 2704 – 2696 Ma Blake River Group in the Abitibi greenstone belt hosts numerous cross-sectional views through such complexes. The Rouyn-Pelletier caldera complex is one such example and is dominated by mafic extrusive and intrusive volcanic facies composing a shield-like base (Moore et al., 2016). Four felsic volcanic centres, the Glenwood, Delbridge, Horne and Quemont complexes, are found clustered in and around the stratigraphic top of the complex and located within a 4 km by 4 km area within the city limits of Rouyn-Noranda, Quebec. Each of these centres contains significant but variable amounts of base (copper, lead and zinc) and precious (gold and silver) metal mineralization:

Horne (H ore bodies): 6.1 g/t Au; 13 g/t Ag; 2.22% Cu (SIGEOM database)

Horne 5 : 1.58 g/t Au; 16.33 g/t Ag; 0.18% Cu; 0.81% Zn (www.falcores.com)

Quemont : 6.51 g/t Au; 30.85 g/t Ag; 1.31% Cu; 2.43% Zn (SIGEOM database)

Delbridge : 2.75 g/t Au; 109.34 g/t Ag; 0.45% Cu; 10.11% Zn (SIGEOM database)

Glenwood : Four intersections with an average of 5.38, 20.70, 1.99 and 0.68 g/t Au per metre (www.visiblegold.com)

Exact controls on this polymetallic mineralization are unknown but similar volcanic and intrusive facies are present at all four complexes (e.g. Lichtblau, 1989; Barrett et al., 1993; Kerr and Gibson, 1993; Moore et al., 2014). Their relationship to each other is also poorly understood but U-Pb radiometric dating indicates they have a relatively contemporaneous emplacement age of approximately 2702 Ma (Mueller et al., 2012; McNicholl et al., 2014). This study will: 1) define and compare and compare volcanic and intrusive facies at each centre; 2) identify major and minor phases of hydrothermal alteration and 3) compare and contrast styles and extent of mineralization. Although outcrop exposure in this region of the Abitibi is excellent, urban growth and mine development limit surficial mapping so a more multifaceted approach to this project is required.

Apart from the Glenwood complex, outcrop exposure for these centrese is limited. Outcrops of the Glenwood complex are extensively exposed and have recently been mapped in detail and sampled for whole rock geochemical analysis (Moore et al., 2014). At the Delbridge complex, only outcrops to the west of the deposit are still accessible and these were mapped by our team in 2007. Historical samples and drill holes of the mineralized zones are archived at the Geological Survey of Canada and will be used for further petrographic and geochemical analysis.

The Quemont and Horne complexes have been exploited for several decades but mining operations largely ceased after 1990. Outcrops for both complexes are limited by mine and urban development so volcanic and intrusive facies distribution will be largely reconstructed using a combination of whole rock geochemical analysis and diamond drill core logs. Falco Resources Ltd. has been drilling the Horne 5 ore body for the past several years as part of their regional exploration program. Detailed core logging and whole rock geochemical analysis has been completed for a total of 52 holes and this will be used to reconstruct the Horne 5 zone and southern Quemont complex. The northern extent of the Quemont complex is exposed at surface and detailed facies mapping and sampling for lithogeochemical analysis commenced in August, 2016.

Preliminary results have shown these complexes have notable characteristics and similarities:

1) All complexes have massive to brecciated felsic flows that are dominantly rhyodacitic in composition and have a transitional magmatic affinity. These facies have similar rare Earth element (REE) profiles when plotted on multi-element diagrams.

2) Chloritization, sericitization, carbonatization, silicification and albitization are present at all four centres to varying degrees. Minor epidote, hematite and anhydrite are visible in both Quemont and Horne 5 volcanic and intrusive facies.

3) At Delbridge, felsic volcanic facies transition from massive, quartz- and/or feldspar-phyric lavas in the west to dominantly brecciated at re-sedimented facies in the east, similar to the Glenwood complex. This distribution is consistent with an emission centre to the west and extrusion to the east and is in contrast to the north-south-trending units previously proposed (Barrett et al., 1993).

4) Both the Quemont and Horne complexes are dominated by massive to flow breccia facies that range from dacitic to rhyodacitic in composition. Basaltic to andesitic volcanic facies are present both before and after mineralized zones in the Horne complex. Massive to brecciated andesitic facies are also present prior to mineralized zones in the Quemont package.

5) Mineralized horizons of the Horne 5 zone are predominantly hosted within laminated and/or graded volcaniclastic facies until the eastern limit of the drilled area. These far-east holes are dominated by a large mafic intrusion and this becomes the host unit for stringer, semi-massive and massive sulfide mineralized zones.

6) Quemont and Horne facies transition into each other without any discernable boundary. The Horne Creek fault is used to separate the stratigraphy of these individual centres. This fault zone is more extensive than previously believed and ranges in thickness from several metres to several tens of metres in thickness. At this scale, it could potentially be a crustal-scale fault.

Future work will continue to focus on the compilation of drill log data and whole rock geochemical analysis for the Quemont and Horne 5 facies. Data will be formatted in a manner allowing for importation into GEMS and modeled in 3-D. Much of the gold and silver mineralization at all complexes is invisible and hosted within the structure of pyrite crystals. Reflected light petrography and laser ablation-inductively coupled plasma-mass spectrometry (LA-ICP-MS) analysis of pyrite and magnetite crystals is in progress (in collaboration with the Geological Survey of Canada under the Targeted Geoscience Initiative 5 program).

References

Barrett, T.J., Catalani, S., MacLean, W.H., 1993. Volcanic lithogeochemistry and alteration at the Delbridge massive sulfide deposit, Norranda, Quebec. Journal of Geochemical Exploration 48, 135-173.

Kerr, D.J., Gibson, H.L., 1993. A comparison of the Horne volcanogenic massive sulfide deposit and intracauldron deposits of the mine sequence, Noranda, Quebec. Economic Geology 88, 1419-1442.

Lichtblau, A., 1989. Stratigraphy and facies at the south margin of the Archean Noranda caldera. M.Sc. thesis, Département de Sciences de la Terre, Université du Québec à Chicoutimi, Chicoutimi, Québec, Canada, 136 p.

McNicholl, V., Goutier, J., Dubé, B., Mercier-Langevin, P., Ross, P.-S., Dion, C., and 4 others, 2014. U-Pb Geochronology of the Blake River Group, Abitibi Greenstone Belt, Quebec and Implications for Base Metal Exploration. Economic Geology 109, 27-59.

Moore, L.N., Daigneault, R., Aird, H.M., Banerjee, N.R., Mueller, W.U., 2016. Reconstruction and evolution of Archean intracaldera facies: the Rouyn-Pelletier Caldera Complex of the Blake River Goup, Abitibi greenstone belt, Canada. Canadian Journal of Earth Sciences 53, 1-23.

Moore, L.N., Daigenault, R., Genna, D., Hollings, P., Mueller, W.U., 2014. Exogenous and endogenous construction of the subaqueous Glenwood felsic flow complex; Abitibi greenstone belt, Québec, Canada. Precambrian Research 251, 18-140.

Mueller, W.U., Friedman, R., Daigneault, R., Moore, L., Mortensen, J., 2012. Timing and characteristics of the Archean subaqueous Blake River Megacaldera Complex, Abitibi greenstone belt, Canada. Precambrian Research 214-215, 1-27.

Geophysics mapping volcanoes

Jan Mrlina[1]

1 *Institute of Geophysics ASCR, Prague, Czech Republic – jan@ig.cas.cz*

Keywords: gravity survey, magnetics, volcano search.

Geophysical methods, mainly gravimetry and magnetometry, can serve as suitable tools for locating unknown hidden volcanic structures that are not expressed by any typical topographic features. These may be e.g. diatremes and maars with eroded scoria cones or rims of tuff/tephra material, as well as lava flows.

Gravity survey may reveal significant negative anomalies due to low density of the filling of volcanic vents, or positive anomalies over the bodies of compact lava accumulation. Magnetometry would rather show positive anomalies related to most of the volcanic structures due to high content of magnetic minerals in the volcanic rocks (except acid trachytes/phonolites/rhyolites). Geophysical surveys should therefore form part of any investigation of volcanic fields where some unknown volcanoes may still be expected.

Gravity monitoring can reveal hidden mass and fluids movement in a volcano interior, and can therefore contribute to the hazard control at regions with active volcanoes.

Other techniques can also contribute to mapping volcanoes, especially their interior structure. Electric resistivity tomography (ERT) can also identify e.g. the conductive filling of maar lakes, as well as fractured fault zones around a volcano. Seismic would define horizons, like bottom of maar lake, or different sedimentary and volcaniclastic formations.

A volcanic body often exhibits anomalous petrophysical properties of the rocks (hard volcanic rock, breccia, tuff, tephra, etc.), like density, porosity, magnetic susceptibility, resistivity etc. that can be recognized by geophysical measurements.

We, for example, identified a volcanic structure during the gravity mapping in the scale 1:25,000 where a single point with negative anomaly gave origin to a detailed survey discovering a small complex volcano. The structure was located in a negligible topographic depression, with no real indication as for morphological shape (Mrlina et al., 1989). On the contrary, volcanic craters in the Coastal Mts. in Syria are forming extreme inverse conical shapes with flat bottom of great size up to 3 km length and 300 m depth. However, only thanks to geophysical surveying it was possible to locate the volcanic chimneys (Mrlina, 1993).

During gravity investigation of the Cheb Basin in western Bohemian Massif an isometric negative gravity anomaly of unknown origin was revealed. Even recently we have confirmed the anomaly by detailed survey (Fig. 1), but due to lack of magnetic signal we still cannot produce unique interpretation. Here only drilling to 150-200 m would resolve the question.

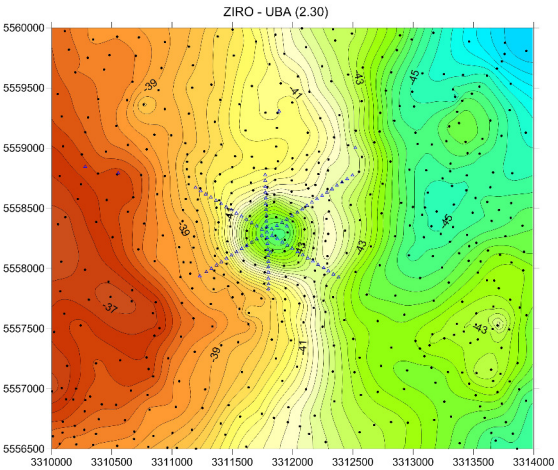

Fig. 1 – Gravity map of the western part of the Cheb Basin in the Bohemian Massif (Czech Republic). The striking negative anomaly under investigation is expected to be also some sort of maar-diatreme volcanic structure. The diameter is about 700 m. The Bouguer Anomaly amplitude reaches almost -4 mGal. Detailed profile study is ongoing.

On the contrary, we have recently found an unknown extraordinary volcano in West Bohemia. Based on observing an unusual topographic element – an almost circular depression (hardly to be seen in the field due to forest), and a gravity-magnetic scouting survey (Mrlina et al., 2007), we found a Quaternary maar near Cheb. The follow-up detailed geophysical survey enabled to position an exploratory well that confirmed the existence of a maar-diatreme volcanic structure filled by Quaternary lake sediments with organic substance that provided material for paleoclimate investigations Mrlina et al., 2009), see Figure 2.

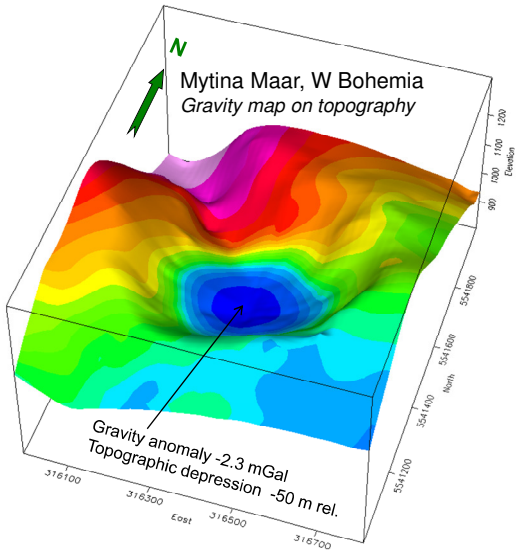

Fig. 2 – Very clear tie between topographic and geophysical signature of a maar structure; however, nobody had noticed this volcano until we did in early 2000s. The anomaly is -2.3 mGal.

The MY-1 well core showed the presence of layers with high content of organic material suitable for paleoclimate investigations. The lake sediments section was 84 m thick, underlain by country rock breccias with volcanic bombs. This depth was in good agreement with the preliminary simple model of Mrlina at al. (2007), who estimated this section to be about 90-100 m.

This case history is a typical example of using geophysics for discovering unknown volcanic structures, especially in cases where there is not enough evidence in topography for the presence of such structure. Gravity survey may locate various structures where the volcanic mass form bodies either with lower density (diatremes, scoria cones, etc.), or higher density (basaltic lava flows, homogeneous compact intrusions, etc.) compared to the country rocks.

We decided to apply also ERT for the definition of resistivity distribution in such structure. As expected, we obtained a very clear resistivity low corresponding to the sedimentary filling of the original maar depression, but also a few low resistivity zones, the principal of which indicated a fractured fault zone connecting another two small Quaternary scoria cone volcanoes in the maar surroundings (Flechsig et al., 2015).

In the Coastal Mts. in western Syria there are numerous volcanic craters with very spectacular topography; however, the aim of geophysical surveying there was to locate the diatreme chimneys that were not indicated by any topographic feature.

We applied gravity, magnetic and resistivity surveying and could locate such chimneys based on very low density and decreased resistivity. The chimneys, surprisingly, were quite small respective to the size of crater whose flat bottom could reach 3 and 1.5 km elliptical axial lengths.

As a specific task, gravity may be used for the location of voids/caves that may often origin in porous lava flows formations, like in Canary Islands, Saudi Arabia, or elsewhere. These areas may represent a hazard of collapse, especially if located in inhabited sites.

Repeated gravity measurements is an important tool for understanding the movement of various fluids, incl. magma, inside an active volcano. The mass displacement can be detected by both permanent observatory measurements, or a campaign style monitoring system. There are examples from Yellowstone, Dead Valley, Etna and other important volcanic areas.

In conclusion, we consider gravity and magnetic surveys as most efficient tools for volcanic structures location. Respective to public life, also gravity monitoring of active volcanoes is an important application of geophysics in this field.

References

Flechsig Ch., Heinicke J., Mrlina J., Kämpf H., Nickschick T., Schmidt A., Bayer T., Günther T., Rücker C., Seidel E. and Seidl M., 2015. Integrated geophysical and geological methods to investigate the inner and outer structures of the Quaternary Mýtina maar (W-Bohemia, Czech Republic). Int J Earth Sci (Geol Rundsch), DOI 10.1007/s00531-014-1136-0

Mrlina J., 1993. Gravity survey in selected localities in Western Syria. Geol.Průzk., 35, 5, 139-142. (in Czech)

Mrlina J., Kämpf H., Geissler W.H. van den Boogart, P., 2007. Assumed Quaternary maar structure at the Czech/German boundary between Mýtina and Neualbenreuth (western Eger Rift, Central Europe): geophysical, petrochemical and geochronological indications Z. geol. Wiss., 35, 4-5: 213-230.

Mrlina J., Kämpf H., Kroner C., Mingram J., Stebich M., Brauer A., Geissler W.H., Kallmeyer J., Matthes H. and Seidl M., 2009. Discovery of the first Quaternary maar in the Bohemian Massif, Central Europe, based on combined geophysical and geological surveys. J. Volc. Geoth. Res., 182, 97-112.

Mrlina J., Pospíšil M., Peška P., 1989, Geophysically disclosed occurrence of neovolcanites near Dobra Voda (Tepla Crystalline complex). Věst.Ústř.Úst.geol., 64, 6, 353-362.

Pitfalls with geological mapping of volcanic terrains: problem of concepts, scales and resolutions

Károly Németh[1] and **Julie Palmer**[1]

[1] *Massey University, Institute of Agriculture and Environment, Turitea Campus, Palmerston North, New Zealand – k.nemeth@massey.ac.nz*

Keywords: lithostratigraphy, volcanic facies, inter versus intra-eruption sequences.

The attempt to find a working geological mapping style that combines traditional stratigraphic methods with complex volcanic terrains has increased in recent years. Many methods recently adopted miss to capture the complex volcanic environment where a volcanic edifice and "*ring plain*" evolved over ka-to-Ma of years. *Unconformity-based lithostratigraphy* has recently been applied to many volcanic terrains [http://www.stratigraphy.org/]. This method is based on the identification and classification of unconformity surfaces associated with a volcanic terrain, similar to sequence stratigraphy as applied to non-volcanic successions. In is undeniable that volcanic edifice growth is commonly interrupted by catastrophic destructive events bounded by a well-defined "*unconformity surface*". The problem, however, is assigning a hierarchy to such surfaces especially to volcanoes that are long-lived and happen to occur in a region susceptible to such catastrophic events. Furthermore, as you go back in geological time identifying and distinguishing such surfaces with sufficient confidence and accuracy that make them useful for geological mapping can be problematic. This issue introduces ambiguity and questions the validity of using such unconformity-bounded surfaces for mapping purposes. Many volcanic edifices are long-lived and contain numerous unconformity surfaces many of which become ambiguous in the older rocks. While many claim that geologic mapping and the description of such unconformity surfaces in volcanic areas allows the definition of formal or informal **Unconformity Bounded Stratigraphic Units** (UBSUs) we argue that such UBSUs in volcanic terrains may not persist in the geological record.

Definition of lithosomatic and lithostratigraphic units have also been claimed as useful tools for the study of the temporal and spatial relationships among constructive and destructive phases of the volcano history, linking the stratigraphic information with tectonic and volcano-tectonic structures. Here we demonstrate several aspects from modern volcanoes and ancient volcanic terrains that this method has numerous flaws and should be used with great care. Volcanic edifices are commonly recognized and defined as lithosomes consisting of a group of lithostratigraphic units on the basis of their common volcanic sources. This approach implies that the classification is based on interpretative aspects of the volcanic terrain. It may introduce artificial boundaries to the classification reducing the genetic aspects of volcanic rock types identified on the field thereby partially violating the main purpose of the geological map, to provide spatial information about the specific processes operating and the rock assemblages produced. While the UBSU approach might work in old terrains, in young terrains (post-Pliocene) it will certainly oversimplify the geological map resulting in the loss of information vital to understanding the architecture of the volcanic edifice. Unconformities in the UBSU approach have a hierarchy. First-order unconformities are angular unconformities defined to be related to major changes in the volcanic and tectonic system. The problem with this approach is that major changes do not always produce readily traceable surfaces. On other hand, major unconformity surfaces representing "*accidental collapse*" in the life of a volcano can appear as dominant feature yet may not have significance in the overall evolution and development of the 3D architecture of the rock assemblages the geological map intends to capture. The problems are further exacerbated by the use of ***supersynthems***, defined as groups of rocks between the above mentioned first-order surfaces, even though these "*packages*" do not represent any fundamental process in the evolution of the volcanic system. Second-order unconformities are commonly used to define ***synthems*** and represent minor hiatuses, changes in the geochemical composition or erosive stages. Finally, third-order unconformities are commonly linked to local gravitational collapse of a volcanic edifice that can be used to define a ***subsynthem***.

At any scale and age of terrain, the geological map must capture both the *processes operating* and the *pathways* the region followed during its geological evolution. The geological map should reflect the geological evolution of the region rather than the evolution of a single or multiple volcanoes. Any volcano contributes sedimentary clasts that

accumulate in the adjacent basin whether it be terrestrial or marine/lacustrine. The relative role of the volcanic detritus will likely increase through time. The volcanic relationship in pre-Pliocene volcanic regions commonly consist of: **1)** volcanic core, where angular unconformities and facies relationships between rock units are clearly evident and **2)** aggradation units contributing volcaniclastic material to a sedimentary basin of any type, reflecting the presence of intrabasinal, or juxtapositioned, volcanism.

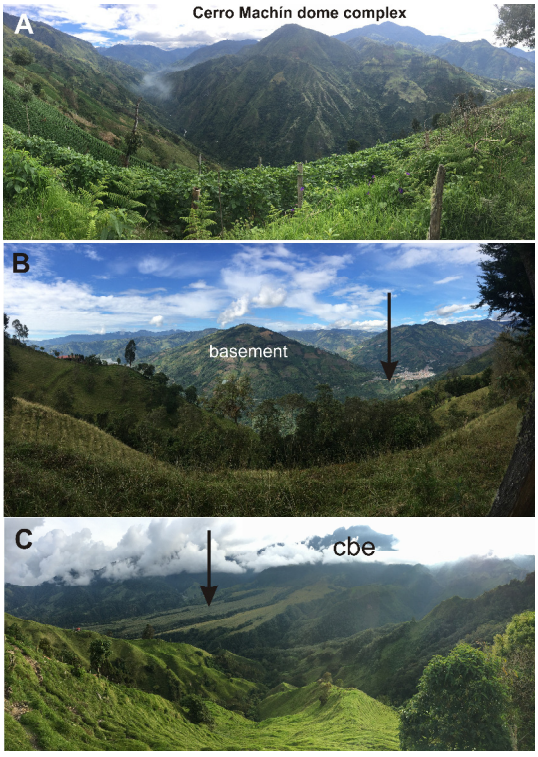

Fig. 1 – Cerro Machín volcano (A) in Colombia sitting on elevated basement that is incised by deep valleys capable to capture primary pyroclasts derived from the volcano by multiple processes. Distal valley networks commonly act as sediment channels for primary and secondary volcanic currents (B), however block-and-ash fans (C) can also form that are closer associated with an edifice (cbe – Cerro Bravo edifice) but still act as "sedimentary catchment areas" collecting primary and secondary volcanic deposits.

When mapping younger volcanics, the volcanic rock units and the volcanic processes they represent will determine the mappable units hence the stratigraphic classification. Hence the geological map must capture the various *eruptive phases*, *episodes* and *epochs* in 2D map form (eg. Manville et al. 2009). The mapping techniques should focus on **1)** identifying deposits formed through *suspension* versus *current deposition* and **2)** recognising *eruption-fed* versus *externally forced process-triggered* deposition. The establishment of *facies architecture* is essential so the link between the volcanoes and the adjacent sedimentary system can be established, without treating them as "*foreign*" bodies or separate entities (eg. Fisher and Smith 1991).

Various young volcanoes in the Central Cordillera in Colombia (Fig. 1) are major providers of volcanic detritus to terrestrial basins. While their eruptions are not always of significant volume and their edifice size is in a medium range, their effect to the surrounding sedimentary basins are dramatic by providing vast volume of volcaniclastics to the deep incised valleys forming valley ponded current deposited units (eruption-fed vs. externally forced). These valley-ponded units are potential volcanic hazards so it is crucial to understand the processes associated with their sedimentation. However, linking the volcaniclastic debris to individual sources is complex and traditional lithostratigraphy is challenging and at times problematic. Furthermore the same region receives suspension deposited ash and eruption-fed volcaniclastic flows, resulting in a complex inter-fingering of multi-sourced deposits. The best approach to mapping these units is to carefully observe and record the field relationships to establish the stratigraphic succession. This is even more important in medial to distal areas where volcaniclastic fans can grow, evolve and form various surfaces with angular relationships within normal sedimentary sequences. Only after completing this work can stratigraphic units be practically applied.

In old (eg. pre-Pliocene) terrains it is useful to follow this lithological approach to defining mapping units. However, such units still need to capture the processes operating at the time of deposition.

The primary purpose of geological maps is to relay the geological evolution of a region at a specific scale. Instead of focusing and ranking various unconformity surfaces the mapping should focus on understanding the processes that produced the rock assemblages both spatially and temporally. Volcanoes are intrabasinal features that are very much a part of the sedimentary environment they formed in (eg. Manville et al 2009).

References

Fisher RV, Smith GA (1991) Volcanism, tectonics and sedimentation. In: Fisher RV, Smith GA (eds) Sedimentation in Volcanic Settings. SEPM Special Publication, Tulsa, Oklahoma USA, pp 1-5

Manville V, Németh K, Kano K (2009) Source to sink: A review of three decades of progress in the understanding of volcaniclastic processes, deposits, and hazards. Sedimentary Geology 220(3-4):136-161.

Volcanic and tectonic evolution of La Reforma caldera, Baja California Sur, Mexico

Claudia Pellicioli[1,3], Laura García Sánchez[2], Susana Osorio-Ocampo[2], Gianluca Groppelli[3], José-Luis Macías[2] and Roberto Sulpizio[3,4]

[1] *University of Milan, Department of Earth Sciences, Milan, Italy – claudia.pellicioli@unimi.it*
[2] *Instituto de Geofisica, Universidad Nacional Autónoma de México, Morelia, Michoacan, México*
[3] *CNR – Department of Environmental Processes Dynamics, Milan, Italy*
[4] *University of Bari, Department of Earth and Geo-Environmental Sciences, Bari, Italy*

Keywords: caldera, tectonics, geological evolution.

La Reforma volcanic district is located in the Santa Rosalia basin, Baja California Sur, Mexico. The fourth largest currently producing geothermal field in Mexico (Tres Virgenes) lies only few kilometers away. The faults pattern responsible for the geothermal fluids production in this area is linked to the Gulf of California opening (10 My) and subsequent rotation of the stress field (Zanchi, 1994) due to the development of a transform plate boundary (3.5 My).

The purpose of the study is to investigate the interplay between regional tectonics and magmatism and to reconstruct the evolution of La Reforma, along with hydrothermal fluids circulation paths and porosity-permeability distribution throughout the area. This will have implications on current and future assessments of geothermal potential in the area. In order to investigate the regional extension of the main faults that affect La Reforma caldera, we also performed a preliminary structural survey in the surroundings of Aguajito volcanic district, located only few kilometers NW from La Reforma.

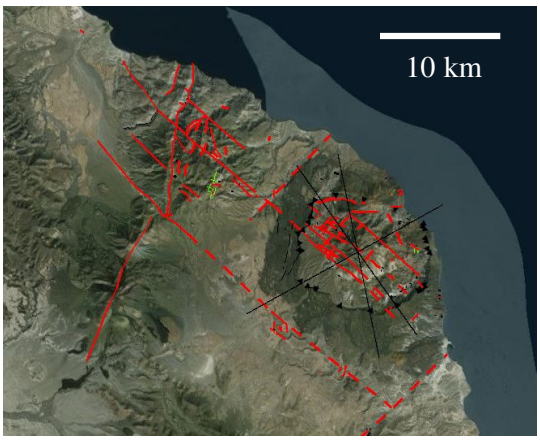

Fig.1– Schematic representation of main faults in the study area (La Reforma on the right, Aguajito on the left and Tres Virgenes on the bottom left).

The interdisciplinary methodology includes geological field surveys, structural stations, volcanological studies and X-Ray analysis for mineral alteration and fluid circulation.

La Reforma caldera

At least four different ignimbrites were found in La Reforma volcanic district. In spite of this, only one caldera collapse can clearly be seen based on morphology. Volumetric estimates of ignimbrites products are believed to help giving an insight on the presence of older caldera collapses covered by subsequent volcanic activity. Following deposition of volcanoclastic and sedimentary sequences during Miocene, a first phase of submarine activity began in La Reforma, with the emplacement of the Cueva Amarilla ignimbrite (Upper Pliocene), interlayered with minor pyroclastic flows, pillow lavas and hyaloclastites. The Grey and Discordia ignimbrites emplaced during lower Pleistocene over a quite uniform area and were followed by La Reforma and the White ignimbrites (García-Sánchez et al., 2015).

Soon after the caldera collapse a phase of resurgence started, with a vertical uplift of pre-caldera and older products to reach the present altitude of about 1200 m a.s.l. Resurgence went along with the emplacement of dykes feeding summit domes and lava flows on top of the White ignimbrite. Resurgence appears to be strongly controlled by regional tectonics. NW-SE transform faults displaying a normal-dextral kinematics in the current stress field mark the presence of a granitic basement slice. These faults did also act as corridors for hydrothermal fluids, as testified by the presence of important sites of Au-Cu mineralization, historically mined by the local population.

Aguajito

Only one ignimbrite, the Aguajito ignimbrite (middle Pleistocene), was found within the Aguajito volcanic center. The evolution of Aguajito has been strongly influenced by regional tectonics. The

clearest example of this is the presence of a NNE-SSW trending fault (Cimarron fault) that fully cross-cuts Aguajito and the Tres Virgenes geothermal field (Garduño-Monroy et al., 1993).

The early stages of Aguajito activity postdate La Reforma magmatism and consists in submarine lava flows, hyaloclastites, shell-bearing sandstones and local submarine pyroclastic flows. The emplacement of the Aguajito ignimbrite suggests the presence of a caldera collapse (Garduño-Monroy et al., 1993). However, the growth of two distinct stratocones on top of the Aguajito ignimbrite makes it difficult to see any morphological evidence of a caldera. The last stage of Aguajito evolution is the emplacement of domes and related lava flows on top of the stratocones (Osorio-Ocampo et al. (2015)).

The interplay between tectonics and magmatism in Aguajito appears more complicated than in neighboring La Reforma. The boundaries between the two stratocones trend either NW-SE or N-S, suggesting a strong tectonic control at the time of their emplacement. The Azufre NW-SE trending fault dissects the Cimarron fault in the south-western part of Aguajito and presently acts as a corridor where hydrothermal fluids have strongly altered the volcanic succession at surface (Wong et al., 2006). Finally the Cimarron fault seems to have had a primary role in controlling magma rise, as magmatic activity appears to have moved from the N (Aguajito) to the S (El Virgen, last eruption in Pleistocene-Holocene).

Work done so far has allowed improving the existent cartography and understanding of La Reforma and Aguajito evolution. 1:50,000 scale geological maps of both volcanic districts are currently at the stage of being revised and refined for publication. Still many points remain to be investigated. Among these the most important one regards the chance of having caldera collapses older than La Reforma collapse. Analysis of faults, fractures and veins measurements is currently ongoing to produce a structural model for the La Reforma volcanic district. In addition to field data, the structural model will include results coming from the analysis of deformational mechanisms along fault planes and the estimate of relative permeability of different ignimbrites litotypes. This will allow making few points about preferential circulation pathways for hydrothermal fluids.

References

García-Sánchez L. et al., 2015. V23B-3104 ABSTRACT Stratigraphy of Reforma caldera, Baja California Sur, Mexico. AGU FALL MEETING, San Francisco, 2015.

Garduño-Monroy V.H., Vargas-Ledezma H. and Campos-Enriquez J.O., 1993. Preliminary geologic studies of Sierra El Aguajito (Baja California, Mexico): a resurgent-type caldera. Journal of Volcanology and Geothermal Research, 59 (1993) 47-58.

Osorio-Ocampo L.S. et al., 2015. V23B-3100 ABSTRACT Stratigraphy of pyroclastic deposits of El Aguajito caldera, Baja California Sur, Mexico. AGU FALL MEETING, San Francisco, 2015.

Wong V. and Munguía L., 2005. Seismicity, focal mechanisms and stress distribution in the Tres Vírgenes volcanic and geothermal region, Baja California Sur, Mexico. Geofísica Internacional (2006), Vol. 45, Num. 1, pp. 23-37.

Zanchi A., 1994. The opening of the Gulf of California near Loreto, Baja California, Mexico: from basin and range extension to transtensional tectonics. Journal of Structural Geology, Vol. 16, No. 12, pp. 1619 to 1639.

The significance of debris avalanche deposits in the architecture of the Călimani-Gurghiu-Harghita volcanic range (Eastern Transylvania, Romania)

Ioan Seghedi[1], Alexandru Szakács[1,2], Zoltán Pécskay[3], Viorel Mirea[1] and Péter Luffi[1]

[1] *Institute of Geodynamics, Romanian Academy, J.-L. Calderon 19-21, 020032 Bucharest, Romania – seghedi @geodin.ro*
[2] *Sapientia University, Department of Environmental Sciences, 4 Matei Corvin Str., 400112 Cluj-Napoca, Romania*
[3] *Institute of Nuclear Research, Hungarian Academy of Sciences, P.O. Box 51, Bem ter 18/c, H-4001, Debrecen, Hungary*

Keywords: Neogene volcanism, debris avalanche deposits, volcanic facies, Eastern Transylvania.

Unraveling the structure of the Neogene Călimani-Gurghiu-Harghita volcanic range (CGH) represents a complex and provocative geological issue. The first general volcanological interpretation (Rădulescu et al., 1964) resulted from extrapolation of field observations in the Gurghiu volcanic area to the whole range. In that view, the overall structure of the chain has been divided into two superposed compartments, which formed during two distinct stages. The lower compartment, outcropping mainly along the western periphery and coined as the "volcano-sedimentary formation" was thought to be generated during an initial, dominantly explosive volcanic activity, whereas the upper compartment comprising the axial stratovolcanic edifices was thought to be built up onto the lower compartment. New volcanological observations supported by K/Ar dating led to an alternative structural model in which the volcaniclastic deposits at the periphery of the CGH represent the medial-distal facies of the adjacent composite volcanoes (Szakács & Seghedi, 1995). Although debris-avalanche deposits (DAD) have been recognized locally at that time, their extent was unknown and their significance was poorly understood.

Concomitantly, the increasing number of K-Ar age data (Pécskay et al., 1995) confirmed the migration of the volcanism from NNW to SSE along the range as suggested earlier (e.g., Rădulescu et al., 1972; Peltz et al., 1987). The almost continuous volcanic activity between 10.2-0.03 Ma built up a row of closely spaced, juxtaposed or partially overlapping medium- sized composite volcanoes; two of these (Călimani; Fâncel-Lăpuşna) evolved to the caldera stage almost in the same time interval (7.0-6.8 Ma) (Fig. 1).

The moderately eroded composite volcanoes of CGH are medium-sized (1000-1500 m relative heights) and their volume systematically decreases southwards (Szakács et al., 1997). Their generally well-preserved cone morphology is limited to the central and proximal facies.

More recently, two major DADs have been identified at the western periphery of CGH (Szakács and Seghedi, 2000). The largest one belonging to the Rusca-Tihu volcano (Călimani Mts.) has displaced ca. 26 km^3 volcanic debris along a 55 km runout distance. The second one originated in the Vârghiş volcano (North Harghita Mts.) has dispersed ca. 13 km^3 of material along a 50 km long runout distance.

The assignment of the volcaniclastic deposits at the western periphery of CGH to different eruption centers has taken into account the various genetic types (pyroclastic, debris-avalanche, debris flow). In some cases, establishing the volcanic source proved to be difficult because of the rather monotonous petrography and geochemistry characterizing the entire range.

Our detailed geological mapping, petrographic observations, and K-Ar geochronology conducted over the past five years enabled a more realistic and comprehensive view about the origin and emplacement history of the volcanoclastic deposits including various DADs in the CGH.

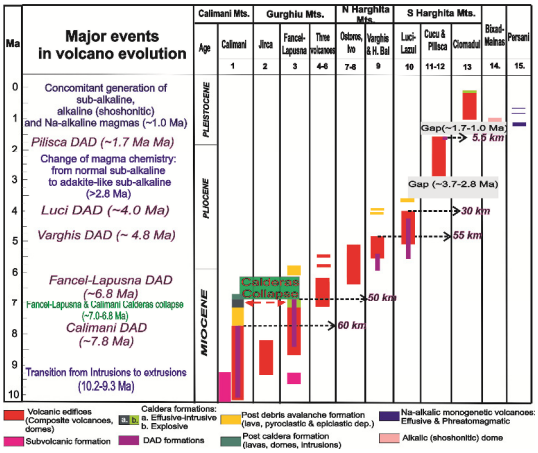

Fig. 1 – Simplified time sequence of the main debris avalanche events and other "major events" in the evolution of the Călimani-Gurghiu-Harghita chain (DAD runout distances are shown by the dashed arrows).

Major volcanic edifice failure events, besides caldera-forming eruptions which were considered as "major events" shaped the volcanic evolution of CGH. We identified and outlined three

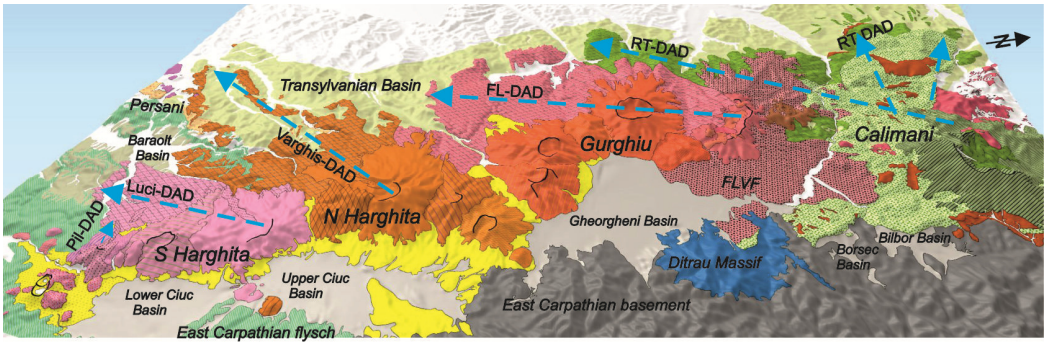

Fig. 2 - 3D view of the simplified volcanological map of the CGH Mts., highlighting the Rusca-Tihu DAD (RT), Fâncel-Lăpuşna DAD (FL), Vârghiş DAD, Luci DAD and Pilişca DAD (Pil) showing the runout distribution (blue arrows)

new, previously unknown, DADs in the Gurghiu and South Harghita Mts. The major DADs are typically represented by thick (tens of m) chaotic mega-breccia with an unsorted, massive, polymictic character. They are extremely heterogeneous at the outcrop scale, displaying sudden lateral variations in their texture and lithology. DAD-specific features such as jigsaw cracks, breccia-in-breccia, and plastic deformations (soft sediment deformation) are common.

Several volcanoes (Rusca-Tihu in the Călimani Mts., at ~7.8 Ma, Fâncel-Lăpuşna at 6.8 Ma in the Gurghiu Mts.; Vârghiş at ~4.8 Ma in the North Harghita and Luci sector collaps of Luci-Lazu volcano at ~4.0 Ma in the South Harghita) experienced edifice-failure events and generated large-volume DADs (Fig. 1). A small volume DAD originating in the ~1.7 Ma Pilişca volcano (South Harghita Mts.) was also identified (Fig. 1).

We suggest that most of the edifice failure events (excepting Fâncel-Lăpuşna), are closely related to a series of tectonic processes including the opening and southward propagation of the Borsec/Bilbor, Gheorgheni, Upper and Lower Ciuc intermountain basins and growth of new volcanoes. The contemporaneous formation of basins and activation of the volcanism, the southward propagating fault system and the geometry of the faults and alignment of volcanic centers indicate strike-slip and normal faulting systems (e.g., Fielitz & Seghedi, 2005). All the DADs were emplaced toward SSW direction from their source volcano, most likely following the preexisting topography sloping toward the Transylvanian Basin (Fig.2).

The Fâncel-Lăpuşna DAD is apparently closely related to the Plinian caldera-forming event (F-L Volcaniclastic Formation) and the collapse of the southern volcano flank (Fig 2). In the South Harghita Mts., the Luci DAD has strongly influenced the evolution of the Baraolt Basin, which acted as a depocenter for the DAD and associated volcaniclastic /epiclastic deposits. Hence, several small-size lacustrine basins developed atop the Luci DAD, where diatomites were accumulated. The new volcanological observations indicate that the medial-distal volcanic facies on the western periphery of CGH is volumetrically dominated by DADs (>75%) in association with debris flow deposits, and are locally overlapped by proximal-medial facies products of the neighboring younger composite volcanoes.

Acknowledgements

Financial support by grant PN-II-ID-PCE-2012-4-0137 of the Romanian Ministry of Education and Scientific Research is acknowledged.

References

Fielitz W., Seghedi I., 2005. Late-Miocene-Quaternary volcanism, tectonics and drainage system evolution in the East Carpathians, Romania. Tectonophysics 410, 111-136

Pécskay Z., et al., 1995. K-Ar datings of Neogene-Quaternary calc-alkaline volcanic rocks in Romania, Acta Vulc. 7, 53-61.

Peltz, S.; Vâjdea, E.; Balogh, K.; Pécskay, Z., 1987. Contributions to the chronological study of the volcanic processes in the Călimani and Harghita Mts. (East Carpathians, Romania) D. S. Inst. Geol. Geofiz., Bucureşti, 72–73/1, (1985; 1986), 323-338

Rădulescu, D. P., et al., 1964. Contribuţii la cunoaşterea structurii geologice a muntilor Gurghiu. Ann. Com. Geol., 33, 87-151.

Rădulescu, D. P., Pătraşcu, Ş., Bellon, H., 1972. Pliocene geomagnetic epochs: new evidence of reversed polarity around the age of 7 m.y. Earth Planet. Sci. Lett., Amsterdam, 14/1, 70- 72

Szakács A., Seghedi I., 1995. The Călimani-Gurghiu Harghita volcanic chain, East Carpathians, Romania: Volcanological features, Acta Vulc., 7, 145-153.

Szakács A, et al., 1997. Rates of migration of volcanic activity and magma output along the Călimani-Gurghiu-Harghita volcanic range, East Carpathians, Romania. Przglad Geologiczny 45, 10/2: 1106.

Szakács A., Seghedi I. (2000) Large volume volcanic debris avalanche in the East Carpathians, Romania. in H. Leyrit & C. Montenat (eds) "Volcaniclastic rocks, from magma to sediments", H., Gordon Breach Science Publishers, p. 131-151.

Morphological features of debris avalanches deposits from Molodoy Shiveluch Volcano

Alina Shevchenko and Viktor Dvigalo

Institute of Volcanology and Seismology FEB RAS, Petropavlovsk-Kamchatsky, Russian Federation – al.vic.shevchenko@gmail.com

Keywords: andesitic volcano, debris avalanche, photogrammetry.

Molodoy Shiveluch is the most active andesitic volcano of the Kamchatka Peninsula. It is located at the junction of the Aleutian and Kamchatkan volcanic arcs. Its edifice was formed due to the lava domes growth, with their subsequent destruction by large explosions and gravitational processes. The southern foot of the volcano, where the bulk of the erupted material is carried out, is covered with pyroclastic flows and debris avalanches deposits of different ages.

The November 12, 1964, Molodoy Shiveluch catastrophic eruption destroyed several coalescing lava domes nested within a horseshoe-shaped caldera. As a result, a new double-shaped avalanche caldera was formed. The diameter of its northern part was 1750 m, and of the southern part was 2050 m. The volume of the collapsed material was 1.03 m^3. The debris avalanche covered 104 km^2 of the southern foot of the volcano. Pyroclastic flows that followed the collapse covered fanwise the area of 45.5 km^2. The thickness of the front of the debris avalanche deposits varies mostly from 1 to 8 m. In some places it is up to 20 m thick. The thickness of the pyroclastic flows has reached 10 m.

Deposits, possibly related to the previous large eruption of 1854, underlay the deposits from the 1964 catastrophic eruption. Though these deposits only fragmentarily protrude from the 1964 deposits (total area is 2.6 km^2), we can say with confidence that there are starkly different morphologies in their surfaces (Fig. 1, fig. 2).

The surface of the 1964 collapse deposits is similar to the surfaces of large mountain landslides and has a number of ridges elongated in the direction of movement. Previously, Melekestsev et al. (2003) assumed that these ridges had been formed due to the explosive-collapse nature of the avalanche movement. However, Dufresne and Davis (2009) presented landslide deposits that had the same ridges on the surface. Therefore, gravitational collapse is a sufficient precondition for the formation of such ridges, and their presence can't indicate the explosive origin of the avalanche.

The surface of the visible fragments of the underlying deposits is creased into wavelike folds stretched along the front of these deposits. Such folds could have been formed as a result of viscous-plastic flow. On the flanks of the fragments, especially in less flat areas, folds stretch along the slope in the form of levees. The wavelength of the folds varies from 13 to 40 m, and their heights reach 14 m. Most of the folds are straight. Their axial surfaces are vertical, and their limbs are symmetrical. Inter-limb angles range from 20˚ to 50˚.

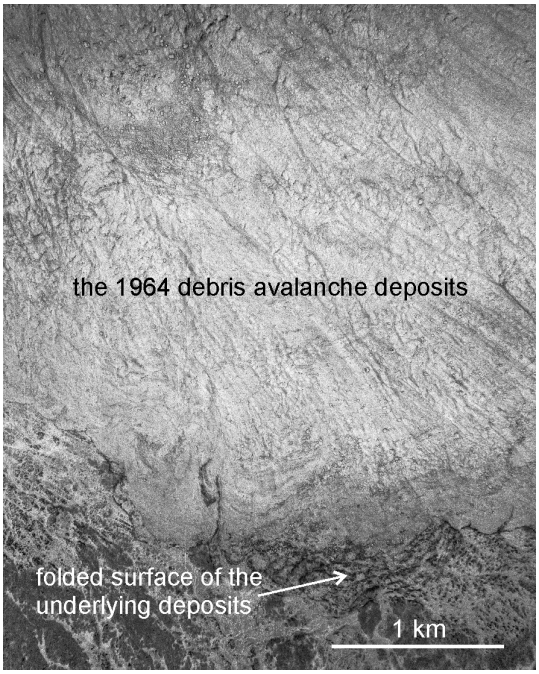

Fig. 1 – Aerial photo of southeastern sector of the Molodoy Shiveluch deposits field. Photo by L.B. Dmitriev and G.S. Shteinberg, November 17, 1964.

Previously, there were two suggestions for the appearance of such a relief. According to Melekestsev et al. (2003), these folds were formed as a result of the impact of the 1964 explosive material on the watered underlying deposits. Belousov et al. (1999) termed these deposits "bulldozer facies" since, in the opinion of the authors, they were folded by the 1964 debris avalanche that bulldozed the underlying surface.

However, interpretation and photogrammetric processing of recently found aerial photographs of November 17, 1964, showed that these deposits had been folded long before the 1964 eruption. In the photographs obtained five days after the events of 1964, we can see trees (10 m in average height) growing on the ridges of the folds and in the depressions between them. The trees' trunks stand vertically and have no signs of damage. The trees are felled only in the areas prone to the lahars of 1964. Consequently, the 1964 eruption may have no relation to the origin of the folds.

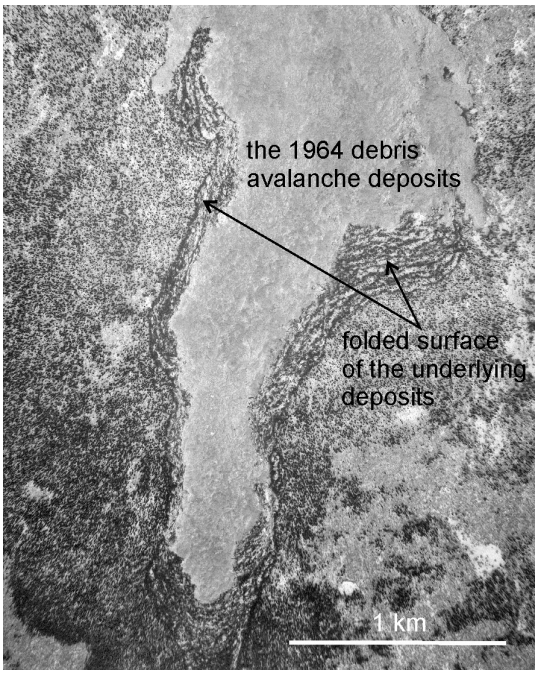

Fig. 2 – Aerial photo of the central part of the Molodoy Shiveluch deposits field. Photo by L.B. Dmitriev and G.S. Shteinberg, November 17, 1964.

There is also no correlation between the hinge lines of the folds and the front line of the 1964 deposits. In some places, the folds go under the surface of the 1964 deposits almost at right angles.

The formation of the folds due to the impact of the 1964 debris avalanche was impossible because of the very small thickness (first meters) of the avalanche front in these areas. It is hard to imagine that an avalanche with a thickness of up to 3 m formed up to 14-metre-thick folds on the underlying surface. Meanwhile, in the areas adjacent to the 1964 deposits front of high thickness (up to 15 m), no folds are observed. Besides, in some places we can observe large folds protruding through the thin surface of the 1964 deposits at a distance from the front.

Therefore, we can suggest that it was not the 1964 debris avalanche that formed this folded surface, but, on the contrary, the form of the bedding of the collapse material was caused by the already existing relief, which predetermined the movement of the 1964 debris avalanche so that its material accumulated in the local depressions, colliding with the folds.

Unfortunately, the materials of aerial photography of Molodoy Shiveluch that was performed in the 1940's are not available. So we can only guess what the morphology and location of the studied deposits had been like before the 1964 eruption.

In any case, it is necessary to find out how the described folded terrain was formed. We think that photogrammetric method has done everything it could, and the answer to this question is to be given by further direct geological studies.

References

Belousov A., Belousova M., Voight B., 1999. Multiple edifice failures, debris avalanches and associated eruptions in the Holocene history of Shiveluch volcano, Kamchatka, Russia. Bull. Volcanol. 61, 324-342.

Dufresne A., Davies T.R., 2009. Longitudinal ridges in mass movement deposits. Geomorphology. 105, 171-181.

Melekestsev I.V., Dvigalo V.N., Kirsanova T.P., Ponomareva V.V., Pevzner M.M., 2003. The 300 years of Kamchatka volcanoes: the Young Shiveluch. An analysis of the dynamics and impact of eruptive activity during the 17-20th centuries. Part I. 1650-1964. Vulkanol. Seismol. 5, 3-19 (in Russian).

The challenge of mapping in poorly-exposed volcanic areas: an Introduction

Alexandru Szakács[1, 2], Ioan Seghedi[1]

[1] *Institute of Geodynamics, Romanian Academy, Bucharest, Romania*
[2] *Department of Environmental Sciences, Sapientia University, Cluj-Napoca, Romania*

Keywords: volcano geology, mapping, fieldwork

Mapping is the first fundamental step in unraveling and understanding geological evolution at any scale, from regional to local. In volcanic areas it is extremely difficult, as compared, for example, with sedimentary terraines, basically because the complicated/irregular geometry of volcanic rock bodies. The outcome of mapping is strongly dependent on the age/degree of erosion and outcrop availability, besides scale, map-type and researcher expertise/subjectivity.

Decades-long fieldwork experience in Miocene volcanic areas in Romania led us to the recognition that mapping in older and poorly exposed volcanic areas requires different methodological approaches as compared to active/recent volcanic regions. Because the heavy soil and vegetation coverage, exposures are unevenly present: continuous outcrops (100x m long) along some major valleys alternate with few and small (1x to 10 x m) outcrops along smaller tributaries and ridges and with large (km^2-scale) areas of no any exposure. Exposed contacts between rock bodies or formations are thus extremely rare to absent. In such circumstances correlation between established cartographic entities is largely based on interpolation and extrapolation, sometimes over large no-outcrop areas. Researcher experience and even subjectivity play an important role in the final outcome of the mapping. Remote sensing techniques are hardly applicable because erosion and soil/vegetation coverage. Topographic features are sometimes relevant – in particular when rocks of contrasting hardness are in contact – and used in tracing geologic boundaries on map. One more complicating factor in mapping older volcanic areas is that early volcanic products and/or basement formations may crop out punctually – i.e. in one single or very few exposures - from beneath younger formations. This helps, however, to cover a longer volcanic history as compared to active/recent volcanoes. Post-volcanic tectonics is another problem.

For these reasons maps realized in ancient and poorly-exposed volcanic areas look quite different from those obtained for recent/active volcanoes. Also, their level of confidence is much lower.

The recently developed and promoted lithostratigraphic concept and methodology (e.g. Branca et al., 2011) is successfully applied in mapping active/recent volcanic areas such as, for example, those in Italy, Azores, Madeira. Some aspects of that approach - the "synthemic/UBU approach", for instance -, essentially based on identification, ranking and mapping of unconformities in the volcanic successions, is still under debate. If there is a whole spectrum of exposure conditions – i.e. from almost continuous exposure at some active volcanoes to almost no exposure at many ancient volcanoes – the field conditions met in many volcanic areas worldwide are closer to the no-exposure end-member of that spectrum. It seems inevitable that in such circumstances the lithostratigraphic approach and methodology, successful in well-exposed areas, has to be adapted and/or completed with new perspectives and methodologies. One significant issue, for instance, is the fact that in poorly-exposed areas discontinuities between synthemic units identified in outcrops are absent or, at most, accidental, so their correlation and ranking extremely difficult, hence they cannot be used as objective features to systematize and order lithostratigraphic entities such as synthems, subsynthems, etc. Rather, discontinuities will eventually emerge at the end of the mapping process, as interpreted features, while processing all fieldwork and analytical information. Instead of field-identifying and tracking unconformities as the basic time-marker entities of volcanic evolution in well-exposed areas, features/formations resulted from major events, either constructive or destructive (i.e. "master-events", as defined and conceptualized elsewhere; Szakács and Canon-Tapia, 2010) such as sector collapse, or caldera formation, are to be considered as the major milestones of volcano evolution. They have the advantage of being easily mappeable due to their large volumes and wide dispersal areas. Also they are quite frequent in volcanic areas dominated by large composite volcanoes such as the Miocene-Pleistocene Călimani-Gurghiu-Harghita range in the East Carpathians, Romania. However, in the case of

small-sized volcanoes which did not underwent such major destructive events, this approach is less effective. Due to their small size, and generally less complex structure, such volcanoes can be mapped by combining outcrop observation with topography and geophysics within the lithosomatic approach.

Another approach in defining map units in volcanic areas is that emerging from the volcanic facies concept which helps systematizing volcanological information in function of dispersal areas of volcanic products with respect to their sources. Defining the spatial position of a certain formation of volcanic rocks or of a volcanic sequence with respect to their source area(s) is a crucial step in order to understand volcanic structures/edifices and evolution.

Taking in to account our experience in ancient volcanic areas, and learning from expertise gained by others in active/recent volcanic areas, we may suggest that a flexible combination – according to the level of exposure and age of volcanism - of the UBU-based lithostratographic approach with the facies-based approach and the "major/master-event"-based approach might lead to the best results in mapping volcanic terraines. Each of these three approaches has to be considered in terms of map units and corresponding Legend symbols. To develop such a combined system of map symbols, as part of an envisaged "Guidelines in volcano mapping", could be a major and attractive task of the IAVCEI Commission on Volcano Geology.

Acknowledgements

We thank IVCEI and Institute of Geodynamics for their contribution for the success of the workshop.

References

Branca S., Coltelli M, Groppelli G. (2011) Geologic evolution of a complex basaltic stratovolcano, Mount Etna, Italy. *Ital.J.Geosci.* (Boll.Soc.Geol.It.), 130, 3, 306-317, doi: 10.3301/IJG.2011.13

Szakács A., Canon-Tapia E. (2010) Some challenging new perspectives of volcanology. In Canon-Tapia, E. and Szakács, A, eds., What is a Volcano? Geological Society of America Special Paper 470, 123-140, doi: 10.1130/2010.2470(9)

Reconstructing the facies architecture and depositional settings of Miocene pyroclastic sequence, Tokaj - Slanske Mountains, Carpathian-Pannonian region

János Szepesi[1], Ildikó Soós[1], Réka Lukács[1], Roberto Sulpizio[2], Gianluca Groppelli[3], and Szabolcs Harangi[1,4]

[1] *MTA-ELTE Volcanology Research Group, Budapest, Hungary – szepeja@gmail.com*
[2] *Dipartimento di Scienze della Terra e Geoambientali, Università degli Studi di Bari, Italy*
[3] *CNR-Istituto per la Dinamica dei Processi Ambientali, Milano, Italy*
[4] *Department of Petrology and Geochemistry, Eötvös University, Budapest, Hungary*

Keywords: silicic explosive volcanism, ignimbrite, pyroclastic density currents, Hernád through

Introduction

The older volcanic successions are erosional relics of complex volcanic centres (Cas and Wright 1987). The original extent and geometry may be severely modified (erosion, tectonics) and the reconstruction of lateral facies connections and vertical succession could be more complicated. In this respect, the Carpathian-Pannonian Region (CPR) provides an advantage due to its mature and commonly erosion-modified volcanic landforms to see the deeper architecture of formed volcanoes as well as their succession (Lexa et al. 2010). The petrographic and quantitative studies of volcaniclastic rocks widely applied (Cas and Wright 1987, Branney and Kokelaar 2002m Sulpizio et al. 2007) and provide useful tool for understanding the explosion dynamics and depositional processes on volcanic slopes. Beside the wide range of regional applications in the CPR, this approach has not been applied yet in the investigated region.

Geological settings

The Miocene (from ca. 15 Ma to 10 Ma) volcanic activity of the Tokaj-Slanske Mountains (TSM) in the northeast segment of the Pannonian Basin was characterized by intense silicic volcanism in addition to eruption of andesitic-dacitic magmas. The Miocene (12,3-11,7 Ma old (Pécskay et al 1987) Abaújvár-Telkibánya ignimbrite forms a small (30 km^2) pyroclastic accumulation field (fig 1.). The explosive sequence represents an important stratigraphic marker below the subsequent lava domes (eastern part, Telkibanya Lava Dome Field). The subsidence of Hernád through (Middle-Late Miocene) was very destructive and caused continuous disruption and burial at the western part of the succession. After the Pliocene pediment formation, a 150-300 m high western sloping surface formed. The Pleistocene regional uplift of Mountain region was combined with renewal subsidence of Hernád Trough which led to rapid incision of the tributary valleys along the re-activated Miocene fault set (N-S, NW-SE, WNW-ESE). Thus a good outcropping developed allowing a detailed facies reconstruction.

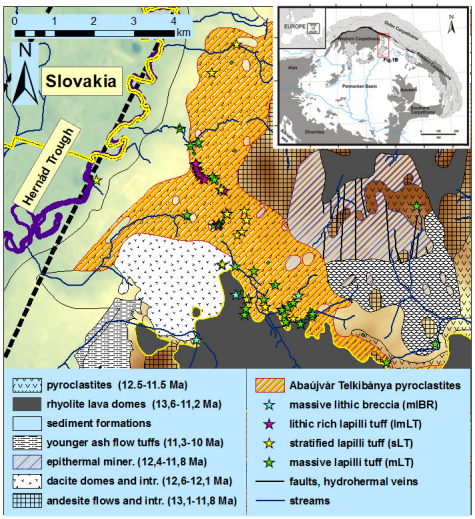

Fig. 1. – Geological sketch of study area with the sampled major lithofacies associations

Lithofacies associations

The deposits have been mapped at a scale of 1:10 000. The lithofacies descriptions for the pyroclastic rocks are based upon lithological characteristic, sedimentary features, grain size sorting and classified using the terminology of Branney and Kokelaar (2002) and Sulpizio et al. (2007). Grain size measurement techniques (sieve, outcrop image analysis, SEM imaging) were applied to evaluate spatial variations in sorting and relative proportion of the components. The identified flow units are bounded by different layers indicating pauses in sedimentation (fall deposits, basal layer of another flow). The lateral connections could be traced using marker horizons of the partly silicified fall deposits. The rare non-volcanic lithics and regional analogues refer that the volcaniclastics overlie clay bedrocks. The settling on older lavas (andesite, rhyolite) can be observable at the eastern margins (fig 1.). The faulting along Hernád Trough and the absence of boreholes makes it difficult to determine the exact

thickness which is approximately 50-80 metre. The succession comprises 3 major explosive lithofacies associations (fig. 2.): (1) massive, non welded lapilli tuff (mLT), (2) well sorted stratified lapilli tuff (sT) and (3) lithic enriched lapilli tuff (lmLT).

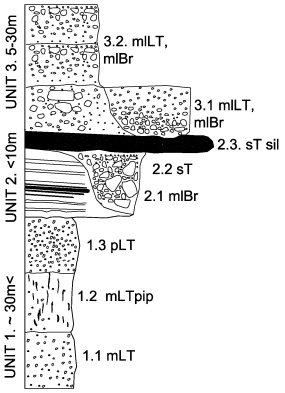

Fig. 2. – Simplified vertical profile of the Abaújvár-Telkibánya ignimbrite: **(1) mLT:** massive lapilli tuff, mLT_{pip}: massive lapilli tuff with fines poor pipes, pLT: pumice rich lapilli tuff **(2) sLT:** stratified lapilli tuff, sT_{sil}: silicified stratified lapilli tuff, **(3) lmLT:** lithic enriched massive lapilli tuff, mlBr:massive lithic breccia layers

(1) The first, mLT dominated part of the succession is most voluminous (30m<). The massive, poorly sorted, non-welded lithics bearing (obsidian, rhyolite) lapilli tuff crops out over the whole area. At the proximal part, the thickest flow unit is over 20 metre. The gas segregation pipes (mLT_{pip}) and charcoal are also common. A fines poor, pumice dominated parts (pmLT) also identified as an individual flow unit. The thinner, distal sheets (~0,5 m) outcrop near the neighbouring dome field (east) within 5 km in distance.

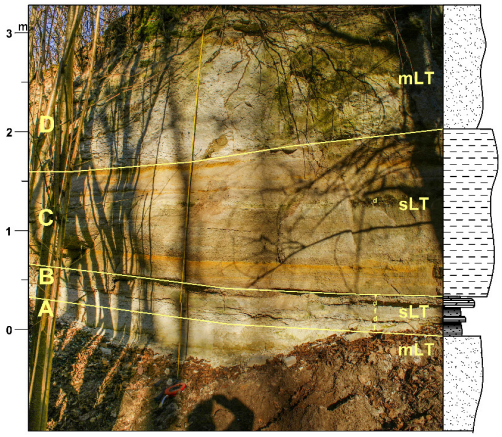

Fig. 3 – Lithofacies architecture in Abaújvár Valley: The stratified lapilli tuff (sLT) interbedding between mLT (A,D) layers. The basal part of the sLT (B) is finely laminated.

(2). The sLT (~ 2-3 m, fig 3.) is mantling the mLT topography and usually consist of cm-dm thick, well sorted, internally laminated beds in a grain size from medium ash to fine grained lapilli. The occasional outcrops also identified with coarse grained pumice lapilli. The most distal, finely (mm) laminated ash contains accretionary lapilli. Subsequent stratified silicification occurred in distinct layers (cm-dm).

(3). The sLT is overlain by poorly to unsorted, lithic enriched volcaniclastic deposits (10 m, lmLT). The mLT layers varied with lmLT parts in normal or reversely graded way. The lithics are dominantly angular glassy lapilli and/or blocks (perlitic glass). Massive, poorly sorted lithic breccias (mlBR) with rounded blocks forms a distinct horizons in the close proximity of the lava domes.

Interpretation of the succession

The facies architecture indicates a small to moderate volume, Late Miocene subaerial silicic succession which developed in the proximity of a tectonically active half-graben structure. The thickest, mLT (1) dominated part deposited as ignimbrite, which followed by fallout deposits of sLT (2). The presence of accretionary lapilli indicate phreatomagmatic activity. The lmLT layers (3) with clast supported zones refers fast sequence of small granular pulses within successive pyroclastic density currents. The unsorted nature of mlBR probably resulted from rapid deposition of lava dome related dense lithic blocks. The settings and stratigraphy are indicative of an extensional tectonic activity induced volcanism where a caldera subsidence associated with subsequent lava dome activity.

Acknowledgements

This study belongs to the Hungarian-Italian MTA-CNR bilateral research project 2016-2018.

References

Branney, M.J., Kokelaar, B.P., 2002. Pyroclastic density currents and the sedimentation of ignimbrites. Geol. Soc. Lond. Mem. 27, 1-152.

Cas R.A.F., Wright J.V., 1987. Volcanic Successions – Modern and Ancient. Allen & Unwin, London, pp 1–528

Lexa J., Seghedi I., Németh K., Szakács A., Konecný V., Pécskay Z., Fülöp A., Kovacs M., 2010. Neogene-Quaternary Volcanic forms in the Carpathian-Pannonian Region: a review Cent. Eur. J. Geosc. 2, 207-270.

Pécskay, Z., Balogh, K., Székyné, F. V., Gyarmati, P. (1987): Földtani Közlöny 117. 237-253.

Sulpizio, R., Mele, D., Dellino, P., La Volpe, L., 2007. Deposits and physical properties of pyroclastic density currents during complex Subplinian eruptions: the AD 472 (Pollena) eruption of Somma-Vesuvius, Italy. Sedimentology 54, 607–635.

Reconstructing the complex evolution of the polycyclic Lausche Volcano

Erik Wenger[1], Jörg Büchner[1], and **Olaf Tietz**[1]

[1] *Senckenberg Museum of Natural History Görlitz, Germany – olaf.tietz@senckenberg.de*

Keywords: Monogenetic volcanoes, Lower Oligocene, Geological mapping.

The Tertiary Lausitz Volcanic Field covers a transboundary area encompassing parts of Eastern Saxony (Germany), Lower Silesia (Poland) and Northern Bohemia (Czech Republic). Volcanism in this region culminated in the Lower Oligocene (32–29 Ma). A petrographic bimodality of the lavas within the Lausitz Volcanic Field is revealed by the appearance of "primitive" basaltoids (nephelinites, basanites, tephrites) as well as slightly younger and geochemically more differentiated volcanics (trachytes, phonolites). The majority of the volcanoes in this area are monogenetic with a rather simple eruptive evolution.

In contrast, the highest volcano, Lausche Hill (Fig. 1), reflects a substantially more complex development. Bedrock outcrops are very limited at this mountain and its geological subsurface is covered by dense vegetation, soil and often mantled by debris. To cope with this unfavourable field situation, the following complementing mapping methods were used: (1) The distribution of loose bedrock fragments was recorded with GPS. (2) A few exploratory excavations were dug and several hand drillings up to 2 m depth were also performed. (3) Data on rock internal structures were collected by flow fabric measurements at outcropping cliffs. (4) Clear morphological features related to geological boundaries were evaluated applying DEM analyses. (5) Previously determined 40Ar/39Ar ages provided temporal information on the volcano's evolution.

The final gathering of the individually ascertained data enabled not only to create a precise geological map of the Lausche Hill, but also to reconstruct its volcanological history. The volcanic edifice consists of two monogenetic volcanoes of different ages which erupted at the same place: A basaltic scoria cone sitting on its initial maar-diatreme volcano was filled by a tephritic lava lake with a lava flow (30.75 ± 0.56 Ma), which overflow the geological framework (Cretaceous sandstones). After a distinct time gap, a phonolithic lava dome extruded (29.05 ± 0.12 Ma). This was accompanied by explosive activity with a collapse breccia and a late-stage magma supply when phonotephrite dykes penetrated the lava dome. According to this evolution, the Lausche Volcano can be defined as small-volume polycyclic volcano.

The study shows that prolonged field mapping in difficult terrain can lead to convincing and valid results, if additional methods are involved and the scientific problem is investigated patiently. Beside the briefly sketched volcanological results, the mapping provides also results for the neotectonic evolution since the volcanic time. The low erosion amounts of the volcanic edifice allow to postulate a very young (neotektonic) uplift event for the Lausche Volcano and the Lausitz Mountains with a culmination by 320 ka (for more details see Wenger et al. 2017).

Fig. 1 – Lausche Hill (792.6 m a.s.l.) seen from Dolní Světlá/Czech Republic (view to northwest).

References

Wenger E., Büchner J., Tietz O., and Mrlina J., 2017. The polycyclic Lausche Volcano (Lausitz Volcanic Field) and its message concerning landscape evolution in the Lausitz Mountains (northern Bohemian Massif, Central Europe). Geomorphology, 147, 193–210

Insights from Askja sand sheet, Iceland as a depositional analogue for the Bagnold Dune Field, Gale Crater, Mars.

Ingrid Ukstins[1] and Michael Sara[1]

[1] *Earth and Environmental Sciences, University of Iowa, Iowa City IA, 52246, USA. Ingrid-peate@uiowa.edu*

Keywords: eolian sedimentation, mafic sand, Bagnold Dunes Mars.

Examining the compositional effect of aeolian transport and sorting processes on basaltic sands is significant for understanding the evolution of the Bagnold dune field, Stimson Fm., and other martian soils and sedimentary units. We use the Askja sand sheet, Iceland, as a testbed to quantify the nature of regolith production and aeolian transport processes in a mafic system. Eolian dominated weathering prevalent at Askja volcano, Iceland, likely also occurred on Mars and Askja mafic volcaniclastic dunes could be the best terrestrial morphological and compositional analogue for Martian dunes.

Basalts from Askja, Iceland have high MgO (5 to 18 wt %) and high Fe_2O_3 (5 to 18 wt %) similar to Martian basalts, which have Fe_2O_3 from 10 to 33 wt % and MgO around 11 wt % (Gellert et al. 2006). Askja is located in the Northern Volcanic Zone of Iceland, and the cold desert climate provides a good weathering analogue for basalts that have been weathered to form mafic volcaniclastic deposits in a 40-km long sand sheet to the E-SE of the Askja caldera complex (Fig. 1). The 2014-2015 Holuhraun eruption was emplaced onto the southeastern part of the sand sheet (Fig. 1) and altered the regional geomorphology and may have impacted the geochemistry of the sand sheet itself by addition of wind-blown ash and crystals, plus weathered material derived from the lava flow (MgO content of ~7.1 wt %). Mangold et al. (2011) found that Icelandic sands show little chemical variability but that study was based on limited samples (12 sand and 12 rock samples).

The Askja sand sheet, between ~10 cm and ~10 m thick, covers 240 km^2. Mountney and Russell (2004) described three distinct sections based on accumulation. The SW section is deflationary and defined by very fine to medium grained basaltic sand with cobbles and boulders of lithologies sourced adjacent to and distal from the sand sheet. The central part is inflating and is dominated by very fine-grained sand, relict lava fields, and small to large sand ripples. The NE portion is also inflating but that accumulation is limited to topographic depressions. The NE, characterized by sand mostly composed of pumice from the 1875 Askja eruption and basalt clasts from local lava fields, was not studied in detail here due to the difference in chemistry.

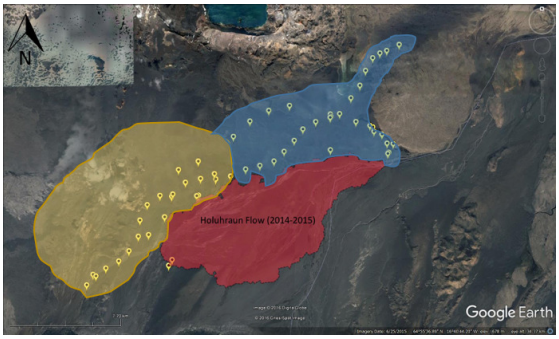

Fig. 1 – Google Earth image of Askja sand sheet sample locations. Yellow shows the deflationary portion of the sand sheet, blue the inflationary section. The red area represents the extent of the 2014-2015 Holuhraun lava flow.

We sampled 36 sites for material at the surface and 10 cm depth along a 25 km traverse and an additional seven sites perpendicular to the main wind direction (E, NE), totaling 225 samples (Fig. 1). We also sampled lava and volcaniclastic deposits that are adjacent to and underlying the sand sheet, which may represent potential sources of the sedimentary material. Chemical composition was determined by standard ICP-MS methods. Sphericity (presented as a percentage describing grain shape relative to a sphere) and other grain size measurements were collected by a Retsch CAMSIZER. High-precision EPMA was used to analyze major and trace element concentrations of glass, mineral and lithic materials, SEM was used to image surface morphology of grains, and LIBS analysis provides a direct comparison to ChemCam data collected on Mars.

Field observations establish the top ~1 cm to be composed of fine- to medium-grained sands composed of basalt lava fragments, volcanic glass, olivine, pyroxene, and plagioclase sourced from mafic lavas and explosive pyroclastic eruptions. Directly beneath is a very fine- to fine-grained consolidated layer largely composed of angular volcanic glass particles. Trenching to a depth of ~1 m indicates the sand sheet is dominated by mm-scale laminations and cross-bedded with varying thickness and grainsize. Most laminations are on the mm-scale, however, there are occurrences of thicker, cm-

scale laminations and the presence of medium-grained sand wedges is also readily apparent.

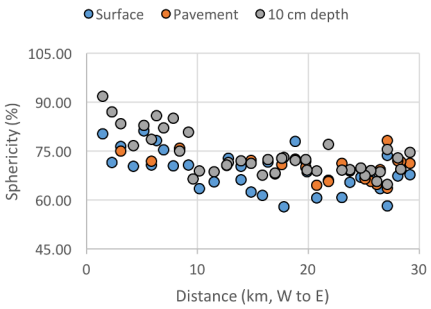

Fig. 2 – Sphericity versus distance along the sand sheet. Blue symbols are surface material, orange are the fine-grained pavement beneath, and grey are from 10 cm depth.

Bulk chemistry of >200 sand samples are similar to Martian crust (SiO_2: 48-52 wt %, MgO: 5-8 wt %, Fe_2O_3: 13-15 wt %). MgO concentrations vary with distance along the sand sheet, increasing by ~1.5 % over ~10 km in the downwind direction (E, NE), then maintaining a relatively consistent concentration of ~6.75 wt % over ~18 km (Fig. 2). This could be due to the influx of new material generated during the Holuhraun eruption (2014-2015). Mean sphericity displays an increase of ~15 % to the E over ~10 km followed by a leveling off between ~65-75 %. This indicates the input of more prismoidal material around 10 km. Also, the material at depth tends to be of higher sphericity than the material on or near the surface of the sand sheet. Notably, the MgO increases while the sphericity decreases and both data sets level off at ~10 km which suggests the two variables are related.

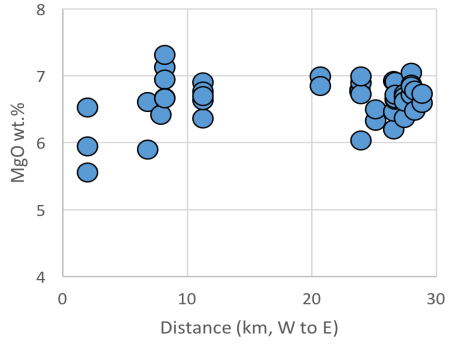

Fig. 3 – Sphericity versus distance along the sand sheet. Blue symbols are surface material, orange are the fine-grained pavement beneath, and grey are from 10 cm depth.

The Bagnold dune field is an active sand sheet composed of rounded to sub-rounded, very fine- to medium- sized (ca. 45 to 500 µm) sand composed of roughly similar proportions of plagioclase, olivine and pyroxene as crystalline components, along with an amorphous component (35 % +/- 15 %) (Ehlmann et al. 2017). Mg, Ni, Fe and Mn are enriched in the coarse fraction, VNIR spectra suggest olivine enrichment. Amorphous components in the sand-sized fraction are Si-enriched and may be impact or volcanic glass. The Stimson Fm., Gale Crater, Mars is a part of the Lower Mount Sharp group, and is a cross-bedded sandstone with visible sand grains. The lithified rock is primarily plagioclase feldspar, pyroxene, magnetite, and ~20-25 wt % XRD amorphous material (Yen et al. 2016). The unaltered sections of the Stimson Fm. have been measured via APXS (Alpha Particle X-ray Spectrometer) to be compositionally similar to Martian crust. Extensive cross-bedding and laminations chronicled by Curiosity are indicative of an ancient eolian-dominated dune system.

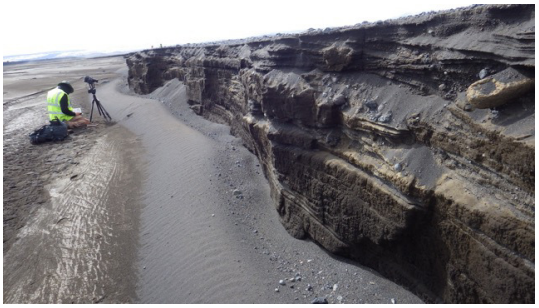

Fig. 4 – Askja sand sheet exposure.

Acknowledgements

Funding provided to I. Ukstins (NASA SSW 14-SSW14-0101) and M. J. Sara (International Programs, CGRER, EES, University of Iowa).

References

Ehlmann, B.L., et al., 2017. Chemistry, mineralogy, and grain properties at Namib and High Dunes, Bagnold dune field, Gale Crater, Mars: A synthesis of Curiosity rover observations. In press, JGR Planets.

Gellert, R., et al., 2006. Alpha particle X-ray Spectrometer (APXS): Results from Gusev crater and calibration report. JGR Planets 111, 2156-2202.

Gellert et al. 2016

Mangold, N., Baratoux, D., Arnalds, O., Bardintzeff, J.M., Platevoet, B., Gregoire, M., Pinet, P., 2011. Segregation of olivine grains in volcanic sands in Iceland and implications for Mars. EPSL 310, 233-243.

Mountney, N.P., Russell, A.J., 2004. Sedimentology of cold-climate aeolian sandsheet deposits in the Askja region of northeast Iceland. Sed. Geol. 166, 223-244.

Yen, A.S., et al., 2016. Cementation and aqueous alteration of a sandstone unit under acidic conditions in Gale Crater, Mars. LPSC XLVII #1694

Correlation of paleomagnetic data and radiometric dating along the Miocene - Quaternary volcanic range of the East Carpathians

Mădălina Vişan[1], Cristian G. Panaiotu[2], Ioan Seghedi[1], Viorel Mirea[1]

[1] *Institute of Geodynamics, Romanian Academy, Jean-Luis Calderon 19-21, 020032, Bucharest, Romania – danamadalina@yahoo.com*
[2] *Paleomagnetic Laboratory, Faculty of Physics, University of Bucharest, Atomiştilor 405, Măgurele, Ilfov, Romania.*

Keywords: paleomagnetism, radiometric dating, volcanism.

In the last five years new paleomagnetic data set (Panaiotu et al., 2012; Panaiotu et al., 2013; Vişan et al., 2016; Panaiotu et al., 2016) were obtained for volcanic rocks of the central-proximal facies of the Călimani-Gurghiu-Harghita range and also from alkali basaltic volcanism of the Perşani Mountains located in the East Carpathians (Romania). Călimani-Gurghiu-Harghita range is around 160 km long and, according to the K-Ar ages, the volcanic activity gradually migrated to the south between the Miocene (~10 Ma) and the Quaternary (~0.03 Ma) (e.g. Pécskay et al., 1995, 2006). The large number of paleomagnetic sampling sites (over 400) and their geographic distribution allowed refining the evolution model of the axial part of the volcanic activity in time and space for the last 10 Ma in the East Carpathians.

The areal distribution of the samples with normal and reversed polarities is in general agreement with geographic and time distribution of volcanism and the magnetic polarity time scale. The evolution of volcanic activity in the main volcanic structures can be correlated with the magnetic polarity time scale as follows (Fig. 1):

1) According to K-Ar ages the main volcanic formations of the Călimani Mountains (Dragoiasa, Budacu and Lomaş and Rusca-Tihu) were mainly emplaced between 9.5 - 7 Ma and they are contemporaneous with the northern volcanic structures of the Gurghiu Mountains (Jirca and Fâncel-Lăpuşna). The geographic distribution of magnetic polarities in these volcanic structures shows the presence of both normal and reversed polarities in agreement with the polarity time scale between 9.5-7 Ma during chrons C4An, C4r and C4n.

2) The Seaca-Tătarca, Borzont, Şumuleu and Ciumani-Fierăstraie volcanic structures (Gurghiu Mountains), show dominant normal polarities, and suggest to be generated during chron C3An (6.7-6.0 Ma);

3) The Ivo–Cocoizaş and Ostoroş volcanic structures (North Harghita), show only reversed polarity and correspond to the chron C3r (6.0 – 5.2 Ma);

4) The Vârghiş volcanic structure (North Harghita), show mixed polarities and, was formed during chron C3n (5.2 - 4.1 Ma);

5) The Luci-Lazu volcanic structure (South Harghita), show dominant reversed polarities and was generated during chron C2Ar (4.2 - 3.6 Ma);

6) The Cucu volcanic structure (South Harghita), show dominant normal polarities, being formed during chron C2An (3.6 - 2.5 Ma);

7) The Pilişca volcanic structure (South Harghita) show dominant reversed polarities, corresponding to the chron C2r (2.5 - 1.9 Ma) and partially during chron C1r (until 1.6 Ma according to the K-Ar ages);

8) The Malnaş and Bixad domes (South Harghita), both show normal polarity, can be correlated according to K-Ages with chron C2n (1.9 - 1.7 Ma) or could be younger (Jaramillo);

9) The Balvanyos extrusive dome (South Harghita) with normal polarity has erupted during chron C1r1n (1.07 – 0.98 Ma);

10) Ciomadul volcanic structure with normal polarity (South Harghita) was generated during chron C1n (0.78 – 0 Ma) that correspond with both K-Ar and U–Th/He and U–Th zircon ages (Szakács et al., 2015; Harangi et al., 2015);

11) The Perşani Mountains basalts were erupted in short episodes between 1.2 – 06 Ma which correspond to chron C1r (Racoş – 12 Ma, Turzun and Comana volcanic structures), C1r1n (Măguricea and Gruiu volcanic structures), C1r1r (Bărc – Bogata upper lavas) and C1n (Dâlma and Mateiaş volcanic structures).

The main conclusions are:

1) The geographic distribution of the magnetic polarity data is in agreement with the currently accepted model of a progressive migration of the volcanic activity from North to the South.

2) Starting with the southern volcanic structures from the Gurghiu Mountains (younger than 7 Ma), the magnetic polarities distribution highlights the fact that in most volcanic structures the eruption period lasted for less than 1 Ma, usually with similar time interval with the one inferred from K-Ar age determinations.

3) The mean paleomagnetic directions show the absence of vertical axis rotations during the migration of the volcanism.

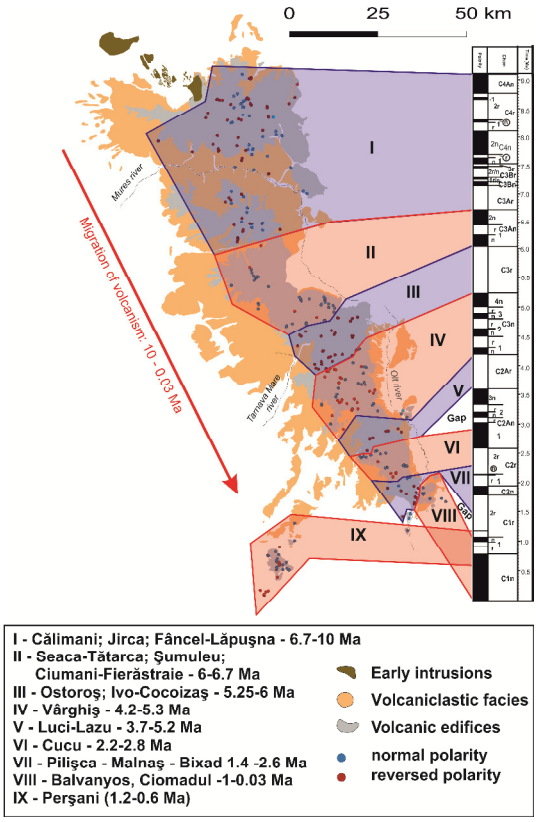

Fig. 1 – Duration of main volcanic activity based on the correlation of the geographical distribution of magnetic polarity data and radiometric ages. The Polarity Time Scale is after Lourens et al. (2004).

Acknowledgements

This work was supported by several grants of the Ministry of National Education, CNCS – UEFISCDI PN-II-ID-PCE-2012-4-0177, PNII-IDEI 974/2007, PNII-IDEI 151/2007 and PN-II-ID-PCE-2012-4-0137

References

Harangi S., Lukács R., Schmitt A.K., Dunkl I., Molnár K., Kiss B., Seghedi I., Novothny Á., Molnár M., 2015. Constraints on the timing of Quaternary volcanism and duration of magma residence at Ciomadul volcano, east–central Europe, from combined U–Th/He and U–Th zircon geochronology. Journal of Volcanology and Geothermal Research 301, 66–80

Lourens, L., Hilgen, F., Shackleton, N. J., Laskar, J. & Wilson, D., 2004. The Neogene Period, pp: 409-440 *in* *A Geological Time Scale*, ed. Gradstein, F. M., Ogg. J. G. & Smith, A. G., Cambridge University Press, Cambridge.

Panaiotu, C.G., Vişan, M., Tugui, A., Seghedi, I., Panaiotu, A.G., 2012. Palaeomagnetism of the South Harghita volcanic rocks of the East Carpathians: implications for tectonic rotations and palaeosecular variation in the past 5Ma, Geophys. J. Int, 189, 369–382

Panaiotu, C.G., Jicha, B.R., Singer, B.S., Ţugui, A., Seghedi, I., Panaiotu, A.G., Necula, C., 2013. $^{40}Ar/^{39}Ar$ chronology and paleomagnetism of Quaternary basaltic lavas from the Perşani Mountains (East Carpathians). Phys. Earth Planet. Int. , 221, 1-14.

Pécskay Z., Edelstein O., Seghedi I., Szakács A., Kovacs M., Crihan M., Bernad A., 1995. K-Ar datings of Neogene-Quaternary calc-alkaline volcanic rocks in Romania, Acta Vulcanologica 7, 53-61.

Pécskay, Z. Lexa, J. Szakacs, A. Seghedi, I. Balogh, K. Konecny, V. Zelenka, T. Kovacs, M., Poka, T., Fülop, A., Marton, E., Panaiotu, C., Cvetković, V., 2006. Geochronology of Neogene magmatism in the Carpathian arc and intra-Carpathian area, *Geologica Carpathica*, 57, 511-530.

Szakács, A., Seghedi, I., Pécskay, Z., Mirea, V., 2015. Eruptive history of a low frequency and low-output rate Pleistocene volcano, Ciomadul, South Harghita Mts., Romania. Bulletin of Volcanology, 77:12, DOI 10.1007/s00445-014-0894-7

Vişan, M., Panaiotu, C.G., Necula, C., Dumitru, A., 2016. Palaeomagnetism of the Upper Miocene- Lower Pliocene lavas from the East Carpathians: contribution to the paleosecular variation of geomagnetic field, Scientific Reports, 6, 23411; doi: 10.1038/srep23411.

Romanian Journal of Earth Sciences
Volume 88(91), special issue, October 2017 ISSN 2248 – 2563

CONTENTS